THE KNEE IN MOTION

DYNAMIC CT IMAGING FOR DIAGNOSIS AND EVALUATION OF KNEE DISORDERS

HANS DUNNING

The knee in motion

Dynamic CT imaging for diagnosis and evaluation of knee disorders

Hans Dunning

The knee in motion

Dynamic CT imaging for diagnosis and evaluation of knee disorders

Proefschrift

ter verkrijging van de graad van doctor
aan de Radboud Universiteit Nijmegen
op gezag van de rector magnificus prof. dr. J.H.J.M. van Krieken,
volgens besluit van het college voor promoties
in het openbaar te verdedigen op
vrijdag 22 september 2023
om 10.30 uur precies

door
Hans Dunning
geboren op 29 januari 1989
te Delfzijl

Table of contents

Chapter 1

General introduction
& Thesis outline

General introduction

Approximately 1.71 billion people suffer from musculoskeletal disorders worldwide, making it the leading cause of disability[3]. Due to the aging population this number is rapidly increasing, significantly limiting peoples' mobility, wellbeing and ability to participate in society. As a result, the direct and indirect social and economic burden of musculoskeletal disorders is high and continues to grow. After low back pain, knee pain is the most common musculoskeletal condition, affecting 1 in 5 of the general population and 1 in 4 of young, active adults and adolescents at some point[14].

The knee consists of three bones, the femur (thigh bone), tibia (shin bone) and the patella (kneecap) that are connected by ligaments and tendons. Together these form two joints; the tibiofemoral joint (TFJ) connecting femur and tibia and the patellofemoral joint (PFJ) between the femur and the patella (figure 1). The patella is the largest sesamoid bone in the body and is part of the knee extensor mechanism. While it was initially thought the sole function of the patella was to act as a lever arm for the quadriceps muscle during extension, research indicates that the patella influences motor control of movement[4, 6].
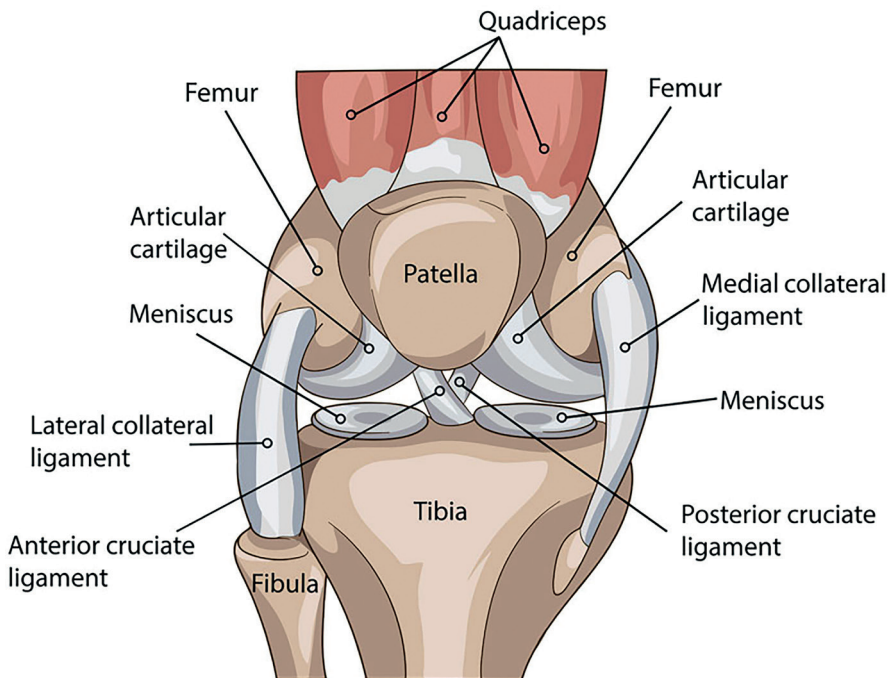

Figure 1. Anatomy of the knee. The knee consist of two joints; the tibiofemoral joint, between the femur and tibia and the patellofemoral joint, between the femur and patella[31].

The TF and PF joint collectively have 12 degrees of freedom (DoF), as the femur, patella and tibia can all rotate and translate along three axis. During flexion and extension of the knee, complex movement occurs in all DoF. From full extension to approximately 30° of flexion, the patella is situated superior to the femoral trochlea and medial and lateral movement is mainly constrained by the soft tissues. At approximately 30° of flexion, the patella engages with the femoral trochlea and bony congruence is the primary restraint for medial or lateral movement[24, 30].

The patellofemoral joint is a source of common pathologies, with patellofemoral pain (PFP) being the most prevalent symptom[27]. Patellofemoral pain and patellar disorders are associated with patellar maltracking, a condition in which the patella follows an unusual path to and through the femoral trochlea. Patellar tracking is governed by an intricate interplay between the soft tissues, neuromuscular control and bony congruence of the patella and femur[22, 24]. If this interplay is severely disrupted, (sub) luxations of the patella from the trochlear groove may occur, which is referred to as patellofemoral instability (PFI). Patella luxations are painful and may cause damage to neighbouring tissues. In the short term, this restricts movement and ability to participate in exercise. On the long term, patellofemoral pain and instability have been associated with osteoarthritis[7].

Although the mechanism behind development of patellar maltracking and patellofemoral instability has not been fully understood, several predisposing factors have been identified, such as[21]:
- Laxity of the medial soft tissue constraints and/or (over)tightness of the lateral soft tissue constraints, which cause the patella to move in lateral direction (too) easily.
- Trochlear dysplasia, a pathological morphology of the femoral trochlea that causes incongruency between the femur and the trochlea reducing (lateral) constraint.
- Patella alta (high riding patella) where the patella has a superior position with respect to the trochlear groove. As a result the patella engages with the femoral trochlea at flexion angles larger than the typical 30°, which can cause the patella to luxate more easily.
- Pathological knee alignment, which can cause the lateral component of forces acting on the patella to become too large, resulting in luxation. Examples are valgus alignment (knock knees) or excessive femoral anteversion, an inward rotation of the femur leading to 'kneeing in'.
- Insufficient neuromuscular control, which can cause altered onset and duration of medial muscle activation during active daily tasks, contributing to more lateral forces and subsequent movement of the patella.

If patellofemoral instability persists, various (surgical) treatments may be considered which aim to restore the normal movement (kinematics) of the knee. As the cause

of patella maltracking often is complex and multifactorial, treatment is equally complex. Choosing the right treatment therefore requires an accurate diagnosis and quantification of biomechanical causes of pain or instability. For this purpose, numerous different classifications and measurements have been developed. These classifications and measurements are made on the basis of both physical examination and/or medical imaging. While physical examination can be performed during knee movement, the results are dependent on the practitioner and therefore difficult to generalise, manifested by weak interrater reliability[1,16,28]. In addition, despite being dynamic, movement during physical examination is often passive (i.e. without muscle activation) rendering the measurement unrepresentative of a physiological situation.

Measurements for patellar maltracking that are based on medical imaging have a slightly better interrater reliability, but these measurements are typically performed on static images, with the patient lying still on their back[11]. Potential vital information that is needed to determine the biomechanical cause of maltracking, such as the effect of joint motion and the influence of the soft tissues and muscles is thereby not captured. As there is a weak correlation between static measurements and dynamic knee kinematics, performing measurements on static images may not be the best method to identify and quantify the patient specific cause of patellar maltracking[13].

For this reason, multiple in-vivo imaging techniques have been developed and researched for the purpose of dynamic diagnosis and postoperative evaluation of (surgical) interventions of the knee[8,10,25,26]. This involves the use of different imaging modalities such as fluoroscopy, dynamic MRI and dynamic CT while applying different loading conditions, such as a squat, lunge or flexion-extension movement against gravity.

In multiple review studies, current state of the art and applications of dynamic imaging for the patellofemoral joint was studied[5,18,23]. These studies concluded that dynamic imaging is able to provide an in-depth understanding of the (patient specific) kinematics of the tibiofemoral and patellofemoral joint and underline the importance of dynamic imaging to identify the biomechanical cause of disorders and evaluation of intervention. However, despite providing potential valuable information, dynamic imaging is rarely used in a clinical setting.

Apart from obvious causes such as the unavailability of dynamic imaging technology, there are other practical causes that prevent widespread use in daily clinical practice. For example, technique dependent limitations, such as time-consuming scan protocols or protocols that require intensive coordination and cooperation of the patient, are unfeasible for frail patients with painful knees. Furthermore, previous dynamic imaging

studies used manual measurements and manually determined coordinate systems, which are necessary for the kinematic description. In the case of dynamic imaging, this is not only too time-consuming for use in clinic practice, but also introduces inter- and intra-rater variability that makes it difficult (if not impossible) to compare and generalise results from different studies[11,19]. Lastly, definitions and methods used to describe tibiofemoral and patellofemoral remain ambiguous[2,15]. This complicates the comparison, combination and interpretation of the complex movements of the tibiofemoral and patellofemoral joint across different studies.

Of the different modalities, dynamic computed tomography (CT) has the most straightforward and least time-consuming scan protocol and therefore seems to be a promising method for use in the clinic and with frail patients. Using a rotating Xray source and a detector plate, a CT scanner is able to create high resolution 3D volumetric images. First generation CT scanners had a single row of detectors, allowing one detector-sized slice to be imaged per rotation[17]. Through improved sensor technology, reconstruction algorithms and increased computational power, current CT scanners can scan multiple slices at higher resolution. Recent innovations in multislice imaging allow imaging of 320 slices at once with a slice thickness of 0.5mm. As a result, 160 mm of axial slices can be imaged per rotation of the gantry. By imaging in quick succession, anatomical structures within the field of view of 160 mm can by dynamically imaged similar to video. This offers possibilities for dynamic diagnostic imaging of knee kinematics and its pathologies.

Dynamic CT or 4DCT was originally introduced in cardiology for coronary angiography and has since then been introduced in other fields such as neurology and orthopaedics [20]. Due to high spatial and temporal resolution, dynamic CT imaging of the knee may offer a means of unravelling the complex aetiology of patellofemoral disorders. Combined with relatively short duration and simplicity of a dynamic CT scan protocol, it is theoretically feasible to use it in a clinical setting. However, before dynamic CT imaging can be implemented in the clinical workflow of patients with patellofemoral disorders, a number of challenges will need to be addressed. This thesis addresses some of these challenges and explores how dynamic CT can be implemented in the clinical workflow of patients with complex knee alignment disorders.

Thesis outline

The aim of this thesis is to implement dynamic CT imaging in the clinical workup of complex knee disorders in order to objectively quantify knee kinematics and the effect of patellofemoral instability. To this purpose, several methods are proposed to automatically extract knee kinematics from dynamic CT images. The results from these

studies provide insights in the limitations of current diagnostic measurements and how dynamic CT imaging could improve diagnosis and treatment of knee disorders of a dynamic nature.

Many different methods can be used to describe and quantify knee kinematics. The method of kinematic description not only influences the results, but also determines the extent to which it can be interpreted, normalised and visualised. Because of the straightforward interpretation and visualisation, anatomical coordinate systems and their position over time are commonly used for the description of knee kinematics. Anatomical coordinate systems are calculated based on the geometry and orientation of bones, and relative motions between them are described around and along the axes of these coordinate systems. However, anatomical coordinate systems are non-identical as a result of anatomical differences within a population. As a result, differences found in the description of knee kinematics may partly be explained by anatomical differences rather than by knee pathologies. The lack of a generally accepted, accurate and consistent knee coordinate system complicates inter-subject comparison of knee kinematics. In **chapter 2** the sensitivity of an anatomical coordinate system to anatomical variations found in a population is determined using a statistical shape model.

In **chapter 3** we determine the sensitivity of the Tibial Tuberosity-Trochear Groove (TT-TG) distance to specific patient positioning inside the CT scanner. The TT-TG distance is a commonly used measurement to determine the insertion of the patellar tendon on the tibia in relation to the femoral trochlear groove and is based on static imaging. The measurement is performed in the coordinate system of the CT scanner assuming that the patient is correctly positioned within the scanner, which may not always be the case. The measurement is often used to determine whether surgical treatment is necessary and therefore has a significant influence on clinical decision making. In this chapter we determine if and to what extent the TT-TG distance measurement is affected by variations in patient positioning during scanning. Furthermore, we determine the extent to which these alignment deviations occur during routine CT scans of the knees where a standard alignment protocol is used.

Knee movement, loading and knee morphology are related and altered knee morphology due to pathology or trauma can therefore affect movement and change tissue loading[9,29]. Therefore, an important question in orthopaedic and trauma surgery is how morphology and function of damaged anatomical structures can be reconstructed in order to restore normal movement. In case of non-congenital defects, such as trauma, the unaffected contralateral joint is commonly used as a guide for treatment. In **chapter 4** the symmetry of the left and right tibial plateau of young healthy individuals are

quantified to determine whether left-right mirroring can be used as a reliable method to optimize 3D surgical planning of patients with fractures in the tibial plateau.

Patellofemoral disorders are commonly associated with patella maltracking but what patellar maltracking exactly involves is complicated and ill-defined. In **chapter 5** normative tibiofemoral and patellofemoral kinematics are determined from 100 healthy volunteers. For this purpose, a fully automatic method of extracting knee kinematics from dynamic CT was developed which is presented in this chapter. In addition to median knee kinematics, the results of this study show the degree of variability present in a healthy population. These results may be used to demonstrate how and to what extent knee disorders affect knee kinematics and provide insights into native knee kinematics. The latter can be used to restore the kinematics of affected knees.

In **chapter 6**, three-dimensional tibiofemoral and patellofemoral kinematics of 39 patients with patellofemoral disorders are compared to 100 healthy volunteers. This section demonstrates whether and to what extent there are statistically significant differences between these populations. Understanding these differences is vital for improving diagnosis and treatment of patellofemoral maltracking disorders and to unravel the complex aetiology.

Finally, in **chapter 7** the results of this thesis are summarized and discussed and indicates for future research are formulated.

References

1. Best MJ, Tanaka MJ, Demehri S, Cosgarea AJ (2020) Accuracy and Reliability of the Visual Assessment of Patellar Tracking. Am J Sports Med 48:370–375

2. Bull AMJ, Katchburian M V., Shih YF, Amis AA (2002) Standardisation of the description of patellofemoral motion and comparison between different techniques. Knee Surgery, Sport Traumatol Arthrosc 10:184–193

3. Cieza A, Causey K, Kamenov K, Hanson SW, Chatterji S, Vos PT (2020) Global estimates of the need for rehabilitation based on the Global Burden of Disease study 2019 : a systematic analysis for the Global Burden of Disease Articles Global estimates of the need for rehabilitation based on the Global Burden of Disease study . Lancet The Author(s). Published by Elsevier Ltd. This is an Open Access article published under the CC BY-NC-ND 3.0 396:2006–2017

4. Cleather DJ (2018) The patella: A mechanical determinant of coordination during vertical jumping. J Theor Biol Elsevier Ltd 446:205–211

5. Dandu N, Knapik DM, Trasolini NA, Zavras AG, Yanke AB (2022) Future Directions in Patellofemoral Imaging and 3D Modeling. Current Reviews in Musculoskeletal Medicine

6. Dejour D, Zaffagnini S, Arendt EA, Sillanpää P, Dirisamer F (2020) Patellofemoral Pain, Instability, and Arthritis. Dejour D, Zaffagnini S, Arendt EA, Sillanpää P, Dirisamer F (eds) JAMA - J. Am. Med. Assoc. Springer Berlin Heidelberg, Berlin, Heidelberg

7. Eijkenboom JFA, Waarsing JH, Oei EHG, Bierma-Zeinstra SMA, Van Middelkoop M (2018) Is patellofemoral pain a precursor to osteoarthritis? Bone Jt Res 7:541–547

8. Elias JJ, Carrino JA, Saranathan A, Guseila LM, Tanaka MJ, Cosgarea AJ (2014) Variations in kinematics and function following patellar stabilization including tibial tuberosity realignment. Knee Surg Sports Traumatol Arthrosc 22:2350–2356

9. Elias JJ, Jones KC, Cyrus Rezvanifar S, Gabra JN, Morscher MA, Cosgarea AJ (2018) Dynamic tracking influenced by anatomy following medial patellofemoral ligament reconstruction: Computational simulation. Knee Elsevier B.V. 25:262–270

10. Esfandiarpour F, Lebrun CM, Dhillon S, Boulanger P (2018) In-vivo patellar tracking in individuals with patellofemoral pain and healthy individuals. J Orthop Res 36:2193–2201

11. Fabricant PD, Heath MR, Mintz DN, Emery K, Veerkamp M, Gruber S, Green DW, Strickland SM, Wall EJ, Brady JM, Chambers CC, Ellis HB, Farr J, Heyworth BE, Koh JL, Kramer DE, Magnussen RA, Redler LH, Sherman SL, Tompkins MA, Wilson PL, Shubin Stein BE, Parikh SN (2022) Many Radiographic and Magnetic Resonance Imaging Assessments for Surgical Decision Making in Pediatric Patellofemoral Instability Patients Demonstrate Poor Interrater Reliability. Arthrosc - J Arthrosc Relat Surg Arthroscopy Association of North America 1–12

12. Freedman BR, Sheehan FT (2013) Predicting three-dimensional patellofemoral kinematics from static imaging-based alignment measures. J Orthop Res 31:441–447

13. GBD 2017 Disease and Injury Incidence and Prevalence Collaborators (2019) Global, regional, and national incidence, prevalence, and years lived with disability for 354 diseases and injuries for 195 countries and territories, 1990–2017: a systematic analysis for the Global Burden of Disease Study 2017. Lancet 393:855–865

14. Grant C, Fick CN, Welsh J, McConnell J, Sheehan FT (2021) A Word of Caution for Future Studies in Patellofemoral Pain: A Systematic Review With Meta-analysis. Am J Sports Med 49:538–551

15. Hiemstra LA, O'Brien CL, Lafave MR, Kerslake S (2021) Common Physical Examination Tests for Patellofemoral Instability Demonstrate Weak Inter-Rater Reliability. Arthrosc Sport Med Rehabil The Authors 3:e673–e677

16. Hounsfield GN (1973) Computerized transverse axial scanning (tomography): Part 1. Description of system. Br J Radiol 46:1016–1022

17. Katchburian M V., Bull AMJ, Shih YF, Heatley FW, Amis AA (2003) Measurement of patellar tracking: Assessment and analysis of the literature. Clin Orthop Relat Res 412:241–259

18. Kedgley AE, McWalter EJ, Wilson DR (2015) The effect of coordinate system variation on in vivo patellofemoral kinematic measures. Knee Elsevier B.V. 22:88–94

19. Kwong Y, Mel AO, Wheeler G, Troupis JM (2015) Four-dimensional computed tomography (4DCT): A review of the current status and applications. J Med Imaging Radiat Oncol 59:545–554

20. Post WR, Fithian DC (2018) Patellofemoral Instability: A Consensus Statement From the AOSSM/PFF Patellofemoral Instability Workshop. Orthop J Sport Med 6:1–5

21. Rathleff MS, Samani A, Olesen JL, Roos EM, Rasmussen S, Christensen BH, Madeleine P (2013) Neuromuscular activity and knee kinematics in adolescents with patellofemoral pain. Med Sci Sports Exerc 45:1730–1739

22. Rosa SB, Ewen PM, Doma K, Ferrer JFL, Grant A (2019) Dynamic Evaluation of Patellofemoral Instability: A Clinical Reality or Just a Research Field? A Literature review. Orthop Surg 11:932–942

23. Scott WN (2007) Insall and Scott, Surgery of the Knee. Vol 2, Capitulo 79

24. Seisler AR, Sheehan FT (2007) Normative three-dimensional patellofemoral and tibiofemoral kinematics: A dynamic, in vivo study. IEEE Trans Biomed Eng 54:1333–1341

25. Sheehan FT, Derasari A, Brindle TJ, Alter KE (2009) Understanding patellofemoral pain with maltracking in the presence of joint laxity: Complete 3D in vivo patellofemoral and tibiofemoral kinematics. J Orthop Res 27:561–570

26. Smith BE, Selfe J, Thacker D, Hendrick P, Bateman M, Moffatt F, Rathleff MS, Smith TO, Logan P (2018) Incidence and prevalence of patellofemoral pain: A systematic review and meta-analysis. PLoS One 13:1–18

27. van Trijffel E, van de Pol RJ, Oostendorp RAB, Lucas C (2010) Inter-rater reliability for measurement of passive physiological movements in lower extremity joints is generally low: A systematic review. J Physiother Elsevier 56:223–235

28. Westphal CJ, Schmitz A, Reeder SB, Thelen DG (2013) Load-dependent variations in knee kinematics measured with dynamic MRI. J Biomech 46:2045–2052

29. Wheatley MGA, Rainbow MJ, Clouthier AL (2020) Patellofemoral Mechanics: a Review of Pathomechanics and Research Approaches. Curr Rev Musculoskelet Med Current Reviews in Musculoskeletal Medicine 13:326–337

30. Hutchins K, Patellofemoral Pain Syndrom (PFPS), *Anatomy of the knee* [image], Lake Washington Physical Therapy, https://www.lakewashingtonpt.com/running-blog/patella-femoral-pain-syndrome-k3gny-2fbwl

Chapter 2

The sensitivity of an anatomical coordinate system to anatomical variation and its effect on the description of knee kinematics as obtained from dynamic CT imaging.

H. Dunning, S.A.W. van de Groes, N. Verdonschot, C.F. Buckens, D. Janssen

Abstract

Introduction: Accurate assessment of knee kinematics is important to investigate knee pathology and the effect of orthopaedic interventions. Anatomical coordinate systems are used to describe knee kinematics but inherently show interpersonal differences. The purpose of this study was to determine the sensitivity of an anatomical coordinate system of the knee to anatomical variation, and to establish its effect on the description of knee kinematics.

Methods: A statistical shape model of the knee was made based on a CT dataset. The statistical shape model was used to generate shapes with a specific variation. A coordinate system was calculated and the rotations relative to a mean coordinate system were calculated. From a dynamic CT dataset, knee kinematics were calculated for a flexion-extension movement. The largest rotational changes of the coordinate systems were then applied to the knee kinematics.

Results: The femoral and tibial coordinate system were relatively insensitive to anatomical variation, while the patellar coordinate system showed a larger sensitivity. Hence, tibiofemoral kinematics could be calculated with an accuracy of <5.01°, while patellofemoral kinematics showed a noticeably larger range of uncertainty (<13.48°).

Conclusion: The findings from this study can be used to investigate whether differences in knee kinematics are due to anatomy or pathology.

Introduction

Accurate assessment of knee kinematics is important to investigate knee pathology and to investigate the effect of orthopaedic interventions. Although knee disorders predominantly cause problems during dynamic activities, current diagnostic imaging and associated radiological measurements are primarily performed on static images. Consequently, crucial information on the effect of joint motion or the influence of soft tissues such as ligaments and muscles is being ignored. The relationship between static radiological measurements and their effect on joint dynamics remain unclear. Surgical interventions based on these measurements may therefore be sub-optimal.

Innovations in the field of multislice CT imaging allow for dynamic CT imaging. After being introduced in the field of cardiology, dynamic CT imaging (4DCT) has made its way to other fields such as orthopaedics[1]. Dynamic CT imaging of the knee during a flexion-extension movement allows in-depth assessment of tibiofemoral and patellofemoral kinematics. However, in order to be able to use 4DCT imaging for diagnostic purposes, suitable joint reference frames are required to describe the joint kinematics.

Over the last decades many methods have been proposed to describe and quantify knee joint kinematics, for example using a finite helical axis[2–5], or using the position and orientation of an anatomical coordinate system over time[6–8]. Because it does not depend on anatomy, the helical axis has shown to be an accurate method to describe and reproduce knee motion, but clinical interpretation, visualization and normalization are complex and not always intuitive[9]. Anatomical coordinate systems, on the other hand, are easier to interpret, but they are inherently non-identical due to inter-subject anatomical differences, introducing uncertainties in the description of kinematics that are related to anatomy rather than movement itself. The lack of a generally accepted, accurate and consistent knee coordinate system complicates inter-subject comparison of knee kinematics. This in turn makes it difficult to quantify the effects of musculoskeletal disorders on joint function and kinematics, and to discriminate between kinematic differences caused by anatomical variation or pathology.

Previously, several studies examined the interrater variation of coordinate systems[7,8,10]. However, these studies have not investigated the influence of inter-subject anatomical differences on the coordinate system, and their effect on the description of knee kinematics. This issue was recognized and addressed by Kedgley et al. who studied the effect of coordinate system rotations based on manually determined landmarks[11]. That study underlined the need for an automated standardized coordinate system, but lacks information on the relationship between the coordinate system variation and anatomical variation.

In a similar study by Morton et al. the effect of landmark variation on the kinematic description of the knee was examined by means of probabilistic analysis[12]. While this study sheds light on the sensitivity of kinematic descriptions to landmark variation, the landmarks were probed manually and landmark variation was not representative for variations that are seen in populations.

In the current paper we investigate the sensitivity of a coordinate system to anatomical shape variations using a statistical shape model. Using knee kinematics extracted from dynamic CT imaging, we investigated how variations of the coordinates system due to common anatomical variation may influence the description and quantification of knee kinematics.

Materials & Methods

In order to investigate the sensitivity of a coordinate system to anatomical shape variations, two imaging datasets were used: a conventional CT dataset for generation of a statistical shape model and a dynamic CT dataset for the extraction of knee kinematics. The statistical shape model was used to quantify the anatomical variation. Next, coordinate systems were assigned to the shape models while perturbating the most prominent shape variations to simulate the effect of anatomical variation on the location and orientation of the coordinate systems. Finally, these variations in coordinate systems were applied to a dataset of dynamic CT scans to determine the effect of anatomical variation on joint kinematics. Figure 1. shows a flowchart of the adopted methodology.
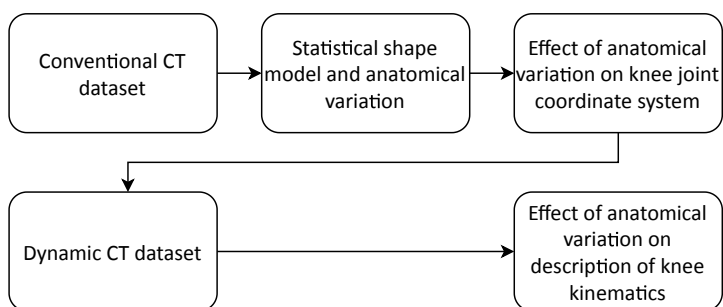
Figure 1. Flowchart of the materials and methods From conventional CT data, statistical shape models of the femur, tibia and patella were made in order to quantify anatomical variation. The effect of anatomical variation on the knee coordinate system was then calculated. From a second dynamic CT dataset, knee kinematics were extracted. The previously found, worst case effect of anatomical variation on the coordinate system was then applied to the coordinate system of the dynamic dataset. From this the effect of anatomical variation on the description of knee kinematics using the anatomical coordinate system was calculated.

The sensitivity of an anatomical coordinate system to anatomical variation and its effect on the description of knee kinematics as obtained from dynamic CT imaging | **23**

2

Conventional CT dataset

An anonymized CT dataset was obtained from the radiology department of the Radboudumc for which ethical approval was given by the local ethical committee. The median voxel dimensions were 0.782x0.782x1 mm. From 79 (17 female, 62 male) complete datasets, the femur, patella, and tibia were manually segmented by an experienced lab technician using Mimics (Materialise, Leuven, Belgium), and stored as surface meshes. Datasets that showed visible defects such as lesions or excessive bone proliferation were excluded.

Dynamic CT dataset

Ethical approval was obtained from the institutional ethical committee to scan 20 patients with patellofemoral instability using a dynamic CT scan protocol.

Patients were scanned with a Canon Aquilion ONE Prisma (Canon medical systems) CT scanner, creating 320 images with voxel dimensions of 0.976x0.976x0.5mm for dynamic scanning and 626 images with the same in plane resolution for the static scan.

A single high resolution scan (field of view 500 mm) was made of both knees in full extension. The scanner table was then moved to the end of the scanner and a pillow was placed in the patient's popliitial fossa, allowing free movement of the knee within the field of view of the scanner (figure 2).

Figure 2. a) High resolution static scan with 50cm field of view. b) & c) Medium resolution dynamic scan from 90 degrees of flexion to full extension and back against gravity, with 16 cm field of view.

Patients were asked to perform a knee extension-flexion movement from 90° to 0° of flexion and back to 90° in approximately 10 seconds. The dynamic scanning sequence was initiated after the patient had performed a few practice runs and the radiologist was satisfied with the pace of movement, in order to minimize any inconsistencies and possible motion artifacts. During the flexion-extension movement 41 CT images were made.

The static and dynamic images were automatically segmented using a trained 3D DenseUNet with Adam optimizer[13]. Each segmented mask was converted to a surface mesh using Matlab R2018b.

Statistical shape model and anatomical variation

To create a statistical shape model (SSM) of the femur, patella, and tibia, the meshes were loaded in Matlab R2018b, where all structures were smoothed (5 iterations, lambda: 0.6), remeshed to improve mesh quality, and downsampled (12000 vertices for tibia and femur, 5000 for the patella). All meshes were registered separately to their corresponding structure (i.e. femur, patella, and tibia) of one randomly chosen knee using a coherent point drift (CPD) algorithm[14]. Correspondence points were established simultaneously.

Principal component analysis was performed on the correspondence points, and eigen-vectors and eigenvalues were calculated using singular value decomposition.

The mean shape was calculated by summing the correspondence points divided by the number of datasets.

The model compactness and generalization ability were determined using a 'leave-one-out' approach. The generalization ability is the ability of the model to describe a shape that was not in the training set and is determined by fitting the SSM to a shape that is left out of the training set and calculating the root mean square error[15–17].

The described variation per principal component, the cumulative described variation and the generalization ability were visualized in a box-line plot (figure 3).

Anatomical coordinate systems

The definition of the anatomical coordinate system was based on the paper by Miranda et al., with minor adaptations. A detailed description on the coordinate system and the adaptions can be found in Chen et al.[18] and Miranda et al[7]. All coordinate frames consisted of three orthogonal axes: the superior-inferior (SI) axis, the medial-lateral (ML) axis and the anterior-posterior (AP) axis. A brief description of the coordinate systems is given below.

First, the inertial axes of the *femur* were calculated using a flood fill algorithm, filling the shape with point masses. In order to calculate the ML axis, the vertices on the articulating surfaces of the femur were identified by fitting separate cylinders through the femoral condyles. The center of mass of the faces corresponding to the articulating

vertices were projected on their respective cylinders resulting in two points, which formed the ML axis. The origin of the coordinate system was defined in the middle of these points. The AP axis was calculated by taking the cross product of the calculated ML axis and the previously calculated 3rd inertial axis (the long axis of the femur). Lastly, the SI axis was calculated as the cross-product of the ML and AP axis, resulting in an orthogonal femoral coordinate system.

For the *patellar* coordinate system, first, the inertial axis and center of mass were calculated. Next, a plane was fitted through the 30% most anterior vertices of the patella, based on the inertial axis. The AP axis was then calculated perpendicular to this plane with its origin in the center of mass of the patella. The sign of the axis was determined in agreement with the external frame. Using an iterative algorithm the vertex furthest away from the center of mass perpendicular to the AP axis was calculated and labelled as the inferior pole. The vector between the center of mass and the inferior pole was taken as the SI axis. Lastly, the ML axis was calculated as the cross product of the AP and ML axis. The origin of the coordinate system was the center of mass.

To determine the *tibial* coordinate system, the method proposed by Miranda et al. was used. The inertial axes of the tibia were calculated using the flood fill algorithm. The largest cross sectional area along and perpendicular to the 3rd inertial axis (the long axis of the tibia) was calculated, after which the tibial plateau was separated with a mesh cutting algorithm. The AP,ML and SI axis correspond to the 2nd, 3rd and 1st inertial axis. The origin was the center of mass of the tibial plateau. Figure 4 shows an example of the *femoral*, *patellar* and *tibial* coordinate system.
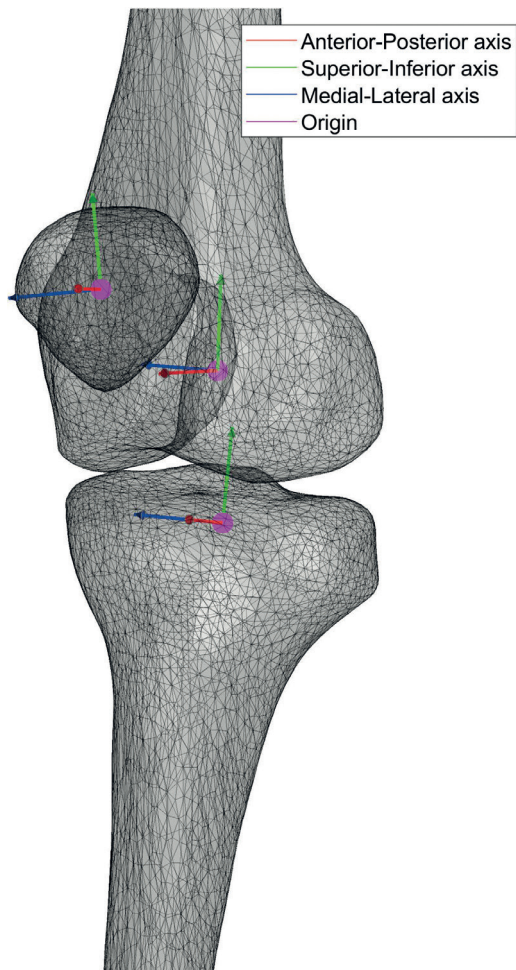
Figure 3. Coordinate system of femur, tibia and patella

The effect of anatomical variation on the knee joint coordinate system

To determine the effect of variation on the coordinate systems, first, the number of principal components (PCs) needed to describe 95% of the shape variation was determined for the femur, patella and tibia separately. By varying each of these isolated PCs from -2 to +2 standard deviations with increments of 0.2 standard deviations, while maintaining all others at zero, 21 shape instances per PC were created.

For each of the shape instances the coordinate system was calculated. The difference in orientation of the axes of the newly calculated coordinate system and that of the mean shape was determined and visualized per PC in a boxplot (Figure 5).

Changing the shape, and scaling in particular, also affects the location of the origin of the coordinate system. When comparing translations between patients, relative numbers

*or ratios should be used. However, this is not possible for rotations. For this reason only
rotations are considered in the current paper.*

Determination of the effect of anatomical variation on description of knee kinematics

The coordinate systems of the femur, patella and tibia were calculated for each of the 20
patients in the 4DCT dataset. The static meshes were then registered onto the dynamic
counterparts using a coherent point drift algorithm (Myronenko 2010). The rotations and
translations of this registration were saved and applied to the static coordinate system,
resulting in41 (the amount of time instances of the dynamic sequence) positions and
orientations of the coordinate system per 4DCT.

The maximal variations of the coordinate system that were found by varying the principal
components of the statistical shape model were then applied to a randomly chosen,
representative (static) coordinate system of the dynamic dataset. This was based on the
principal component showing the largest rotation and was done for both the maximal
negative rotation as the maximal positive rotation. The transformation superimposing
the static and dynamic meshes was applied to the normal and perturbed coordinate
systems to calculate their dynamic position and orientation. By calculating the angles
between the coordinate systems, the (perturbed) kinematics were calculated. The
angles between the 41 femoral, tibial, and patellar coordinate systems, were calculated
in the conventional order (flexion, internal -external rotation, ab-adduction)[19].

Results

SSM

The femoral and tibial model were considerably more compact than the patellar model.
Moreover, the first principal components of the femoral and tibial model described
a large amount of cumulative variation, whereas the variation in the patellar model
was distributed evenly over a larger number of PC's. Six, twenty two and six principal
components were required to describe 95% of the cumulative shape variation of the
femur, patella and tibia, respectively. Respectively, the corresponding generalizability
was 0.6, 0.9 and 0.4 mm.

For all models, the influence of the first principal component was the greatest, and
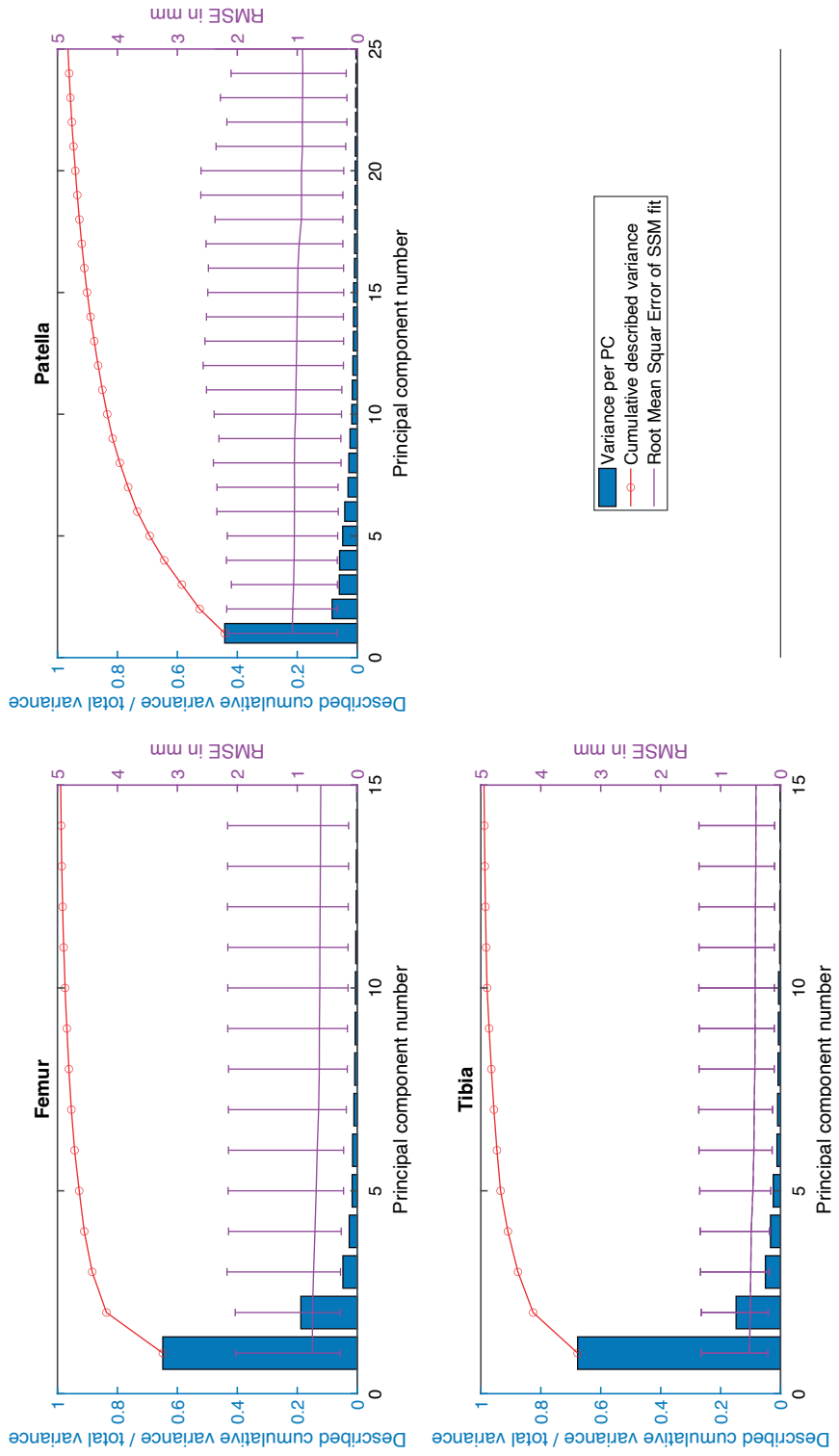comprised a scaling factor. The quality metrics of the SSM are visualized in figure 3.

Figure 4. Quality metrics of statistical shape models. Cumulative described variance (i.e. compactness) and the generalization ability of the Femur, Patellar and Tibial statistical shape model.

Influence on static coordinate system

The femoral and tibial coordinate system showed less sensitivity to common anatomical variation than the patellar coordinate system. Although higher order principal components described an ever decreasing degree of variation, the largest rotations of the coordinate systems were found in higher order pcs. The largest rotations of femur, patella and tibia were found in the 6th, 9th and 5th principal components, respectively. These principal components described approximately 2%, 3% and 3% of the total variation found in that particular model, respectively. The effects of isolated anatomical variation is visualized in figure 5, and the extremes of the rotations are depicted in Table 1.

Rotations								
Femur			Patella			Tibia		
AP	SI	ML	AP	SI	ML	AP	SI	ML
Max +	1.31˚	5.72˚	1.23˚	6.75˚	3.07˚	1.89˚	3.05˚	0.55˚	1.57˚
Max -	-1.11˚	-5.83˚	-1.14˚	-4.87˚	-2.82˚	-1.89˚	-1.62˚	-0.53˚	-1.45˚

Table 1. Overview of the largest rotations of the femur, patella and tibia coordinate system with respect to their counterpart calculated on the mean shape.

Rotation of the coordinate system

The largest rotation of the coordinate system of the femur was found around the SI-axis (-5.83° to 5.72°), corresponding to an internal/external rotational movement of the femur.

The rotation of the tibial coordinate system was largest around the AP axis (-1.61° to 3.05°), corresponding to ab/adduction movement of the tibia. The second largest rotation was around the ML axis (-1.45° to 1.57°), corresponding to a flexion-extension movement.

The largest rotations or the patellar coordinate system was around the AP axis (-4.87˚ to 6.75˚), corresponding to internal and external patellar rotation. The 2nd and 3rd largest rotation were around the SI- (-2.82˚ to 3.07˚) and ML- (-1.89˚ to 1.89˚) axis corresponding to patellar tilt and patellar flexion.
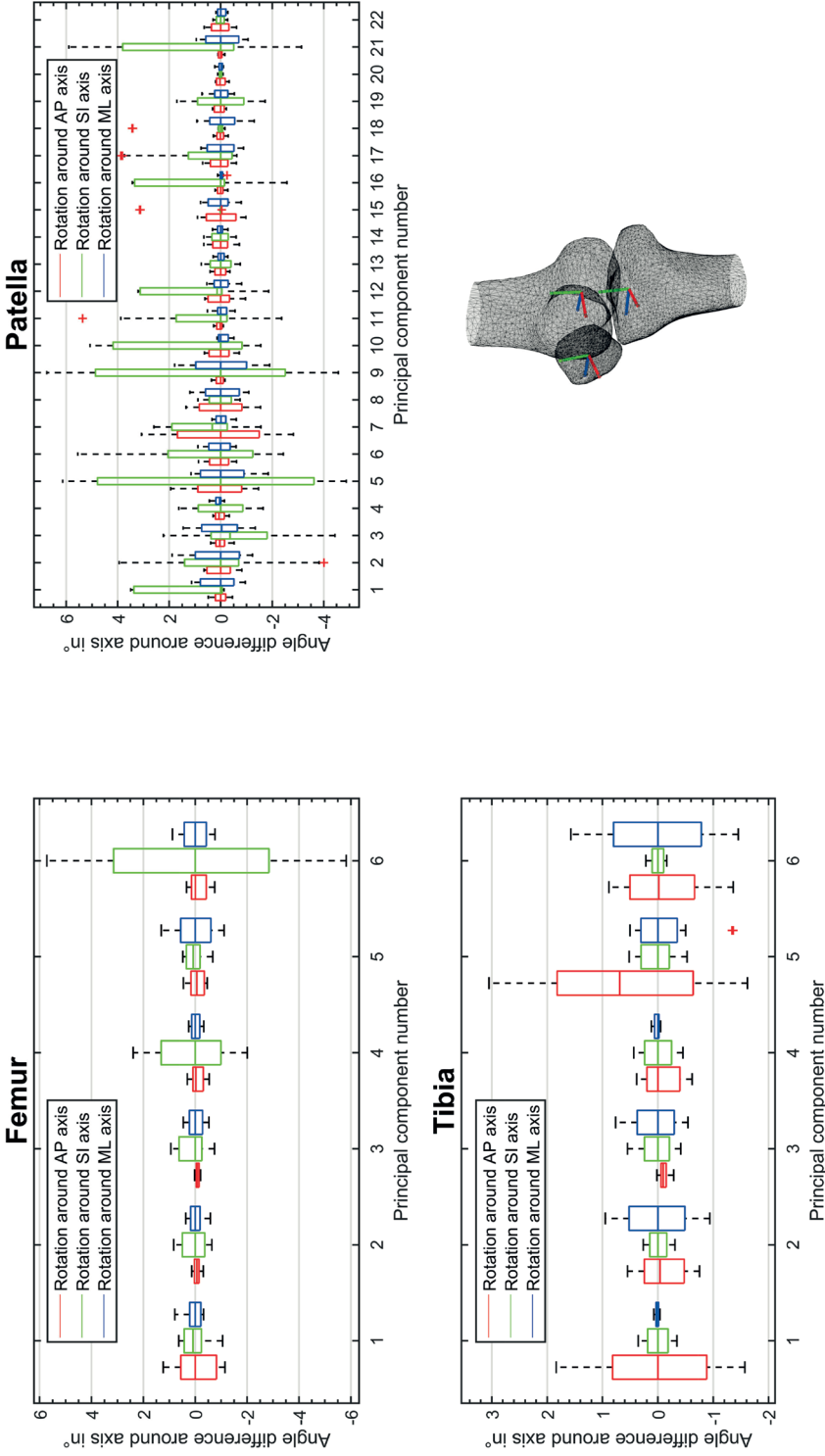
Figure 5. Visualisation of anatomical variation on the calculated femoral, tibial and patellar coordinate system. The figure shows the rotations of the coordinate system calculated on the perturbed anatomy of the corresponding principle component with respect to the coordinate system of the mean shape.

Influence on kinematic description

Rotations of the anatomical coordinate system due to anatomical differences caused variations in the calculation of tibiofemoral and patellofemoral kinematics. The description of the tibiofemoral flexion and internal/external rotation angle was relatively insensitive to the common variation of the coordinate system. Calculating kinematics with the perturbed coordinate system yielded an 'uncertainty' range of 2.52° and 1.09° respectively. Description of ab/adduction was influenced to a larger extent with a 5.01° bandwidth.

The description of patellofemoral kinematics were overall more influenced by common variations in the coordinate system. The flexion angle was the least affected and showed an average uncertainty of 3.53°, followed by the patellar tilt with an uncertainty of 6.65° degrees, and lastly the patellar rotation with an uncertainty of 13.48° degrees. Figure 6 shows the effects of calculating tibiofemoral and patellofemoral kinematics using a non-perturbed and perturbed coordinate system.
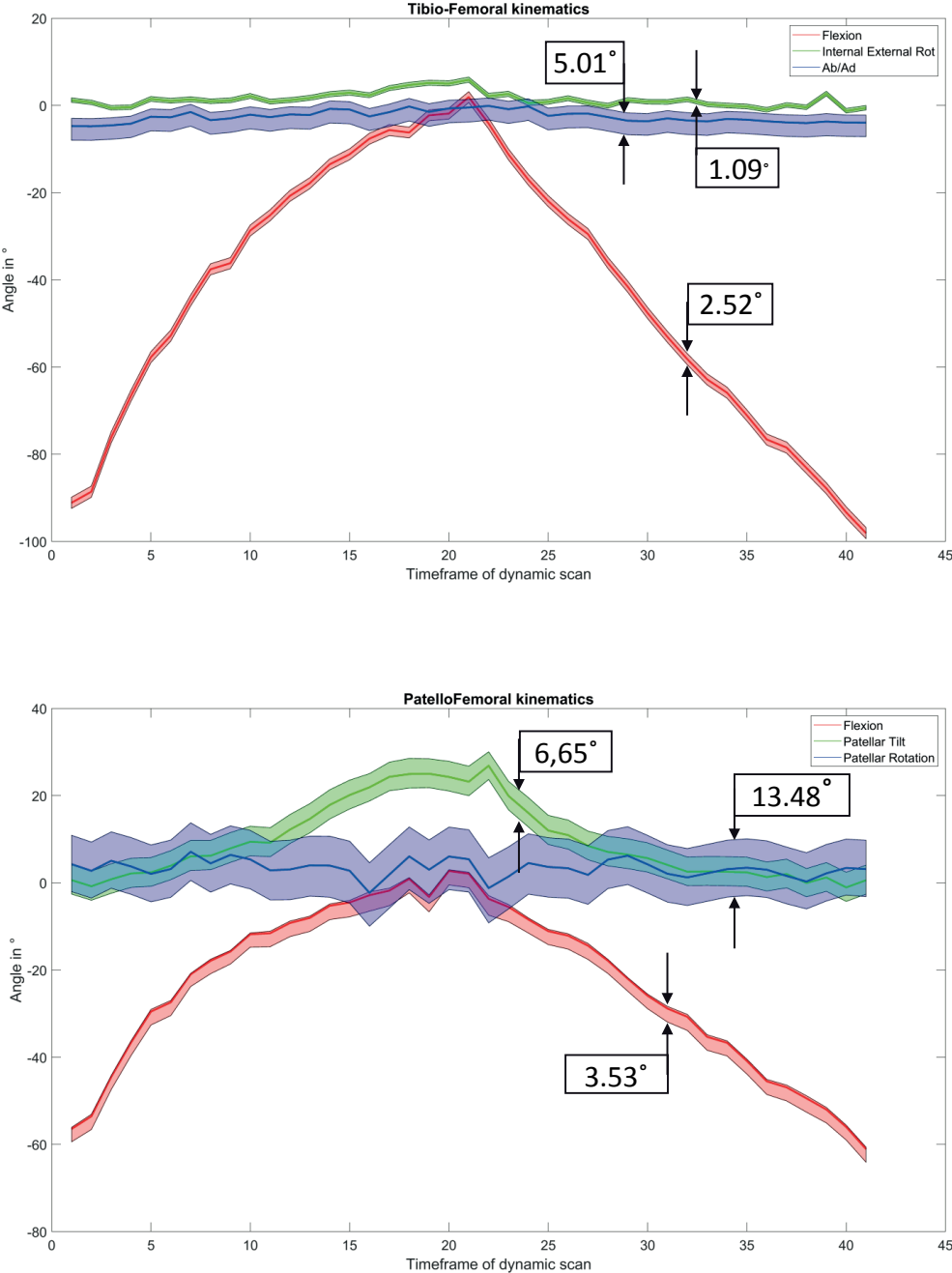
Figure 6. Tibiofemoral and Patellofemoral kinematics with a bandwidth for extremes of rotations found due to anatomical differences.

Discussion

The aim of the current study was to determine the sensitivity of an anatomical coordinate system of the knee to isolated variations in anatomy, and to determine its effect on the quantification of tibiofemoral and patellofemoral kinematics. Our findings suggest that calculation of the tibiofemoral flexion, ab/adduction and internal/external rotation angles calculated with the described anatomical coordinate system is relatively insensitive to anatomical variations found in a population. To our knowledge, this is the first article that links anatomical variation directly to variations in knee kinematics.

The femoral coordinate system showed the largest rotation around the SI axis (- 5.83˚ to 5.72˚) in the 6th principal component, which translates to an internal-external rotation movement. The 6th principal component of the model influenced the femoral rotation. In cases where a severe femoral anteversion is seen, the effect on the description of patellofemoral kinematics should therefore be taken into account.

The largest rotations found in the tibia coordinate system were found to be around the AP and ML axis, which showed considerable variation (AP -1.62˚ to 3.05˚, ML -1.45˚ to 1.57˚). These results are in line with literature (Quintens et al. 2019), which show that the tibial plateau is subject to the largest variation found in the tibia. The tibial variation is reflected in the tibiofemoral kinematics in figure 6, which showed an uncertainty of ±5.01˚ and 1.09˚ and 2.52˚ in the description of ab-adduction, internal-external rotation and flexion angle, respectively of the tibia with respect to the femur. The rotations found for the tibial and femoral coordinate system were in the same range as calculated in the paper by Miranda et al. even though it was calculated on a more diverse range of knee shapes.

The maximum bandwidth of the tibiofemoral kinematics is 5.01 degrees. Considering the wide range of created shapes from -2 to +2, the tibiofemoral axis system can be considered robust and accurate. This accuracy is a meaningful outcome as it affects patellofemoral kinematics, which is often plotted against the tibiofemoral flexion angle. In addition, it offers the possibility to use the tibiofemoral angles for the interpolation of patellofemoral kinematics between two different timeframes of the dynamic dataset, possibly offering new insights and possibilities for better inter-subject comparison.

The patellar coordinate system was more sensitive to anatomical variation, and hence, the description of patellofemoral kinematics showed larger uncertainty, in line with literature[8]. From Figure 5 we can conclude that shape variation of the patella was spread out over a larger number of principal components. This underlines that the patella does not have the distinct landmarks required for a robust coordinate system. This was

also reflected in the description of patellofemoral kinematics (figure 6), where a large uncertainty in patellar tilt and foremost patellar rotation was observed. Description of these parameters is largely influenced by the patellar anatomy. The significant uncertainty in the description of patellar rotation can be accredited to the large variation of the inferior pole of the patella. Although here again, the extreme variation has been applied to determine the kinematic uncertainty, and it is likely to be smaller in practice, this must be taken into account when attempting inter-subject comparison. The high variation of the patella raises the question whether it is possible to calculate a patellar coordinate system that is robust enough to allow accurate inter-subject comparison of rotation, tilt and flexion.

It is difficult to compare the results of the current study with those from the literature, due to differences in coordinate system definitions. Morton et al. investigated to what extent a landmark-based coordinate system changes as a result of variations in landmark placement[12]. Similar to the present study, their research showed tibiofemoral kinematics is more robust to changes in landmarks than patellofemoral kinematics. In addition, as in the present study, the tibiofemoral flexion angle was most robust. Interestingly, the order of the axes that showed most of the rotations is different, which may be due to differences in the definition of the coordinate system.

To our knowledge this is the first study that quantifies the sensitivity of an anatomical coordinate system to anatomical variation. The main strengths of this study are the parameterization of anatomical variation using an SSM, and the use of dynamic CT data for the calculation of knee kinematics. Results from this study can be used to define an accurate and unified description of tibiofemoral and patellofemoral kinematics that allows for discrimination between anatomical and pathological effects on joint movement.

Several limitations should be noted. The first limitation relates to the data that was used for generating the SSM. The RMS error of the SSM is comparable to those found in literature. However, the data that was used to create the SSM was not exhaustive. There may be differences in knee anatomy between people of different ethnicities[21,22]. Adding more and/or diverse data would allow for a better generalization ability, and would more accurately describe all shape variations found in the population. In the current study, the maximum rotations found were used. However, as the box plots show, the majority of the rotations was smaller. Therefore, it is not expected that extending the data set will have a substantial impact on the outcome of this study.

The second limitation relates to the generation of shape instances used for sensitivity analysis of the coordinate system. A typical shape found in a population is a linear

combination of eigenvalues for the principal component that is added to the mean shape. Varying a single PC from -2SD to +2SD while maintaining all others at zero creates a shape instance that is unlikely to exist in reality. The current approach, however, allowed us to assess which specific anatomical variation caused a rotation of the coordinate system.

A third limitation of this study is that the SSMs did not include the relation between the three separate models (i.e. femur, patella, and tibia). Information on congruency of the femur, tibia and patella were therefore lost in the process. Consequently, it was not possible to investigate mutual relationships in form, and to what extent they have a strengthening or cancelling effect on the bandwidth found in the kinematic descriptions.

Lastly, a single coordinate system was evaluated. The way a coordinate system is calculated obviously has an effect on its sensitivity for anatomical variation. The strength of the used coordinate system is that it is based the articulating surfaces and is widely used in literature. As the maximal rotations that were found were applied to a single representative kinematic measurement, it is not an exhaustive description of the possible 'bandwidth' of kinematic measurements of a larger population. However it does provide insight in the expected effect on the kinematic description of the knee joint.

Understanding the impact of surgical interventions on joint biomechanics is important to improve surgical techniques and outcomes. It is difficult to determine the accuracy required for a successful intervention. However, as state of the art surgical navigation allows surgeons to perform surgery with an accuracy within 1mm and 1°, the evaluation of outcomes requires the same accuracy or better. Our results show that possible variation in kinematic measurement as a result of anatomical variation in a population is possibly larger.

In conclusion, the description of both tibiofemoral and patellofemoral kinematics is influenced by anatomical variation. While tibiofemoral kinematic description is insensitive to anatomical variation (<5.01˚ variation), anatomical variation of the patella combined with the lack of distinct features complicate a general, unified coordinate system for the patella. The present study demonstrates the extent of uncertainty that can be expected when describing tibiofemoral and patellofemoral kinematics of a population, and to what extent meaningful comparisons can be made.

References

1. Kwong Y, Mel AO, Wheeler G, Troupis JM. Four-dimensional computed tomography (4DCT): A review of the current status and applications. J Med Imaging Radiat Oncol 2015;59:545–54. https://doi.org/10.1111/1754-9485.12326.

2. Woltring HJ, Huiskes R, de Lange A, Veldpaus FE. Finite centroid and helical axis estimation from noisy landmark measurements in the study of human joint kinematics. J Biomech 1985;18:379–89. https://doi.org/10.1016/0021-9290(85)90293-3.

3. Blankevoort L, Huiskes R, de Lange A. Helical axes of passive knee joint motions. J Biomech 1990;23:1219–29. https://doi.org/10.1016/0021-9290(90)90379-H.

4. Reichl I, Ongaro M. Finite helical axis versus symmetrical axis of rotation approach for the human knee joint: squats, rowing and cycling. Comput Methods Biomech Biomed Engin 2013;16:109–11. https://doi.org/10.1080/10255842.2013.815943.

5. Sheehan FT. The finite helical axis of the knee joint (a non-invasive in vivo study using fast-PC MRI). J Biomech 2007;40:1038–47. https://doi.org/10.1016/j.jbiomech.2006.04.006.

6. Cui X, Kim H, Li S, Kwack K-S, Min B-H. Extraction of anatomical landmarks and axis for 3D coordinate system construction of femur and tibia bone models. Osteoarthr Cartil 2015;23:A246–8. https://doi.org/10.1016/j.joca.2015.02.454.

7. Miranda DL, Rainbow MJ, Leventhal EL, Crisco JJ, Fleming BC. Automatic determination of anatomical coordinate systems for three-dimensional bone models of the isolated human knee. J Biomech 2010;43:1623–6. https://doi.org/10.1016/j.jbiomech.2010.01.036.

8. Renault JB, Aüllo-Rasser G, Donnez M, Parratte S, Chabrand P. Articular-surface-based automatic anatomical coordinate systems for the knee bones. J Biomech 2018;80:171–8. https://doi.org/10.1016/j.jbiomech.2018.08.028.

9. Marin F, Claes L, Sattelmayer G, Mannel H, Dürselen L, Mohr M, et al. Finite helical axes of motion are a useful tool to describe the three-dimensional in vitro kinematics of the intact, injured and stabilised spine. Eur Spine J 2004;13:553–9. https://doi.org/10.1007/s00586-004-0710-8._

10. Lenz NM, Mane A, Maletsky LP, Morton NA. The effects of femoral fixed body coordinate system definition on knee kinematic description. J Biomech Eng 2008;130:1–7. https://doi.org/10.1115/1.2898713.

11. Kedgley AE, McWalter EJ, Wilson DR. The effect of coordinate system variation on in vivo patellofemoral kinematic measures. Knee 2015;22:88–94. https://doi.org/10.1016/j.knee.2014.11.006.

12. Morton NA, Maletsky LP, Pal S, Laz PJ. Effect of Variability in Anatomical Landmark Location on Knee Kinematic Description. J Orthop Res 2007;9. https://doi.org/ 10.1002/jor.20396

13. Li X, Chen H, Qi X, Dou Q, Fu CW, Heng PA. H-DenseUNet: Hybrid Densely Connected UNet for Liver and Tumor Segmentation from CT Volumes. IEEE Trans Med Imaging 2018;37:2663–74. https://doi.org/10.1109/TMI.2018.2845918.

14. Myronenko A. Point Set Registration: Coherent Point Drift. IEEE Trans Pattern Anal Mach Intell 2010;32:2262–75. https://doi.org/10.1109/TPAMI.2010.46.

15. Van Dijck C, Wirix-Speetjens R, Jonkers I, Vander Sloten J. Statistical shape model-based prediction of tibiofemoral cartilage. Comput Methods Biomech Biomed Engin 2018;21:568–78. https://doi.org/10.1080/10255842.2018.1495711.

16. Clogenson M, Duff JM, Luethi M, Levivier M, Meuli R, Baur C, et al. A statistical shape model of the human second cervical vertebra. Int J Comput Assist Radiol Surg 2014;10:1097–107. https://doi.org/10.1007/s11548-014-1121-x.

17. Lu YC, Untaroiu CD. Statistical shape analysis of clavicular cortical bone with applications to the development of mean and boundary shape models. Comput Methods Programs Biomed 2013;111:613–28. https://doi.org/10.1016/j.cmpb.2013.05.017.

18. Chen H, Kluijtmans L, Bakker M, Dunning H, Kang Y, De S Van, et al. A robust and semi-automatic quantitative measurement of patellofemoral instability based on four dimensional computed. Med Eng Phys 2020;78:29–38. https://doi.org/10.1016/j.medengphy.2020.01.012.

19. Grood ES, Suntay WJ. A joint coordinate system for the clinical description of three-dimensional motions: Application to the knee. J Biomech Eng 1983;105:136–44. https://doi.org/10.1115/1.3138397.

20. Quintens L, Herteleer M, Vancleef S, Carette Y, Duflou J, Nijs S, et al. Anatomical Variation of the Tibia – a Principal Component Analysis. Sci Rep 2019;9:1–10. https://doi.org/10.1038/s41598-019-44092-8.

21. Mahfouz M, Fatah EEHA, Bowers LS, Scuderi G. Three-dimensional morphology of the knee reveals ethnic differences. Clin Orthop Relat Res 2012;470:172–85. https://doi.org/10.1007/s11999-011-2089-2.

22. Kim TK, Phillips M, Bhandari M, Watson J, Malhotra R. What Differences in Morphologic Features of the Knee Exist Among Patients of Various Races? A Systematic Review. Clin Orthop Relat Res 2017;475:170–82. https://doi.org/10.1007/s11999-016-5097-4.

2

Chapter 3

Alignment deviations between the longitudinal axis of the CT scanner and femur lead to substantial changes in TT-TG distance

H.Dunning, H. Chen, S.A.W. van de Groes, N.Verdonschot, D. Janssen

Abstract

Background: The TT-TG distance is a commonly used measure to distinguish between healthy and pathological lateral insertion of the patellar tendon on the tibia. Previous studies have reported on sensitivities of the TT-TG distance measurement to patient orientation in the scanner. The aim of this study was to determine the effect of differences in alignment of the femoral SI axis and the longitudinal axis of the CT scanner in the coronal plane (Scanner Femur Angle) on the TT-TG distance.

Methods: One-hundred healthy subjects between 18-35 years underwent a CT scan of both knees. Calculation of the TT-TG distance was automated to ensure reproducibility. The SFA of both knees of all subjects was determined. SFA's of -7° to 7° were simulated, to simulate different orientations of the subject in the scanner. The effect of orientation on the TT-TG distance was calculated.

Results: Image data of 97 healthy subjects were included. The mean TT-TG distance in scanned orientation was 13.28±3.76mm. The mean TT-TG distance was 12.49±3.85mm. The mean SFA was 1.02±2.23°. Simulating changes the SFA resulted in changes in the measured TT-TG distance. For every degree of change in SFA, a change of approximately 1mm in TT-TG distances was observed.

Conclusion: The TT-TG distance is sensitive to changes in the SFA. The prevalence of SFA's unequal to zero and poor recognition on the axial views on which the TT-TG is measured, suggest that errors that complicate intra- and intersubject comparison of the TT-TG distance, are easily introduced.

Introduction

Patellofemoral instability is a knee disorder characterized by (partial) dislocations of the patella from the femoral trochlear groove. Patellofemoral instability is a result of an imbalance in forces that guide the patella to and through the trochlear groove during motion[8]. *During knee flexion* instability include trochlear dysplasia, excessive patellar tilt, lateral or proximal insertion of the patellar tendon on the tibia and valgus malalignment[13].

During knee flexion, the quadriceps muscle exerts force on the patellofemoral joint, transmitting that force through the patellar center and patellar tendon to the tibia[4]. A lateral insertion of the patella tendon on the tibia causes a lateralizing force on the patella. When this force becomes too large, the patella can (sub)luxate.

The lateral insertion of the patellar tendon is commonly quantified with the Tibial Tuberosity – Trochlear Groove (TT-TG) distance, which was widely introduced by Dejour et al[2]. The purpose of the TT-TG distance is to quantify the lateral pull of the patellar tendon on the patella. The TTTG distance has absolute cut-off values to assess clinical pathology. Distances below 15mm are considered normal, between 15-20mm are considered threshold values, and TT-TG larger than 20 is considered too large[6]. For patients with a TT-TG distance larger than 20mm, surgical treatment is considered to medialize the insertion of the patellar tendon, and to restore physiological patellar tracking.

The TT-TG distance is commonly measured on MRI or CT images of the subject in passive supine position. On the axial slices, the slices containing the Tibial Tuberosity (TT) and the Trochlear Groove (TG) are selected and superimposed. The TT and TG points are selected and on the TG slice the Posterior Condylar Line (PCL) is drawn. The distance between the TT and TG parallel to the PCL is the TT-TG distance.

Several publications reported on the effect of patient orientation and pose in the scanner on the TT-TG distance measurement. For example, Tanaka and Saomalainen et al. have shown that the TT-TG decreases with increasing flexion angle[9,11]. This effect was most pronounced in the first 30° of flexion, where the tibia internally rotates with respect to the femur as a result of the screw home mechanism. The screw home mechanism causes a lateral translation of the TT, decreasing the TT-TG distance.

Furthermore, Yao et al. reported on the influence of axial slice orientation on the TT-TG measurement[14]. This paper concluded that in a routine MRI scan up to 5° of abduction/adduction of the femur with respect to the longitudinal axis (z-axis) of the scanner can be

expected, changing the axial slice direction and causing changes in TT-TG measurement approaching 40% of the total measurement. While multiplanar reconstruction (MPR) is able to negate the effect of ab/adduction on the axial slice orientation, this is rarely used in practice.

In a comprehensive meta-analysis, Tan et al. concluded that there were significant differences between the TT-TG distance measured on MRI versus CT[10]. When compared, TT-TG distances measured on CT were significantly larger than those measured on MRI. Furthermore, Ho et al. reported systematic technique dependent differences between CT and MRI[5]. As a result, measurements of the TT-TG distance based on CT and MRI do not seem to be interchangeable.

Visually aligning subjects' legs with the longitudinal axis of the CT scanner as during a routine CT scan, may therefore not provide sufficient standardisation, and may cause differences in measured TT-TG distances that are related to patient positioning rather than a lateral insertion of the patellar tendon. The TT-TG measurement continues to have an important role in distinguishing healthy and pathological insertion of the patellar tendon, and thus affects clinical decision making. It is vital to understand the effect of patient positioning inside the CT scanner on the TT-TG measurement to avoid under- or over-treatment of patients.

The aim of this study is therefore twofold: 1) to determine the extent of differences in the orientation of the SI axis of the femur with respect to the longitudinal (z-axis) of the CT scanner in the coronal plane during a routine CT scan 2) to calculate the effect of this orientation on the TT-TG measurement.

Materials & Methods

Institutional approval was obtained to perform a CT scan on 100 healthy volunteers. One-hundred subjects between the age of 18-35 years, without knee disorders, prior trauma or surgery to the knee, were recruited between 2020 and 2021 as part of an ongoing imaging study. Exclusion criteria were functional- or congenital disorders and diagnosed valgus malalignment. All participants signed an informed consent form prior to participating.

All subjects underwent a high-resolution CT scan (voxel size 0.71x0.71x0.80mm) using the Canon Aquilion One CT scanner. The subject was positioned as during a routine CT scan of the knees; both legs in full extension and with feet pointing up while both legs were visually aligned with the longitudinal (z-axis) of the CT scanner. Data was pseudonymized and the left and right femur, patella, tibia and patellar tendon of all

subjects were segmented using a deep learning network[7]. Segmentation masks were transformed into 3D surface meshes with MATLAB, which were remeshed and smoothed to improve mesh quality[12].

In order to determine to what extent there are differences in the orientation of the SI axis of the femur with respect to the longitudinal (z-axis) of the CT scanner in the coronal plane during a routine CT scan (hereinafter referred to as the Scanner Femur Angle or SFA), coordinate systems for the femur, patella and tibia were calculated. All coordinate systems consisted of a Superior-Inferior (SI), Anterior-Posterior (PD), Medial-Lateral (ML) axis and a coordinate system origin. The calculated femoral SI axis resembles the femoral mechanical axis. A detailed description of the calculation of the coordinate systems can be found in a previously published articles[1,3].

The SFA was calculated for the left and right femur of all subjects, and the mean and standard deviation of the SFA were determined.

Landmarks
To ensure consistency of the measurement, calculation of the TT-TG distance was automated. Therefore the 3D coordinates of the trochlear groove, tibial tuberosity and posterior condylar line were calculated, using a MATLAB algorithm. A detailed description of the landmark calculation, and how they compare to manually selected landmarks, can be found in previously published work[1,3]. The position of the automatically determined landmarks was visually checked by the first author and adjusted if necessary.

To calculate the effect of the SFA on the TT-TG measurement, the femur was first fully aligned with the CT scanner, by respectively aligning the posterior condylar line, femoral AP axis, and femoral SI axis with the x (horizontal) ,y (vertical) and z (longitudinal) axis of the CT scanner. The spatial relationship between the femur, tibia and all landmarks was maintained by applying the same transformation to all structures. The TT-TG distance in this 'neutral' orientation was calculated for all subjects as the difference between the TT and TG along the PCL, and the mean and standard deviation was calculated.

The difference between the TT-TG distance of the left and right knee was calculated in the scanner orientation and in the neutral orientation, to reveal if alignment causes interpersonal differences.

Yao et al. reported a mean SFA of 5°±2.3° in routine MRI scans[14]. Therefore a SFA of -7° to +7° was simulated with 1° increments, with respect to the neutral orientation. This is equivalent to a 7° adduction to 7°abduction orientation of the femur with respect to the longitudinal axis of the scanner. Again, the spatial relations between all structures were

maintained. Figure 1 shows an overview of the femur in neutral orientation, SFA = -7°, SFA = 7° and visualizes the effect on the TT-TG distance. The axial slices corresponding to these orientations are shown below the figure.

As by definition the PCL is always in the same axial slice as the TG, the changing axial slice direction required recalculating the PCL. Therefore, for every orientation in the -7° to 7° range, the new PCL and the TT-TG distance along that line were calculated.
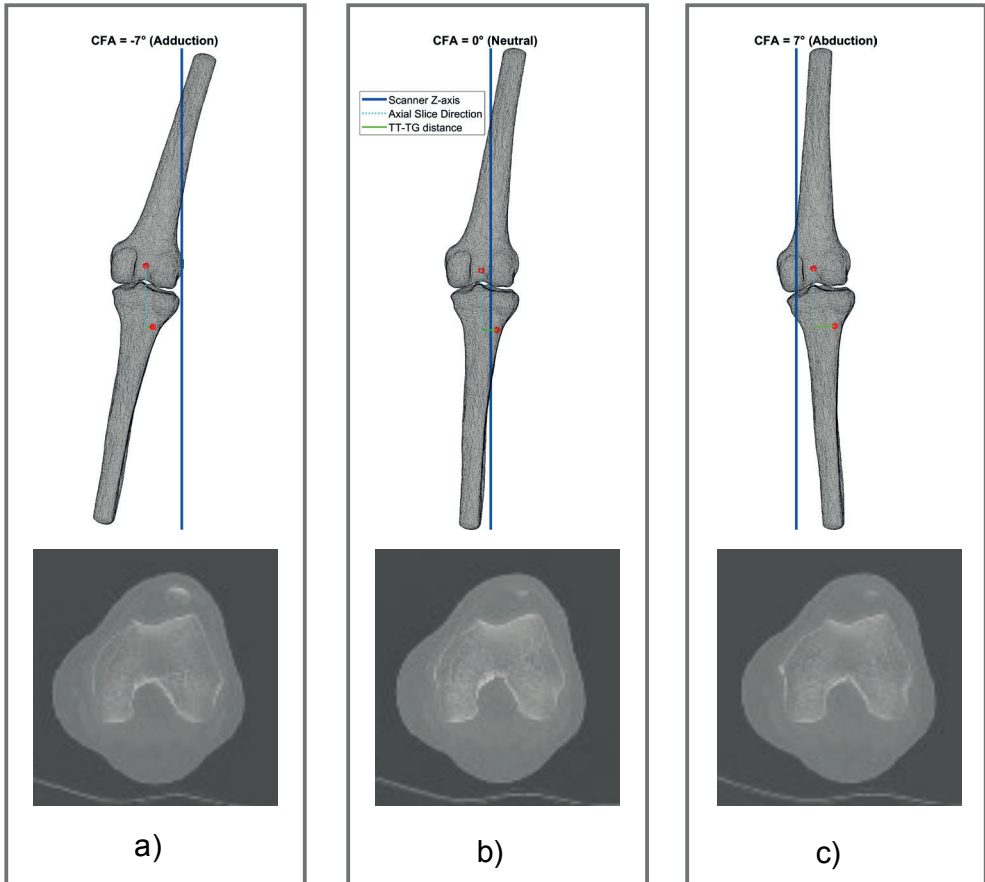
Figure 1. An overview of the different orientations of the femur with respect to the scanner z- axis (blue) and theircorresponding axial slices. The cyan line is parallel to the scanner z-axis and drawn from the TG point to the TT point. The green line is the TT-TG distance. a) The orientation where the SFA = -7° corresponding to an adducted leg. b) The neutral orientation where SFA = 0° and the femur SI axis is fully aligned with the scanner z-axis. c) The orientation where the SFA = +7° corresponding to an abducted leg.

Results

One hundred healthy volunteers were successfully recruited, of which 71 were female and 29 were male. The mean age was 24±3.36 years and all subjects were between 18-35 years old.

Image data of three volunteers showed significant image artifacts and were excluded from further analysis. The remaining data of 97 volunteers was successfully segmented with the deep learning network.

The TG, TT and PCL landmarks were calculated and visual inspection of the position of automatically calculated landmarks did not reveal anomalies. The mean TT-TG distance in scanned orientation was 13.28±3.76mm. All knees were rotated to the neutral orientation and the mean TT-TG distance in neutral orientation was 12.49±3.85mm.

The femur SI axis was never fully aligned with the z-axis of the CT scanner. The mean and standard deviation of the SFA was 1.02±2.23° (range -5.88° to 6.62°) for the left femur and 1.07±2.21° (range -6.17° to 4.96° for the right femur). The mean and standard deviation of the sum of left and right SFA was -0.05°±2.28°.

Simulating changes in the SFA resulted in changes of the measured TT-TG distance. For every degree of change in SFA, a change of approximately 1mm in TT-TG distances was observed. Figure 2 shows the mean change and a trendline of the TT-TG distance for every degree SFA for all knees.
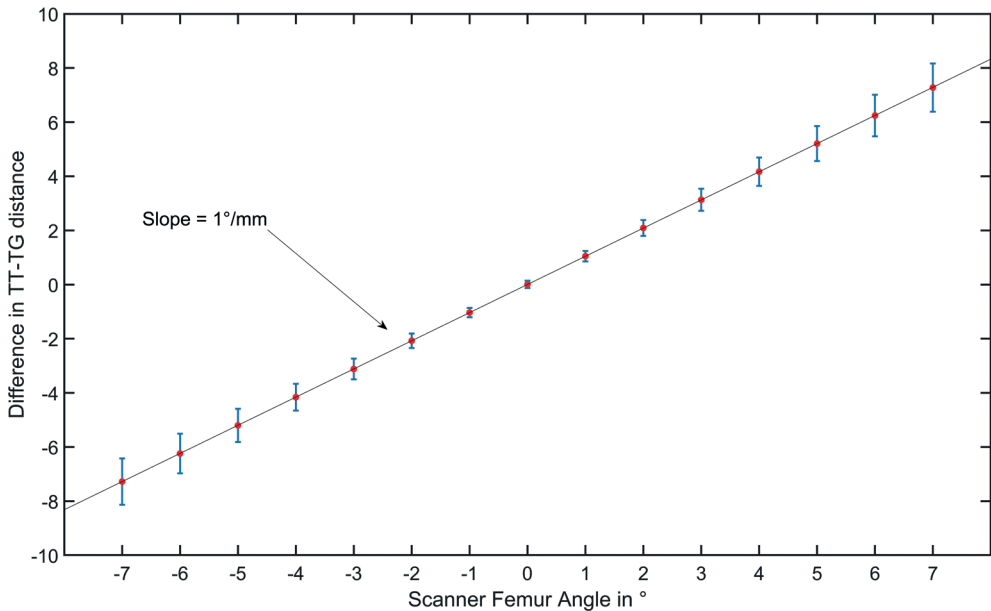
3

Figure 2. A visual representation of the amount of change in TT-TG distance due to altered SFA.

Discussion

The TT-TG distance has an important role in distinguishing healthy and pathological insertion of the patellar tendon, and therefore affects clinical decision making. Previous studies have reported on sensitivities of the TT-TG distance measurement to patient orientation and pose in the CT and MRI scanner and that TT-TG measurements performed on MRI and CT images are not interchangeable. Although it is technically possible to correct any alignment issues after image acquisition using Multiplanar Reconstruction (MPR), this rarely happens in practice. The aim of this study was to determine the effect of differences in orientation of the SI axis of the femur and the longitudinal axis of the CT scanner or scanner femur angle, on the TT-TG measurement and to establish the mean SFA during a routine CT.

The key findings of this study are that the TT-TG distance measurement changes considerably if the SFA changes and that in many cases there is a substantial SFA. Figure 2 shows that for every degree change in SFA the TT-TG distance changes with approximately one millimeter. While the trend in the current data is similar to reported by Yao et al. (0.68mm/1° vs 1mm/1°), the absolute numbers are different[14]. This is to be expected as measurements performed on MRI and CT are not interchangeable, and TT-TG distances measured on CT are significantly larger as a result of systematic differences in techniques[5,10].

The effects as a result of SFA appear larger (~0.29mm/1° vs. 1mm/1°, respectively) than the effect of flexion on the TT-TG distance described in literature[9]. This can possibly be explained by the fact that a pure flexion rotation has no effect on the mediolateral position of the TT or TG, but the change in TT-TG distance is likely caused by internal/external rotation of the tibia in the first degrees of flexion. However, changes in TT-TG due to slight flexion or ab/adduction can likely co-exist and complement each other, resulting in even larger variability.

The mean SFA was 1.94°±1.49° and the maximum of 6.62°, while the sum of the SFA of the left and right femur was 0.05°±2.28°. This indicates that while the patient as a whole is generally aligned with the scanner z-axis, both femora are not. Furthermore, what becomes apparent from the axial views in figure 1, is that deviations in SFA of this magnitude (-7° to 7°) are hardly recognizable on the axial slices of the femur on which the measurement is performed. The combination of the significant effect of SFA on the TT-TG distance, the prevalence of SFA's unequal to zero and poor recognition on the axial views on which the TT-TG is measured, indicate that there may be substantial differences of the measured TT-TG distance that are the result of patient orientation rather than lateral insertion of the patellar tendon.

Furthermore, although the sum of left and right SFA is centered around zero, the standard deviation is substantial (2.2816°). This may cause differences in TT-TG distance between the left and right knee. For this reason, caution is required when using the contralateral side as a guide during treatment of patients with patellar maltracking, for example for planning a tibial tubercle osteotomy.

The change in TT-TG measurement as a result of SFA can be partly explained by trigonometry: an increased SFA will cause an increased TT-TG distance. As the posterior condylar line changes as a result of the rotation and cylindrical form of the femoral condyles this effect might be enhanced or negated.

It is important to note that the choice of aligning the femoral SI axis with the scanner z-axis, rather than for example the tibial SI axis, was made for practical reasons and was considered the best method of conveying the importance of alignment. This study did not investigate whether this is the most effective way, and using the tibia alignment likely produces similar results. It may therefore not matter which structure is aligned, as long as it is done consistently.

Several limitations of the current study should be noted. Firstly, simulations were used in this study to investigate the effects of malalignment, rather than repeated CT scans with the aim to limit radiation exposure of participants. Unforeseen effects may

therefore not have been taken into account. However, the accuracy of rotations as in the present study cannot be imitated in an imaging study. No substantial differences in results between the effects of virtually relative to actual rotations are to be expected.

Secondly, this study was conducted on healthy subjects. The results of this study may therefore not be directly translatable to patients with patellofemoral instability, who may have a non-standard anatomy. However, this study indicates that TT-TG values are influenced by changes in SFA; it is highly likely that these differences are similar in healthy and pathological patient cohorts.

This paper showed that the TT-TG measurement is highly sensitive to the SFA and stresses the importance of consistent alignment for reproducible TT-TG distance measurements. Due to physiological knee angles and poor visibility of alignment during the scan, alignment of both limbs with the scanner during scanning is challenging. It is therefore obvious to do this during post-processing, ideally using an automatically calculated anatomical coordinate system. This results in a TT-TG quantification that is consistent and performed in an objective, reproducible manner allowing more accurate intra- and intersubject comparison. As there is currently no widely accepted and available method to align the knee during scanning, the orthopaedic community should be aware of this sensitivity and, where possible, apply manual correction through interpolation to minimise differences.

References

1. Chen H, Kluijtmans L, Bakker M, et al. A robust and semi-automatic quantitative measurement of patellofemoral instability based on four dimensional computed. *Med Eng Phys*. 2020;78:29-38.

2. Dejour H, Walch G, Nove-Josserand L, Guier C. Factors of patellar instability: An anatomic radiographic study. *Knee Surgery, Sport Traumatol Arthrosc*. 1994;2(1):19-26.

3. Dunning H, van de Groes SAW, Verdonschot N, Buckens CF, Janssen D. The sensitivity of an anatomical coordinate system to anatomical variation and its effect on the description of knee kinematics as obtained from dynamic CT imaging. *Med Eng Phys*. 2022;102(January):103781.

4. Herrington L, Nester C. Q-angle undervalued? The relationship between Q-angle and medio-lateral position of the patella. *Clin Biomech*. 2004;19(10):1070-1073.

5. Ho CP, James EW, Surowiec RK, et al. Systematic technique-dependent differences in CT versus MRI measurement of the tibial tubercle-trochlear groove distance. *Am J Sports Med*. 2015;43(3):675-682.

6. Krishnan H, Eldridge JD, Clark D, Metcalfe AJ, Stevens JM, Mandalia V. Tibial tuberosity-trochlear groove distance: does it measure up? *Bone Jt Open*. 2022;3(3):268-274.

7. Li X, Chen H, Qi X, Dou Q, Fu CW, Heng PA. H-DenseUNet: Hybrid Densely Connected UNet for Liver and Tumor Segmentation from CT Volumes. *IEEE Trans Med Imaging*. 2018;37(12):2663-2674.

8. Post WR, Fithian DC. Patellofemoral Instability: A Consensus Statement From the AOSSM/PFF Patellofemoral Instability Workshop. *Orthop J Sport Med*. 2018;6(1):1-5.

9. Suomalainen JS, Regalado G, Joukainen A, et al. Effects of knee flexion and extension on the tibial tuberosity–trochlear groove (TT–TG) distance in adolescents. *J Exp Orthop*. 2018;5(1):1-6.

10. Tan SHS, Lim BY, Chng KSJ, et al. The Difference between Computed Tomography and Magnetic Resonance Imaging Measurements of Tibial Tubercle-Trochlear Groove Distance for Patients with or without Patellofemoral Instability: A Systematic Review and Meta-analysis. *J Knee Surg*. 2020;33(8):768-776.

11. Tanaka MJ, Elias JJ, Williams AA, Carrino JA, Cosgarea AJ. Correlation between Changes in Tibial Tuberosity-Trochlear Groove Distance and Patellar Position during Active Knee Extension on Dynamic Kinematic Computed Tomographic Imaging. *Arthrosc - J Arthrosc Relat Surg*. 2015;31(9):1748-1755.

12. Tran AP, Yan S, Fang Q. Improving model-based functional near-infrared spectroscopy analysis using mesh-based anatomical and light-transport models. *Neurophotonics*. 2020;7(01):1.

13. Varatojo R (2010) Clinical Presentation of Patellofemoral Disorders. Patellofemoral Pain, Instab Arthritis Springer Berlin Heidelberg, Berlin, Heidelberg, pp 35–39

14. Yao L, Gai N, Boutin RD. Axial scan orientation and the tibial tubercle-trochlear groove distance: Error analysis and correction. *Am J Roentgenol*. 2014;202(6):1291-1296.

3

Chapter 4

The symmetry of the Left and Right Tibial Plateau; a Comparison of 200 Tibial Plateaus

N. van der Gaast, H. Dunning, J.M. Huitema, A. Waters, R.L. Jaarsma, J.N. Doornberg, M.J.R. Edwards, S.A.W. van de Groes, E. Hermans

Abstract

Introduction: The tibial plateau is one of the crucial weight-bearing areas of the body. Fractures of the tibial plateau are intra-articular and therefore often technically challenging to treat. This study aims to investigate the symmetry of the left and right tibial plateau in young healthy individuals to determine whether left-right mirroring can be reliably used to optimize preoperative 3D virtual planning for patients with tibial plateau fractures.

Methods: One hundred healthy subjects, without previous knee surgery, severe knee trauma, or signs of osteoarthritis were included for a previous dynamic imaging study of the knee. The subjects underwent a CT scan, scanning the left and right knee with a slice thickness of 0.8mm. 3D surface models of the femur, patella, and tibia were created using a convolutional neural network. The 3D models of the left and right tibias were exported to MATLAB © and the tibias were mirrored. The mirrored tibias were superimposed on the contralateral tibia using a coherent point drift surface matching algorithm. Correspondence points on both surfaces were established, the mean root squared distance was calculated and visualized in a boxplot and heatmaps.

Results: The overall mean difference between correspondence points on the left and right tibial plateau is 0.6276mm ± 0.0343mm. The greatest differences between correspondence points were seen around two specific surfaces on the outside the tibial plateau; where the distal tibia was cut 15mm below the tibial plateau and around the tibiofibular joint.

Conclusion: The differences between the left and right tibial plateau are small and therefore, we can be confident that the mirrored contralateral, unfractured, tibial plateau can be used as a template for 3D virtual preoperative planning for young patients without previous damage to the knee.

Introduction

The tibial plateau is one of the crucial weight-bearing areas of the body. Fractures of the tibial plateau are intra-articular and therefore often technically challenging to treat. A bimodal distribution is seen in age; high-energetic trauma for younger patients in contrast to relatively low-energetic traumas in older patients with osteoporosis[1]. Patients with tibial plateau fractures are highly susceptible to complications including knee stiffness, posttraumatic osteoarthritis, and non- or mal-union[2]. Anatomic reconstruction of the articular surface is key to prevention of these complications. Recognition and understanding of the fracture and its fracture lines are crucial for determining the optimal surgical approach for fracture reduction [3]. Preoperative planning could be important for the patients' prognosis, and the choice of surgical technique has proven to be of impact on the functional recovery of the knee according to recent studies[3-5].

Currently, radiographs and two- and three-dimensional (3D) computed tomography are used for surgical planning[6-9]. Since these images are static and virtual reduction is not possible, it can be difficult for surgeons to create an optimal strategy for surgical reduction. Consequently, surgeons are continuously looking for improvements in preoperative planning when treating complex fractures. Three-dimensional (3D) virtual planning is a relatively new tool that might improve the insight into fracture characteristics and thereby improve fracture reduction and decrease complications, blood loss, and operating time[4,10,11]. 3D Virtual planning can be provided by expert programs such as Sectra Medical Systems AB © (Linköping, Sweden) and Materialise © (Leuven, Belgium). These programs are gaining popularity and the additional value of these programs is currently being investigated.

For surgical planning, the contralateral, unfractured tibial plateau, is already used as a template for optimal reduction of the fractured tibial plateau[3,12]. Several studies have been performed on assessing limb symmetry using different methods[13-16]. In a study by Quintens et al.[15], statistical shape modeling was used to gain insight into anatomical variations of the tibia using a principal component analysis based on five parameters of the tibia. Small differences in shape variation were found between the left and right tibial plateau. Whilst this demonstrates that there is a difference in shape variation within a population, it is less indicative of the left-right difference within one patient. Similarly, a study by Jang et al.[16] compared 3D morphometric measurements on ten fresh frozen cadavers and found small within-subject differences of 1.1 ± 0.6 mm between the left and right proximal tibia of one subject. Although both previous named studies suggest a small difference between the left and right tibia, they can only draw a limited conclusion because of indirect left-right comparison, high age of participants, and small sample sizes. Therefore, we aim to investigate the symmetry of the left and right tibial

4

plateau in young healthy individuals to determine whether left-right mirroring can be used to optimize preoperative 3D virtual planning for patients with tibial plateau fractures.

Methods

Data for this study was collected for a previous study on dynamic, four-dimensional (4D), imaging of the knee, which was approved by our local ethics committee (Ethics approval number: NL 72784091). The secondary use of this data was approved by all subjects in a written informed consent file. The procedures used in this study adhere to the tenets of the Declaration of Helsinki. One hundred healthy subjects, without previous knee surgery, severe knee trauma, or signs of osteoarthritis, were included. In the context of the ongoing imaging study, healthy individuals underwent a CT scan (Canon Aquilion One), scanning both knees with a slice thickness of 0.8mm. The images had voxel sizes of 0.782x0.782x0.8mm. For this study, 3D surface models of the femur, patella, and tibia were created using a convolutional neural network[17]. The 3D models of the left and right tibias were exported to MATLAB©. (The MathWorks Inc, Natick, Massachusetts, United States) The left tibias for each participant were mirrored in the sagittal plane. The mirrored left tibias were superimposed on the contralateral right tibia using a computer-based Coherent Point Drift surface matching algorithm[18]. The target and superimposed surface models were cut 15mm below the tibial plateau. The resulting surfaces were again superimposed to ensure alignment of the proximal tibia and to avoid point drift due to points outside our region of interest. Correspondence points were identified on both surfaces. The root mean squared distance between correspondence points on both surfaces was calculated in millimeters and visualized in heatmaps. (Fig.1 Overview of methods).
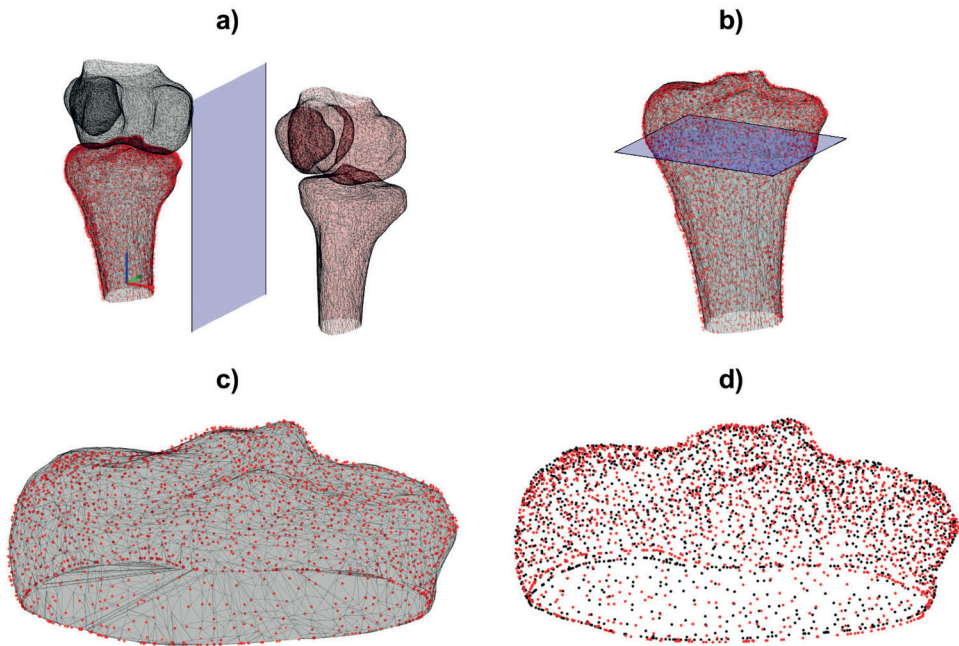
Figure 1. Overview of methods. a) The left tibia (red) is mirrored along the sagittal plane (blue). The surface of the mirrored left tibia is superimposed with the surface of the right tibia (black). b) The superimposed, mirrored left tibia and right tibia are cut 15 mm below the tibial plateau in an axial plane (blue). c) The resulting proximal parts of both tibias are again superimposed to prevent malposition due to distal surface points. d) Correspondence points are established (red & black) and the Euclidean distance between these points is calculated.

Results

The mean age of the participants was 24.1 years (range 18-34 years, 71 females, 29 males). The overall mean squared distance between correspondence points on the left and right tibial plateau is 0.6276mm ± 0.0343mm. The differences between all correspondence points were illustrated in a boxplot (Fig. 2 Boxplot of the Euclidean distance of all correspondence points on the left and right tibia). The greatest differences between correspondence points were seen around two specific surfaces of the tibia; where the distal tibia was cut 15 mm below the tibial plateau and around the tibiofibular joint (Fig. 3 Overview of artefacts: a) Heatmaps were used to illustrate artefacts at (a) the cut-off edges of the tibia, and (b) the tibiofibular joint). The greatest left to right difference, of the subject with the largest mean difference, was 1.6mm. This difference was found on the medial plateau (Fig. 4 Heatmap investigating the largest distance between correspondence points observed in one subject's tibial plateau (posterior view)).
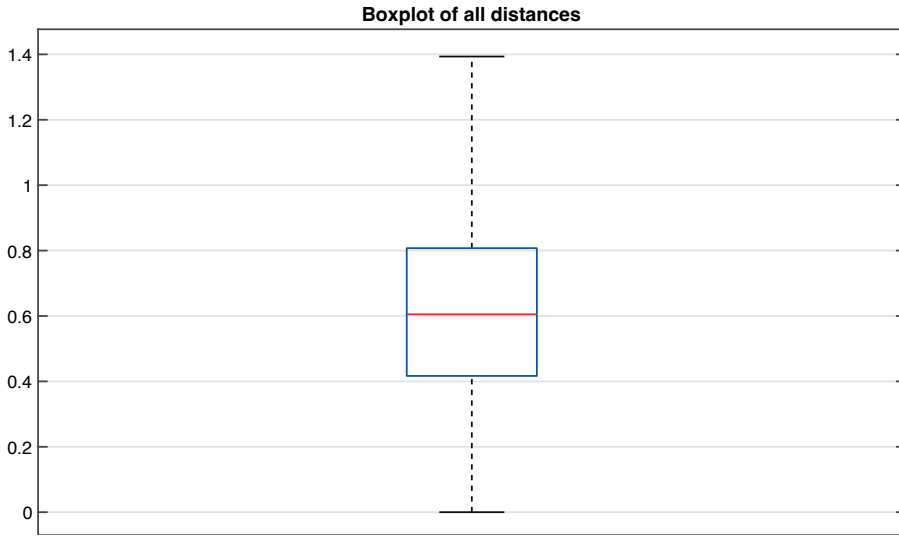
Figure 2. Boxplot of the Euclidean distance of all correspondence points on the left and right tibia
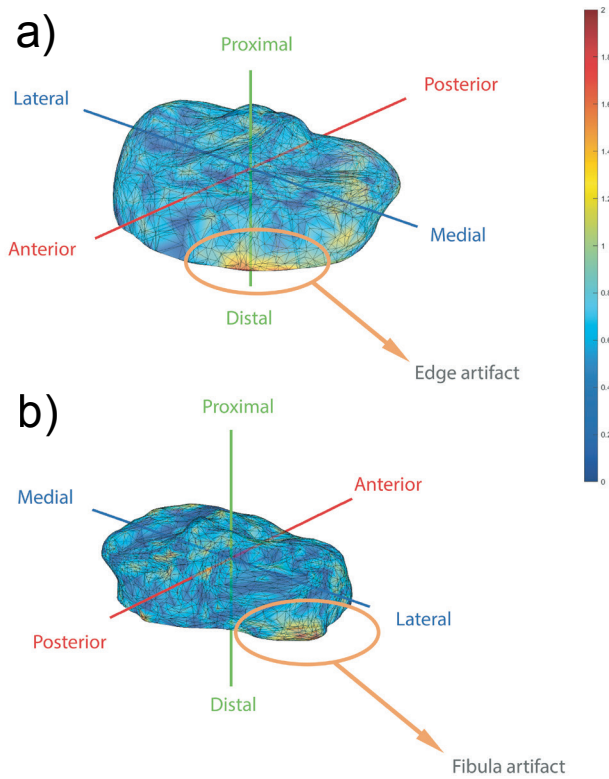

Figure 3. Overview of artifacts: a) Heatmaps were used to illustrate artifacts at (a) the cut-off edges of the tibia, and (b) the tibiofibular joint.
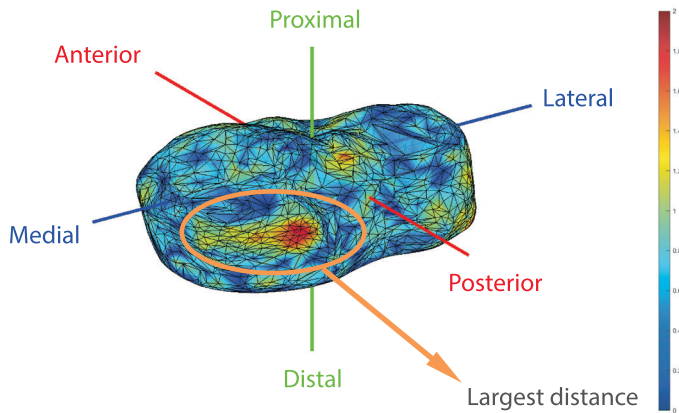
Figure 4. Heatmap investigating the largest distance between correspondence points observed in one subject's tibial plateau (posterior view).

Discussion

This study aimed to investigate the equality of the left and right tibial plateau in hundred healthy living subjects to establish whether mirroring the contralateral tibial plateau can be used to optimize the surgical reduction using 3D virtual planning software for patients with tibial plateau fractures. The overall average distance of correspondence points based on surface matching of the left and right tibial plateau was 0.6276mm ± 0.0343mm.

The distance of 0.6276mm lies in the range of one voxel size, which was 0.782x0.782x0.8mm in this study. To translate this difference into clinical practice; differences in one voxel size are only recognizable in one slice of an axial CT scan of 0.8mm. Increasing the resolution of the CT scans, could have potentially decreased the distances between the correspondence points. In current literature, the indication for surgical reduction of a tibial plateau fracture varies between a step-off and/or a gap of more than 2-5mm of the articular surface[4,19-21]. The average measured distance of 0.6276mm between correspondence points on the left and right tibia is only a small difference within these clinical margins. Therefore, we are confident that this small difference is not clinically relevant, indicating the contralateral, unfractured, tibial plateau can be used as a template for reduction of the fractured tibial plateau.

Moreover, the knowledge from this study could not only be implemented for 3D virtual planning, but could also be used to address the quality of the postoperative reduction by comparing the postoperative CT scan of the fractured knee and the unfractured contralateral knee. However, for this comparison, it is critical to have access to a CT scan

with significant quality to ensure reduction of scattering of the osteosynthesis material. The clinical feasibility of this warrants further research evaluation.

For the participant with the greatest overall left-right difference, there was a localized difference of 1,6mm on the posterior side of the medial plateau. As figure 4 illustrates, the overall distances of the same subject were small, indicating that this is not a superimposing error. This abnormality could be a result of a previous unrecognized posttraumatic injury to the posterior side of the medial meniscus. Despite screening participants for a history of major knee trauma, unrecognized trauma cannot be completely ruled out. In this specific subject, we think this could be a result of twist injury.

A potential limitation of this study is that there were some challenges with the segmentation of the CT scans. The discrimination of bone and soft tissue can be a difficult task in areas with low contrast. For example, around the tibiofibular joint, artificially high distances were be measured due to a poor discrimination of the junction of the tibia and fibula. However, these differences are minimal and do not influence the articular surface of the tibial plateau. Second, cutting the distal tibia 15 mm below the tibia plateau, complicates the determination of correspondence points around this cut off point. This may also have introduced artificially high distances. However, this results only in localized differences, which, due to the high number of total points, only slightly overestimates the average distance of all correspondence points.

Concluding, based on our comparison of 100 CT scans of the knee in healthy, young individuals without previous damage to the knee, the differences between the left and right tibial plateau are negligible, and therefore, we are confident that the mirrored contralateral, unfractured, tibial plateau can be used as a template for the reduction of a fractured tibial plateau using 3D virtual preoperative planning.

References

1. Yoon, R.S., F.A. Liporace, and K.A. Egol, *Definitive fixation of tibial plateau fractures.* Orthop Clin North Am, 2015. 46(3): p. 363-75, x DOI: 10.1016/j.ocl.2015.02.005.
2. Papagelopoulos, P.J., et al., *Complications after tibia plateau fracture surgery.* Injury, 2006. 37(6): p. 475-84 DOI: 10.1016/j.injury.2005.06.035.
3. Ozturk, A.M., et al., *Surgical advantages of using 3D patient-specific models in high-energy tibial plateau fractures.* Eur J Trauma Emerg Surg, 2020 DOI: 10.1007/s00068-020-01378-1.
4. Marsh, J.L., et al., *Articular fractures: does an anatomic reduction really change the result?* J Bone Joint Surg Am, 2002. 84(7): p. 1259-71.
5. Wu, W.Y., et al., *Preoperative Plan with 3D Printing in Internal and External Fixation for Complex Tibial Plateau Fractures.* Orthop Surg, 2019. 11(4): p. 560-568 DOI: 10.1111/os.12466.
6. Castiglia, M.T., et al., *The Impact of Computed Tomography on Decision Making in Tibial Plateau Fractures.* J Knee Surg, 2018. 31(10): p. 1007-1014 DOI: 10.1055/s-0038-1627464.
7. Doornberg, J.N., et al., *Two-dimensional and three-dimensional computed tomography for the classification and characterisation of tibial plateau fractures.* Injury, 2011. 42(12): p. 1416-25 DOI: 10.1016/j.injury.2011.03.025.
8. te Stroet, M.A., et al., *The value of a CT scan compared to plain radiographs for the classification and treatment plan in tibial plateau fractures.* Emerg Radiol, 2011. 18(4): p. 279-83 DOI: 10.1007/s10140-010-0932-5.
9. Wicky, S., et al., *Comparison between standard radiography and spiral CT with 3D reconstruction in the evaluation, classification and management of tibial plateau fractures.* Eur Radiol, 2000. 10(8): p. 1227-32 DOI: 10.1007/s003300000326.
10. Suero, E.M., et al., *Use of a virtual 3D software for planning of tibial plateau fracture reconstruction.* Injury, 2010. 41(6): p. 589-591.
11. Thomas, T.P., et al., *ASB Clinical Biomechanics Award Paper 2010 Virtual pre-operative reconstruction planning for comminuted articular fractures.* Clin Biomech (Bristol, Avon), 2011. 26(2): p. 109-15 DOI: 10.1016/j.clinbiomech.2010.12.008.
12. Nie, W., et al., *Preliminary application of three-dimension printing technology in surgical management of bicondylar tibial plateau fractures.* Injury, 2019. 50(2): p. 476-483 DOI: 10.1016/j.injury.2018.12.019.
13. Auerbach, B.M. and C.B. Ruff, *Limb bone bilateral asymmetry: variability and commonality among modern humans.* Journal of Human Evolution, 2006. 50(2): p. 203-218 DOI: https://doi.org/10.1016/j.jhevol.2005.09.004.
14. Radzi, S., et al., *Assessing the bilateral geometrical differences of the tibia – Are they the same?* Medical Engineering & Physics, 2014. 36(12): p. 1618-1625 DOI: https://doi.org/10.1016/j.medengphy.2014.09.007.
15. Quintens, L., et al., *Anatomical Variation of the Tibia - a Principal Component Analysis.* Scientific reports, 2019. 9(1): p. 7649-7649 DOI: 10.1038/s41598-019-44092-8.
16. Jang, K.M., et al., *Three-Dimensional Evaluation of Similarity of Right and Left Knee Joints.* Knee Surg Relat Res, 2017. 29(4): p. 307-315 DOI: 10.5792/ksrr.16.076.
17. Li, X., et al., *H-DenseUNet: Hybrid Densely Connected UNet for Liver and Tumor Segmentation From CT Volumes.* IEEE Trans Med Imaging, 2018. 37(12): p. 2663-2674 DOI: 10.1109/tmi.2018.2845918.
18. Myronenko, A. and X. Song, *Point set registration: coherent point drift.* IEEE Trans Pattern Anal Mach Intell, 2010. 32(12): p. 2262-75 DOI: 10.1109/tpami.2010.46.

4

19. Schatzker, J., R. McBroom, and D. Bruce, *The tibial plateau fracture. The Toronto experience 1968--1975.* Clin Orthop Relat Res, 1979(138): p. 94-104.

20. Meinberg, E., et al., *The Fracture and Dislocation Classification Compendium 2017 – "Nearing the Finish Line".* Injury, 2017. 48(4): p. 793-794 DOI: https://doi.org/10.1016/j.injury.2017.03.032.

21. Mthethwa, J. and A. Chikate, *A review of the management of tibial plateau fractures.* Musculoskelet Surg, 2018. 102(2): p. 119-127 DOI: 10.1007/s12306-017-0514-8.

Chapter 5

Fully automatic extraction of knee kinematics from dynamic CT imaging; normative tibiofemoral and patellofemoral kinematics of 100 healthy volunteers

H. Dunning, S.A.W. van de Groes, C.F. Buckens, M. Prokop,
N. Verdonschot, D. Janssen

Abstract

Background: Accurate assessment of knee kinematics is important in the diagnosis and quantification of knee disorders and to determine the effect of orthopaedic interventions. Despite previous studies showing the usefulness of dynamic imaging and providing valuable insights in knee kinematics, dynamic imaging is not widely used in clinics due to a variety of causes. In this study normative knee kinematics of 100 healthy subjects is established using a fully automatic workflow feasible for use in the clinic.

Methods: One-hundred volunteers were recruited and a dynamic CT scan was made during a flexion extension movement. Image data was automatically segmented and dynamic and static images were superimposed using image registration. Coordinate systems for the femur, patella and tibia were automatically calculated as well as their dynamic position and orientation.

Results: Dynamic CT scans were made with an effective radiation dose of 0.08 mSv. The median tibial internal rotation was 4° and valgus rotation is 5° at full flexion. Femoral rollback of the lateral condyle was 7 mm versus 2 mm of the medial condyle. The median patella flexion reached 65% of tibiofemoral flexion and the median tilt and rotation were 5° and 0° at full flexion, respectively. The median mediolateral translation of the patella was 3 mm (medially) in the first 30° of flexion.

Conclusion: The current study presents TF and PF kinematic data of 97 healthy individuals, providing a unique dataset of normative knee kinematics. The short scanning time, simple motion and, automatic analysis make the methods presented suitable for daily clinical practice.

Introduction

Knee disorders such as ligament injury or patellofemoral instability affect the dynamic functioning of the knee joint. Accurate assessment of knee kinematics is therefore important in the diagnosis and quantification of such disorders, and to determine the effect of orthopaedic interventions. Current diagnostic imaging in clinical practice, however, is predominantly taken while the subject is in passive, supine position. During imaging, potential important information on the effect of joint motion and the influence of soft tissues such as ligaments, tendons and muscles is thereby not captured[1]. To assess the potential added information during dynamic scanning, there is a need for objective and accurate determination of subject-specific knee kinematics, and the possibility of comparing them with normative kinematics, in a clinical setting.

In order to diagnose subject-specific knee kinematics and pathologies, several in-vivo dynamic imaging techniques of the knee joint have been developed using a variety of different modalities such as MRI, Fluoroscopy, CT or a combination of these techniques[1,2]. In these studies various loading conditions and dynamic tasks were investigated[3–6]. Unfortunately, these studies mainly focus on patellofemoral kinematics (PF) and very rarely the combination of tibiofemoral (TF) and PF kinematics, while these are known to influence each other[7].

In two comprehensive review studies, the current state of dynamic imaging for the patellofemoral joint was studied[2,8]. Both review studies conclude that dynamic imaging provides valuable insight into knee kinematics and pathologies and underline the need for objective and accurate determination of subject-specific knee kinematics. However, these studies also reveal a number of limitations that need to be addressed before implementation of dynamic imaging in general clinical practice is possible. For instance, due to differences in modalities, loading conditions, range of motion, and analysis methods it is difficult to compare and generalise dynamic imaging studies. Secondly, practical limitations such as time consuming scanning sequences in case of dynamic MRI require intensive coordination and cooperation of the patient. Thirdly, dynamic imaging provides a multitude of data compared to conventional static imaging, rendering manual assessment by a radiologist too time-consuming, and is prone to variabilities that complicate intra- and intersubject comparison.

To overcome these limitations, a fully automatic analysis method was developed that is able to simultaneously extract tibiofemoral and patellofemoral kinematics from dynamic CT imaging. The short duration and simplicity (no loading rigs, or moving frequency required) of the scan protocol and automatic segmentation and kinematic quantification allows for use in daily clinical practice and ensures fast and consistent determinations

5

of knee kinematics. In the current study we used this method to determine PF and TF kinematics in a cohort of 100 healthy subjects, with the objective to establish normative knee kinematics from dynamic CT imaging that can be used as a baseline dataset in future clinical studies investigating various types of knee joint pathology.

Methods

Prior to the current study, a dose reduction study was performed to ensure the radiation dose was below the maximum limit for healthy volunteers (protocol dose 0.08 mSv). Institutional approval was obtained to perform a dynamic CT scan on healthy volunteers. One-hundred volunteers from the age of 18 years were included with a maximum of 35 years to avoid altered kinematics due to early onset arthrosis. Subjects were not allowed to have any previous knee pathologies, prior trauma or surgery to the knee. This was checked by briefly discussing their medical background regarding these subjects. Reports on dysfunction, pain or prior surgery were reason for exclusion. Further exclusion criteria were functional or congenital disorders and severe valgus or varus malalignment. The exclusion criteria were assessed by the first author during an intake interview. Sex, age and BMI of all participants were determined and recorded. All participants signed an informed consent form prior to participating.

A single high resolution static scan (voxel size 0.71x0.71x0.80mm) of both legs was made of the subject in supine position (Canon Aquilion One). The field of view was 500 mm and included the distal half of the femur, the proximal half of the tibia and the full patella. The subject was then moved to the end of the scanner table, and an angled pillow was placed in the popliteal fossa, with both legs hanging freely over the edge of the scanner table (see figure 1). Subsequently, subjects were asked to assume a relaxed, semi-seated position, so the movement could be easily performed with minimal effort.

Figure 1. Overview of the scan protocol and corresponding CT images . a) A high resolution static scan is made of the patient in supine position on the scanner table. b&c) The subject is moved to the end of the scanner table and an angled pillow is placed in the popliteal fossa. The subject is asked to fully extend and flex both legs in approximately 10 seconds.

Subjects were asked to move both legs from approximately 90° of flexion to full extension and back again in approximately 10 seconds. The movement was practiced prior to the actual scan, so that a smooth and full extension-flexion movement was completed within the scanning time. During the dynamic scan, 41 images were made while the subject moved both knees. The field of view during dynamic scanning was 160 mm. A subject positioning protocol was used to ensure that the entire patella, and parts of the proximal tibia and the distal femur were continuously within the field of view during the scan. Prior validation studies have demonstrated that dynamic CT imaging is accurate (~1° and 1mm of x,y,z rotation and translation) and comparable to other dynamic imaging techniques[9,10]. Given the high similarity in image acquisition, similar accuracies are expected in this study.

The left and right femur, patella, tibia and patellar tendon of all subjects were segmented with a deep learning network[11]. The deep learning algorithm had a DICE coefficient of 0.99 for the femur, 0.98 for the tibia and 0.96 for the patella compared to manual segmentations, demonstrating that the algorithm is capable of performing accurate and precise segmentations. Segmentation masks were automatically transformed into 3D surface meshes (MATLAB), and remeshed and smoothed without manual intervention, in order to improve mesh quality[12].

As the field of view of the dynamic scans is too small for accurate landmark and axes determination, the femur, patella and tibia of the static scans were superimposed by subsequent pointcloud- (Coherent Point Drift) and image-registration (Elastix 5.0.1)[13,14]. Although the accuracy of (image) registration is notoriously difficult to determine, the algorithms used in this study are well established and have demonstrated high accuracies and will likely introduce minimal inaccuracies. All spatial transformations were saved in an Elastix transform file. Coordinate Systems (CS) were calculated for every static femur, patella and tibia, similar to those described by Miranda et al.[15]. Each orthogonal coordinate system consisted of Superior-Inferior (SI), Anterior-Posterior (AP) and Medial-Lateral (ML) axis. The sensitivity of the coordinate system was determined in a previous publication, which concluded that with common anatomy, the kinematics of the knee can be described with acceptable certainty[16]. A detailed description of the calculation of the femoral and tibial coordinate systems can be found in Chen et al.[17]. Furthermore a detailed description of the calculation of the patellar coordinate system can be found in a previous publication[16].

The transformations found in the dynamic scans were applied to each relative coordinate system to calculate their dynamic position and orientation. The angles between SI, AP and ML axes of the femur, patella and tibia were calculated according to the sequence described by Grood & Suntay[18]. Rotations of the tibia and patella were all calculated

5

with respect to the femur (i.e. the femur was fixed in space). As data were collected at even time intervals (fastest acquisition speed of the scanner) and subjects were allowed to move freely, images were taken at different knee flexion angles between subjects. Therefore, spherical linear interpolation was used to calculate the rotations of the patella and tibia with respect to the femur for every degree of tibiofemoral flexion. Similarly, for the interpolation of translations, piece-wise linear interpolation was used.

To counteract differences in angles as a result of anatomical variation, to objectively describe motion and to allow intersubject comparison, any rotational and translational offsets were negated similar to Amis et al., who assumed all rotations and translations to be zero at full extension[19]. Therefore, the smallest tibiofemoral flexion angle was calculated for both knees for every subject. In that position, the direction of the AP and ML axes of the femur were copied to the patellar and tibial AP and ML axes which essentially negates any rotations for that specific TF flexion angle. The orientation of the SI axis (flexion angle) was left unaffected.

Femoral Rollback was calculated by projecting the femoral trans epicondylar axis on the tibial plateau, specifically the centroids of the medial and lateral condylar articulating surface that, when connected, make up the femoral ML axis.

Rollback was separately calculated for the medial and lateral condyle as the translation of the projected points, similar to the method by Gray et al.[20]. Lastly, the patellar mediolateral translation was calculated by calculating the distance between the patellar and femoral CS origin along the ML axis of the femur. Similar to the rotations, the mediolateral patellar translation and femoral rollback were negated at the smallest tibiofemoral flexion angle (i.e. in extension)[19].

An overview of how TF and PF rotations and translations were calculated can be found in figure 2.

To ensure usefulness and smoothness while allowing maximal range of flexion angles, the median and percentiles were only calculated and visualized at flexion angles which at least 65% of all subjects were able to reach within the scan time. This percentage was iteratively determined by maximizing range of motion (ROM) and number of subjects reaching that ROM. At least 65% of the subjects were able to reach TF flexion angles of 6-85° during the extension movement. For the flexion movement, 65% of the subjects were able to reach TF flexion angles of 6-70°.

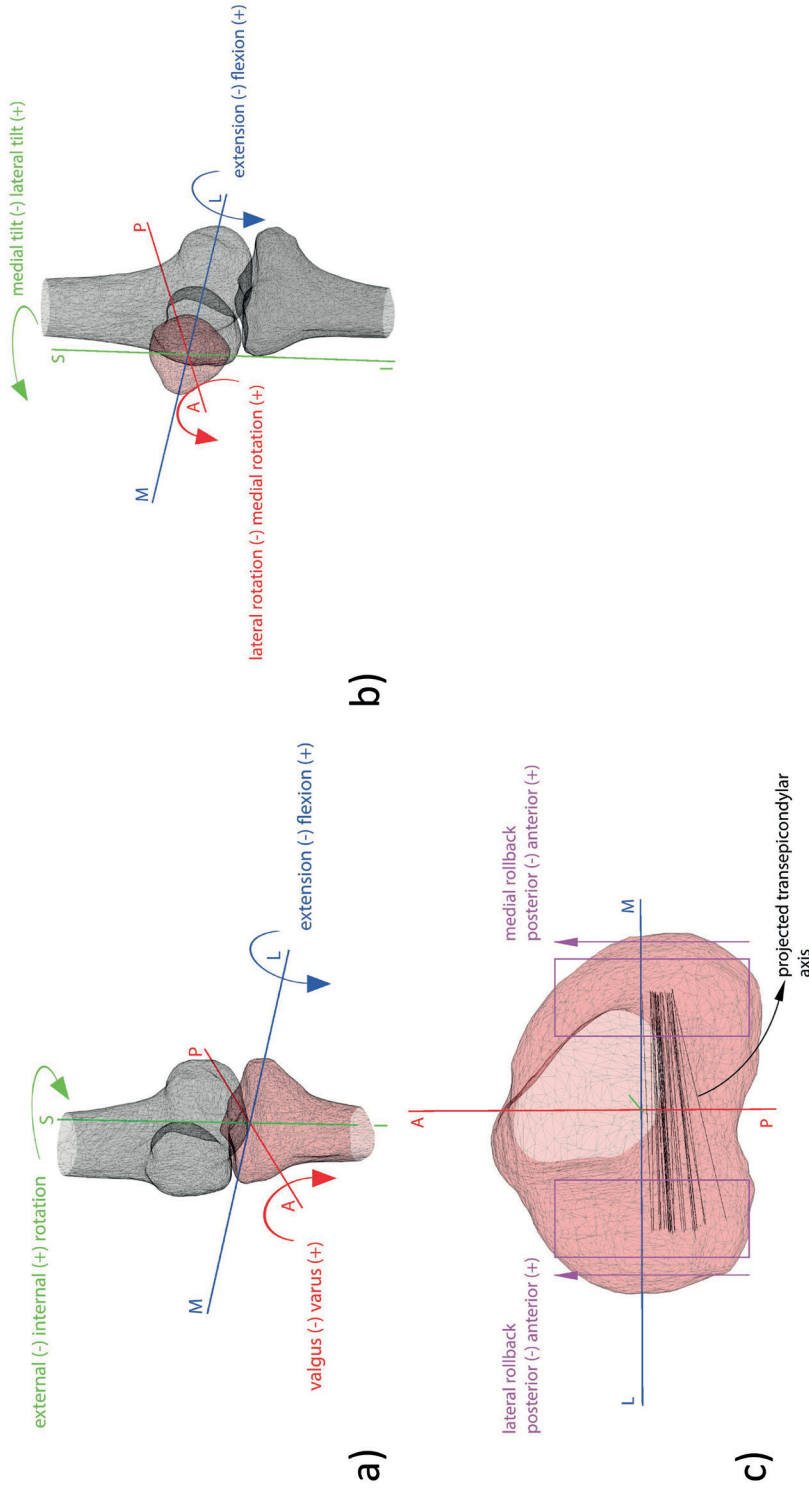**Figure 2.** Overview of TF & PF rotations and femoral rollback. The example is a left knee. a) Tibiofemoral Rotations b) Patellofemoral rotations. Mediolateral patellar translation is measured along the ML axis of the femur. c) Femoral rollback is calculated by projecting the trans epicondylar axis of the femur onto the tibia plateau. The anterior and posterior movement is measured separately on the medial and lateral side.

5

Results

One hundred healthy volunteers were successfully recruited, of which 71 were female and 29 were male. The mean age was 24 years with a standard deviation of 3.36 years. All subjects were in the age range of 18-34 years old. The mean BMI of all subjects was 19±2.8. Forty-one images were made during 11.3 seconds of active movement, resulting in a framerate of 3.6 frames per second. The effective radiation dose associated with the scan protocol was 0.08 mSv .

Of the 100 dynamic CT datasets, 3 datasets showed substantial image artifacts which prohibited automatic segmentation and registration, and the data were therefore excluded. As both knees were scanned, a total of 197 knees was analyzed. Remaining data was successfully segmented, registered and coordinate systems for the femur, patella and tibia were successfully calculated.

The median, 25-50 percentile and 12.5-87.5 percentile of tibiofemoral and patellofemoral kinematics are visualized in figure 3-5. For visibility, the extension and flexion movements are visualized in separate subplots. The overall flexion range of all subjects was 3.37°±8.03° to 89.31°±8.78°.

There was a slight internal rotation of the tibia from 85° to approximately 30° of flexion, followed by external rotation from 30° to 6° of flexion. The variance between subjects was approximately 10° at larger flexion angles, and gradually decreased with lower flexion angles, resulting in a narrowing area between the percentiles plots. Both median and percentiles followed a slightly different path during the extension and flexion movement.

A small valgus angle of the tibia with respect to the femur was observed at higher flexion angles, which decreased with decreasing flexion angle. Similar to the internal external rotation, the variance in the measured varus-valgus angles was largest at higher flexion angles, with differences of ±15°, which became smaller with decreasing flexion angles. Both median and percentiles followed a slightly different path during the extension and flexion movement.

Femoral Rollback was largest at higher flexion angles, both medially and laterally. With decreasing flexion, rollback decreased. Femoral rollback overall was larger on the lateral side compared to the medial side. Both median and percentiles followed the same (inversed) path during the extension and flexion movement.

The median, 20-50 percentile and 12.5-87.5 percentile of medial and lateral femoral rollback and are visualized in figure 3b.
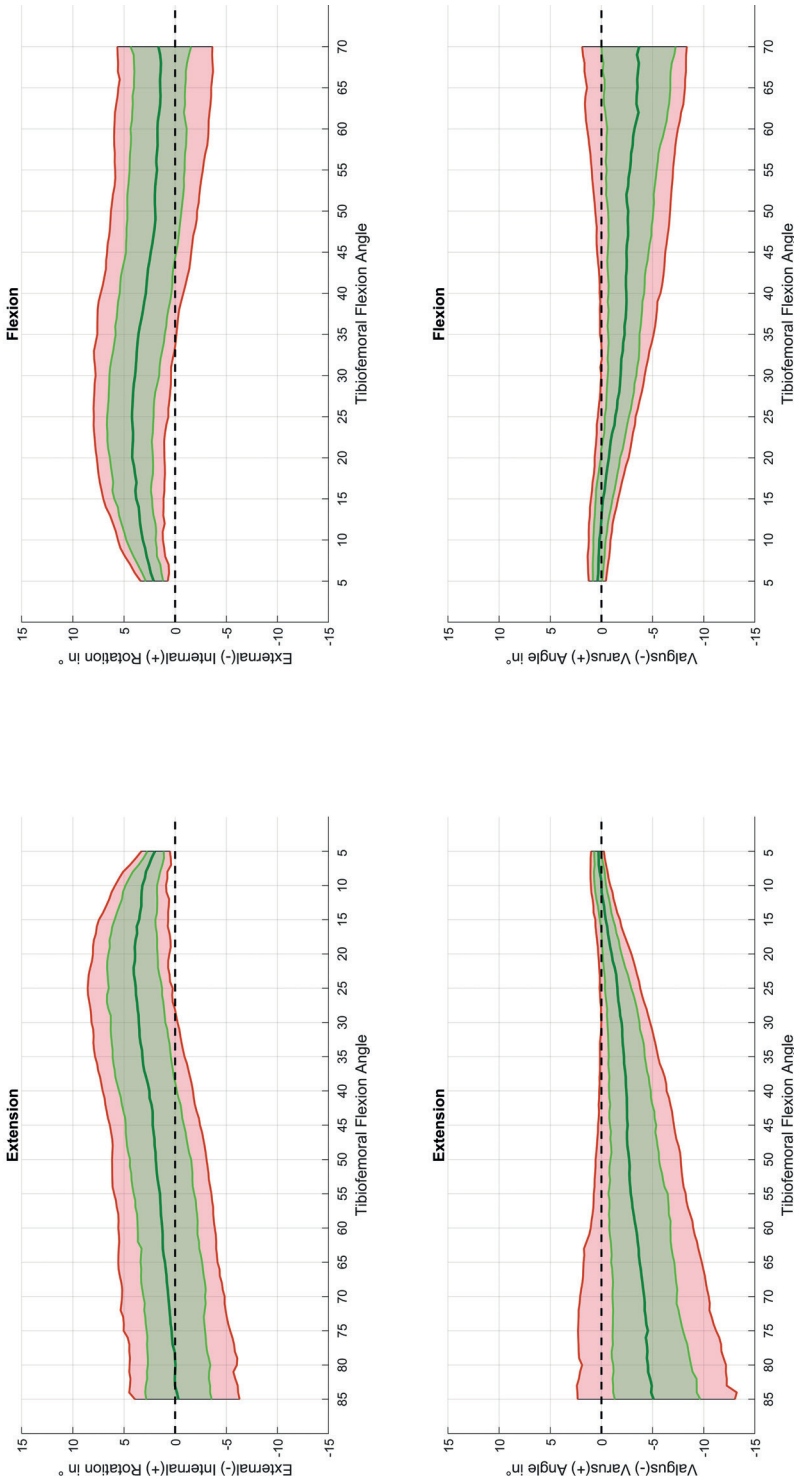
Figure 3a. Percentile plot of tibiofemoral kinematics during the extension-flexion movement, green line = media, red area = 12.5-87.5 percentile. Top = internal (+) external (-) rotation, bottom = Varus(-) Valgus(+) angle. (+). The horizontal axis contains the tibiofemoral flexion angle, the vertical axes are labelled. To ensure smoothness and readability of the plots, measurements are only displayed between 6°-85° of flexion, as these angles were achieved by at least 65% of all subjects.

Femoral Rollback
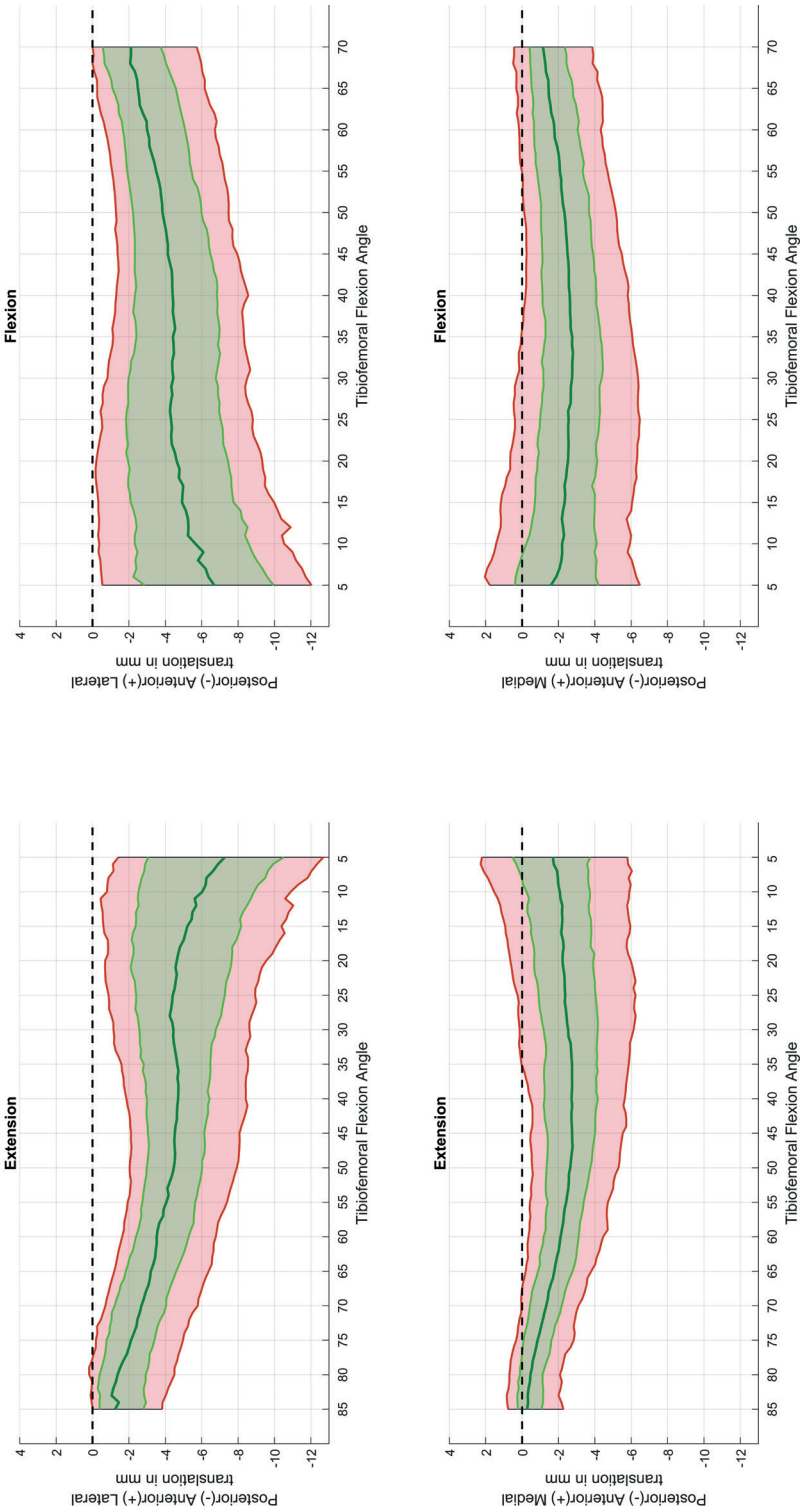
Figure 3b. Percentile plot of the femoral rollback off the lateral (upper) and medial (lower) condyle during an extension-flexion movement. (+). The horizontal axis contains the tibiofemoral flexion angle, the vertical axes are labelled To ensure smoothness and readability of the plots, measurements are only displayed between 6°-85° of flexion, as these angles were achieved by at least 65% of all subjects.

Patellofemoral flexion reached approximately 2/3rd of tibiofemoral flexion throughout movement and patellar flexion decreased with decreasing tibiofemoral flexion. The variance was approximately 10° over the complete range of motion.

The patella was most laterally tilted at high TF flexion angles, which generally decreased with decreasing flexion. Patellar tilt remained roughly equal between 50°-20° of TF flexion and decreased to zero nearing full extension. The variance was approximately 10° and decreased to 5° nearing full extension.

The patellar rotation was centred around 0° with a variance of approximately 10° at full flexion which decreased to 0° with decreasing TF flexion. The largest change in variance occurred at TF flexion angles larger than 30°.

The median, 20-50 percentile and 12.5-87.5 percentile of patellofemoral flexion, patellar tilt and patellar rotation are visualized in figure 4a/b.

The patella moved medially in the first 25°of TF flexion and remained stable after that. The median translation was ±2.5mm and the variance ±10mm.

5
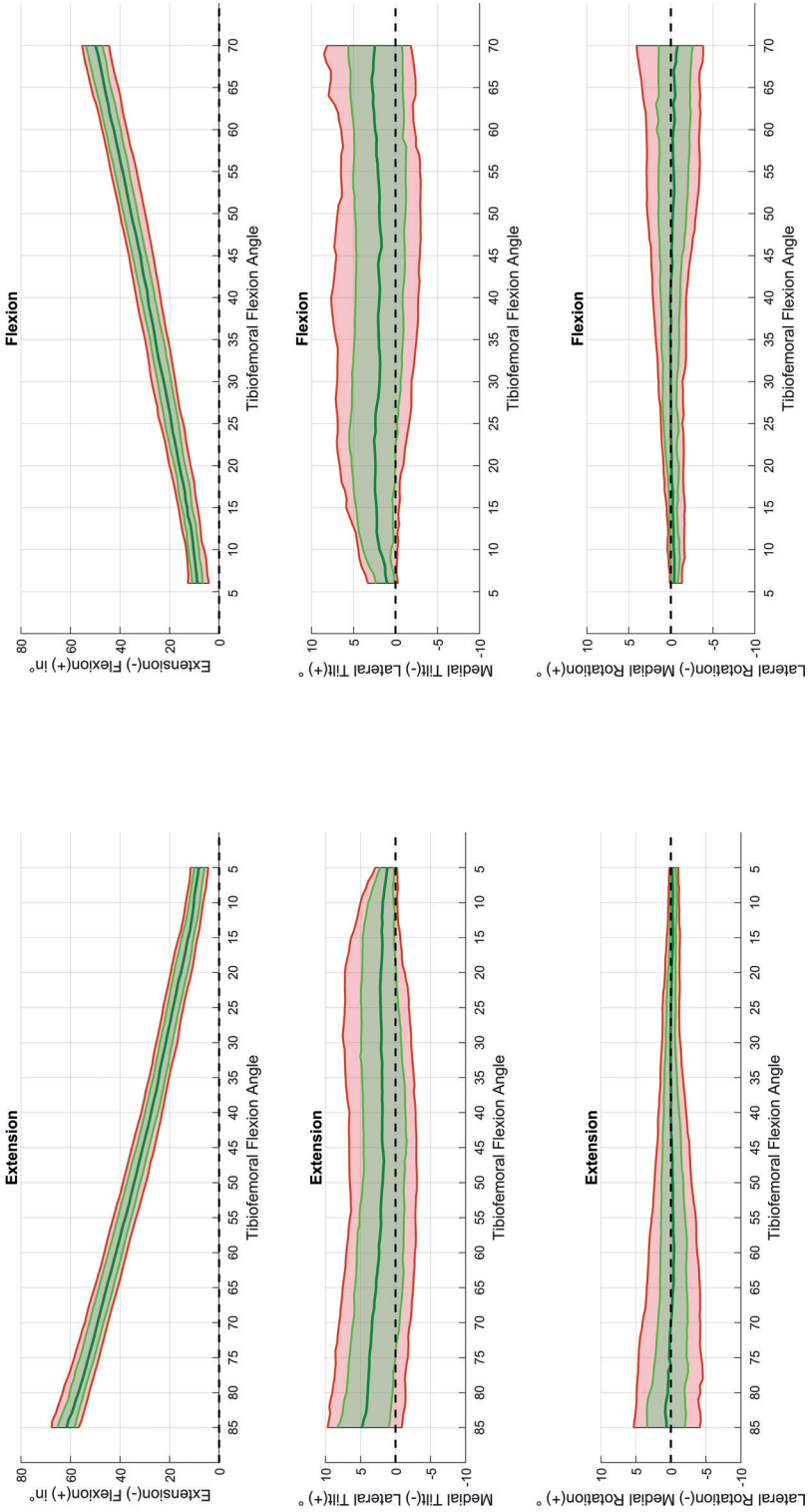
Figure 4a. Percentile plot of Patellofemoral Kinematics, green line = median green area = 25-50 percentile red area = 12.5-87.5 percentile. Top = Extension (-) Flexion (+), middle = Medial Tilt(-) Lateral Tilt(+), bottom = Medial Rotation (-) Lateral Rotation (+). The horizontal axis contains the tibiofemoral flexion angle, the vertical axes are labelled. To ensure smoothness and readability of the plots, measurements are only displayed between 6°-85° of flexion, as these angles were achieved by at least 65% of all subjects.

Patellar Mediolateral Translation
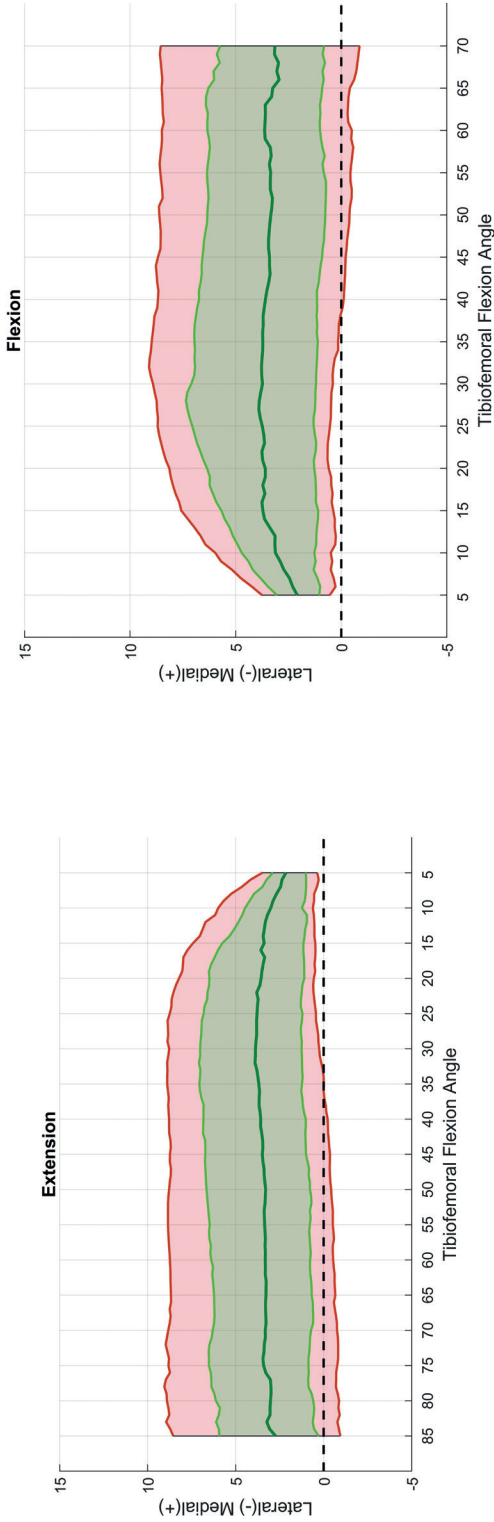
Figure 4b. Percentile plot of the mediolateral translation of the patella with respect to the femur during an extension-flexion movement. (+). The horizontal axis contains the tibiofemoral flexion angle, the vertical axes are labelled. To ensure smoothness and readability of the plots, measurements are only displayed between 6°-85° of flexion, as these angles were achieved by at least 65% of all subjects.

5

Discussion

In-vivo patient specific dynamic assessment of knee kinematics has the potential to expand upon static measurements in the diagnosis and quantification of knee disorders and to determine the effect of orthopaedic interventions. Despite previous studies showing the usefulness of dynamic imaging and providing valuable insights in knee kinematics, dynamic imaging is not widely used in clinics. In the current study we introduce a fully automatic analysis method to extract tibiofemoral and patellofemoral kinematics and applied it to a cohort of 97 healthy subjects to establish normative knee kinematics as a reference for the analysis of knee joint pathology.

Dynamic CT imaging allows for a combination of high spatial- and temporal resolution over a large range of motion compared to other modalities. For example, compared to dynamic MRI where spatial and temporal resolution are a trade-off and flexion range is limited by the MR coil[21].

The protocol involves a simple, single movement which does not require repetitions nor specific timing, which makes it feasible for subjects with painful knees. Together with the fast automatic analysis this makes the presented methods suitable for use in daily clinical practice. As the effective radiation dose (0.08 mSv) is low compared to natural background radiation and routine CT, it is broadly applicable at relatively low-risk.

The current study presents TF and PF kinematic data of 97 healthy individuals, providing a unique dataset of normative knee kinematics. Unfortunately there is no gold standard regarding dynamic imaging to which the results of this study can be compared. However, the kinematics found in the current study are highly similar to those reported in literature. Internal and external rotation of the tibia in the studies by Seisler- and Sheehan et al. is highly comparable to the current study. In all cases there is small internal rotation with increasing flexion angle, especially in the first 30°, which can be attributed to the screw home mechanism[4,5]. Similarly, a publication by Shandiz et al. studying changes in knee kinematics after total knee arthroplasty (TKA), shows a comparable internal tibial rotation in participants prior to TKA[22].

Whereas there is little to no valgus rotation of the tibia in the studies of Seisler & Sheehan, our data suggests a median varus alignment of 5° at 85° of TF flexion. This difference may be caused by the use of different coordinate systems, where a valgus rotated, or externally rotated femoral ML axis causes a more valgus description during knee flexion[23].

Similarly to what is found in other studies, femoral rollback is larger at the lateral condyle than the medial condyle, as a result of medial pivoting[24,25]. Moreover, despite differences in loading conditions, movement task and range of motion, both magnitude and path of the medial and lateral condyle show large resemblance with the study from Gray et al.[20]. This study investigated joint motion with biplane fluoroscopy during normal walking, and found mean posterior translations of ±5mm for the lateral condyle and ±2.5mm for the medial condyle as well as a short period of anterior movement of the medial condyle starting around 20° of TF flexion, similar to our results.

In addition to similar tibiofemoral kinematics, patellofemoral kinematics in this study is also highly similar to aforementioned studies. Patellofemoral flexion is nearly identical during flexion and extension movement, and has a constant variation around the median of approximately 5°.

The patellar tilt shows an increase in the first 30° of tibiofemoral flexion, followed by a very subtle decrease. This initial increase may be caused by contraction of the quadriceps, causing a lateral pull on the patella. Around 20° of tibiofemoral flexion the medial facet of lateral wall of the trochlea comes into contact with the lateral facet of the patella, causing a small medial tilt. Both the median and variance (percentiles) show large similarity to Esfandiarpour and Amis et al[3,19].

Patellar rotation is centered around zero, similar to Sheehan- , Seisler- and Amis et al.[4,5,19]. Here we see differences with the study of Esfandiarpour, which shows a medial patellar rotation of approximately 5°.

The patella shows a lateral movement of the patella during extension and at TF flexion angles smaller than ±30°, at which the patella moves out of the femoral trochlea. In literature, the mediolateral displacement of the patella is calculated and visualized in many different ways. For example, Tanaka et al. used the bisect offset which determines the fraction of the patella lateral of the femoral trochlear groove[26]. Suzuki et al. who used dual fluoroscopy to establish patellar tracking used displacement of the patellar origin with respect to the femoral origin, similar to Amis et al. and the current study[27]. In a comprehensive literature review, Yu et al. compared patellofemoral joint kinematics of 12 studies using different techniques and modalities. That study showed that there is a large variability in patellar ML translation among different studies and indicates that different movement tasks, loading conditions and analysis methods have a substantial impact on measured displacement.

Overall, our data shows that there is considerable variance in knee kinematics even within a healthy population. This variation should be taken into account when

5

comparing patients and healthy subjects, as it may complicate distinguishing the two at an individual level. The amount of variation at a specific flexion angle is related to the angle at which rotations around the SI, and AP axis were negated and are therefore specific to this study. In case of the translations, part of the variation can be explained by knee size differences, where larger knees show more translation than smaller knees. Some studies use the epicondylar width in an attempt to negate size differences. We have not chosen to do so in the current study, as the validity of this method is unclear.

Both tibiofemoral and patellofemoral kinematics show small differences for the extension and flexion movement. As this difference is most pronounced in patellofemoral kinematics, this may be a result of concentric versus eccentric contraction of the quadriceps muscle. It may therefore be necessary to consider these movements separately.

There are limitations of this study that should be considered. First, is the negation of the offsets in rotation and translation of both tibia and patella at the lowest TF flexion angle. This assumes full alignment of the patellar and tibial ML and AP axes with those of the femur at the smallest flexion angle (i.e. extension), where in practice this is not the case. Due to a natural variation in pose and anatomy, there will be a range of different starting-positions and -orientations. The variations in kinematics are highly dependent on the flexion angle at which rotations around the SI and AP axis were negated and from this cannot be concluded that higher flexion angles are associated with larger variance in kinematics. Furthermore, as not every subject was able to reach 0° of TF flexion, negation of rotations and translations at the smallest TF angle will introduce variations. However, the introduced variations as a result of negating rotations will be small and have no effect on the calculated median and percentiles. Moreover, the current approach allows us to solely investigate movements relative to the extended position, rather than a combination of movement and different starting positions and orientations.

Secondly, the choice of coordinate system has a major influence on the kinematic description[8,16,28,29]. The choice of coordinate system together with natural variation in anatomy and pose are a possible explanation for offsets, or different starting positions and orientations[23]. The absolute numbers from this study, may therefore not by directly comparable to studies where other coordinate systems are used. Negating the data, may reduce these differences. Moreover, as was previously mentioned, differences with other studies are small and trends are similar and movement patterns of the tibia as well as the patella relative to the femur are similar to those reported in the literature.

Lastly, it is known that knee kinematics are different for different tasks and loading conditions. A flexion extension movement is not a challenging or error-prone movement. Episodes of, for example, instability of the knee joint will therefore most likely not occur during the scan as these are usually associated with weightbearing activities. It is unclear whether the occurrence of such episodes is necessary for a better understanding of the underlying cause, and the same applies for other knee disorders. Knee kinematics are dependent on loading conditions. In this study, data were gathered under non-weightbearing conditions. For example, varus/valgus rotation is significantly different in a weightbearing versus non-weightbearing situation[30]. As a result, values found in this study cannot be extrapolated to a weightbearing situation. Interestingly, multiple studies have found that tibiofemoral and patellofemoral rotations and translations are more pronounced in non-weightbearing versus weightbearing conditions[31–33]. Due to large forces acting on the knee joint during weight-bearing, the effect of smaller, less powerful but important structures for knee kinematics such as the MPFL, Iliotibial band or lateral retinaculum may be less apparent. Therefore, a flexion extension movement against gravity might provide better insight into the more subtle aspects of knee kinematics, and therefore kinematic disorders. The presented method of real-time dynamic CT-scanning proved to be easily applicable in a clinical setting. Although not all CT scanners are capable of dynamic imaging, it has a large potential to investigate numerous knee disorders in vivo. Dynamic imaging and associated image analysis offers a new set of challenges. Applying existing measurements made for static imaging to dynamic imaging data can have results that are counterintuitive or difficult to explain. To fully exploit these techniques, existing dogmas and static measurements should therefore be reconsidered, and new diagnostic methods must be developed. These automatized, 3D, dynamic methods will therefore likely change the personalized diagnostic capacity for patients with knee pathologies and will further optimize treatment options and evaluation methods in order to improve patient care.

5

References

1. Katchburian M V., Bull AMJ, Shih YF, Heatley FW, Amis AA. Measurement of patellar tracking: Assessment and analysis of the literature. Clin Orthop Relat Res 2003;412:241–59. https://doi.org/10.1097/01.blo.0000068767.86536.9a.

2. Rosa SB, Ewen PM, Doma K, Ferrer JFL, Grant A. Dynamic Evaluation of Patellofemoral Instability: A Clinical Reality or Just a Research Field? A Literature review. Orthop Surg 2019;11:932–42. https://doi.org/10.1111/os.12549.

3. Esfandiarpour F, Lebrun CM, Dhillon S, Boulanger P. In-vivo patellar tracking in individuals with patellofemoral pain and healthy individuals. J Orthop Res 2018;36:2193–201. https://doi.org/10.1002/jor.23887.

4. Seisler AR, Sheehan FT. Normative three-dimensional patellofemoral and tibiofemoral kinematics: A dynamic, in vivo study. IEEE Trans Biomed Eng 2007;54:1333–41. https://doi.org/10.1109/TBME.2007.890735.

5. Sheehan FT, Derasari A, Brindle TJ, Alter KE. Understanding patellofemoral pain with mal-tracking in the presence of joint laxity: Complete 3D in vivo patellofemoral and tibiofemoral kinematics. J Orthop Res 2009;27:561–70. https://doi.org/10.1002/jor.20783.

6. Elias JJ, Carrino JA, Saranathan A, Guseila LM, Tanaka MJ, Cosgarea AJ. Variations in kinematics and function following patellar stabilization including tibial tuberosity realignment. Knee Surg Sports Traumatol Arthrosc 2014;22:2350–6. https://doi.org/10.1007/s00167-014-2905-9.

7. Salsich GB, Perman WH. Patellofemoral joint contact area is influenced by tibiofemoral rotation alignment in individuals who have patellofemoral pain. J Orthop Sports Phys Ther 2007;37:521–8. https://doi.org/10.2519/jospt.2007.37.9.521.

8. Yu Z, Yao J, Wang X, Xin X, Zhang K, Cai H, et al. Research Methods and Progress of Patellofemoral Joint Kinematics: A Review. J Healthc Eng 2019;2019. https://doi.org/10.1155/2019/9159267.

9. Zhao K, Breighner R, Holmes D, Leng S, McCollough C, An K-N. A Technique for Quantifying Wrist Motion Using Four-Dimensional Computed Tomography: Approach and Validation. J Biomech Eng 2015;137:074501. https://doi.org/10.1115/1.4030405.

10. Adachi T. Accuracy Verification of 4D-CT Analysis of Knee Joint Movements : A Pilot Study Using a Knee Joint Model and Motion-capture System 2021:1–14.

11. Li X, Chen H, Qi X, Dou Q, Fu CW, Heng PA. H-DenseUNet: Hybrid Densely Connected UNet for Liver and Tumor Segmentation from CT Volumes. IEEE Trans Med Imaging 2018;37:2663–74. https://doi.org/10.1109/TMI.2018.2845918.

12. Tran AP, Yan S, Fang Q. Improving model-based functional near-infrared spectroscopy analysis using mesh-based anatomical and light-transport models. Neurophotonics 2020;7:1. https://doi.org/10.1117/1.nph.7.1.015008.

13. Myronenko A, Song X. Point set registration: Coherent point drifts. IEEE Trans Pattern Anal Mach Intell 2010;32:2262–75. https://doi.org/10.1109/TPAMI.2010.46.

14. Klein S, Staring M, Murphy K, Viergever Ma., Pluim J. <emphasis emphasistype="mono">elastix</emphasis>: A Toolbox for Intensity-Based Medical Image Registration. IEEE Trans Med Imaging 2010;29:196–205.

15. Miranda DL, Rainbow MJ, Leventhal EL, Crisco JJ, Fleming BC. Automatic determination of anatomical coordinate systems for three-dimensional bone models of the isolated human knee. J Biomech 2010;43:1623–6. https://doi.org/10.1016/j.jbiomech.2010.01.036.

16. Dunning H, van de Groes SAW, Verdonschot N, Buckens CF, Janssen D. The sensitivity of an anatomical coordinate system to anatomical variation and its effect on the description of

knee kinematics as obtained from dynamic CT imaging. Med Eng Phys 2022;102:103781. https://doi.org/10.1016/j.medengphy.2022.103781.

17. Chen H, Kluijtmans L, Bakker M, Dunning H, Kang Y, v/dGroes, Sebastiaan M.J.Sprengers A, et al. A robust and semi-automatic quantitative measurement of patellofemoral instability based on 4D computed tomography" n.d.

18. Grood ES, Suntay WJ. A joint coordinate system for the clinical description of three-dimensional motions: Application to the knee. J Biomech Eng 1983;105:136–44. https://doi.org/10.1115/1.3138397.

19. Amis AA, Senavongse W, Bull AMJ. Patellofemoral Kinematics during Knee Flexion-Extension : An In Vitro Study 2006:2201–11. https://doi.org/10.1002/jor.

20. Gray HA, Guan S, Thomeer LT, Schache AG, de Steiger R, Pandy MG. Three-dimensional motion of the knee-joint complex during normal walking revealed by mobile biplane x-ray imaging. J Orthop Res 2019;37:615–30. https://doi.org/10.1002/jor.24226.

21. Garetier M, Borotikar B, Makki K, Brochard S, Rousseau F, Ben Salem D. Dynamic MRI for articulating joint evaluation on 1.5 T and 3.0 T scanners: setup, protocols, and real-time sequences. Insights Imaging 2020;11. https://doi.org/10.1186/s13244-020-00868-5.

22. Akbari Shandiz M, Boulos P, Saevarsson SK, Yoo S, Miller S, Anglin C. Changes in knee kinematics following total knee arthroplasty. Proc Inst Mech Eng Part H J Eng Med 2016;230:265–78. https://doi.org/10.1177/0954411916632491.

23. Lenz NM, Mane A, Maletsky LP, Morton NA. The effects of femoral fixed body coordinate system definition on knee kinematic description. J Biomech Eng 2008;130:1–7. https://doi.org/10.1115/1.2898713.

24. Von Eisenhart-Rothe R, Lenze U, Hinterwimmer S, Pohlig F, Graichen H, Stein T, et al. Tibio-femoral and patellofemoral joint 3D-kinematics in patients with posterior cruciate ligament deficiency compared to healthy volunteers. BMC Musculoskelet Disord 2012;13. https://doi.org/10.1186/1471-2474-13-231.

25. Pinskerova V, Johal P, Nakagawa S, Sosna A, Williams A, Gedroyc W, et al. Does the femur roll-back with flexion? J Bone Jt Surg - Ser B 2004;86:925–31. https://doi.org/10.1302/0301-620X.86B6.14589.

26. [26] Tanaka MJ, Elias JJ, Williams AA, Demehri S, Cosgarea AJ. Characterization of patellar maltracking using dynamic kinematic CT imaging in patients with patellar instability. Knee Surgery, Sport Traumatol Arthrosc 2016;24:3634–41. https://doi.org/10.1007/s00167-016-4216-9.

27. Suzuki T, Hosseini A, Li JS, Gill TJ, Li G. In vivo patellar tracking and patellofemoral cartilage contacts during dynamic stair ascending. J Biomech 2012;45:2432–7. https://doi.org/10.1016/j.jbiomech.2012.06.034.

28. Kedgley AE, McWalter EJ, Wilson DR. The effect of coordinate system variation on in vivo patellofemoral kinematic measures. Knee 2015;22:88–94. https://doi.org/10.1016/j.knee.2014.11.006.

29. Grant C, Fick CN, Welsh J, McConnell J, Sheehan FT. A Word of Caution for Future Studies in Patellofemoral Pain: A Systematic Review With Meta-analysis. Am J Sports Med 2021;49:538–51. https://doi.org/10.1177/0363546520926448.

30. Fritz B, Fritz J, Fucentese SF, Pfirrmann CWA, Sutter R. Three-dimensional analysis for quantification of knee joint space width with weight-bearing CT: comparison with non-weight-bearing CT and weight-bearing radiography. Osteoarthr Cartil 2022;30:671–80. https://doi.org/10.1016/j.joca.2021.11.019.

5

31. Draper CE, Besier TF, Fredericson M, Santos JM, Gary S, Delp SL, et al. Differences in Patello-femoral Kinematics between Weight- Bearing and Non-Weight-Bearing Conditions in Patients with Patellofemoral Pain. J Orthop Res 2010;29:312–7. https://doi.org/10.1002/jor.21253.

32. Victor J, Labey L, Wong P, Innocenti B, Bellemans J. The influence of muscle load on tibiofemo-ral knee kinematics. J Orthop Res 2010;28:419–28. https://doi.org/10.1002/jor.21019.

33. Souza RB, Draper CCE, Fredericson M, Powers MDCM. Femur Rotation and Patellofemoral Joint Kinematics: A Weight-Bearing Magnetic Resonance Imaging Analysis 2010;40:277–85. https://doi.org/10.2519/jospt.2010.3215.

5

Chapter 6

Dynamic CT imaging in clinical practice; a pilot study in patients with patellofemoral instability.

H. Dunning, S.A.W. van de Groes, C.F. Buckens, M. Prokop,
N. Verdonschot, D. Janssen

Abstract

Introduction: Patellofemoral pathologies are commonly associated with patellar maltracking. Multiple studies have investigated the potential of dynamic imaging in the diagnosis of knee disorders, particularly patellar maltracking. However, dynamic imaging is still largely confined to research settings and is not widely used in clinical practice. The aim of this study was to assess the feasibility of utilizing dynamic CT in clinical practice and to investigate its ability to differentiate between healthy and pathological knee kinematics.

Methods: Two dynamic datasets were acquired: a normative dataset of 100 healthy subjects and a dataset of 21 patients with patellofemoral instability. During the scan, subjects were asked to perform a flexion extension movement. Tibiofemoral and patellofemoral kinematics were automatically extracted and statistical analysis was performed to determine differences.

Results: All subjects were able to complete the scan protocol and statistical differences between patients and healthy subjects were demonstrated. Compared to healthy individuals, patients exhibited more external tibia rotation, smaller varus angle during flexion, greater translation of the lateral femoral condyle, increased patella tilt, and greater mediolateral translation of the patella.

Conclusion: The proposed method appears feasible for use in daily practice and the scan protocol is executable for both healthy subjects and patients with painful knees. The analysis methods enable differentiation between pathological and healthy kinematics, and provide valuable insights into possible biomechanical causes of knee disorders.

Introduction

Patellofemoral pathologies frequently occur in conjunction with abnormal patellar tracking[8,18]. Factors influencing patellar tracking include bony congruence of the patella and femur, neuromuscular control and soft tissues surrounding the joint[26,28]. The cause of maltracking is often complex and multifactorial, making it challenging to determine the most effective treatment approach for individual patients.

To determine the cause and extent of disorders, various measurements have been developed based on physical examination and/or medical imaging. Although physical examination can be performed during movement, measurements are often difficult to generalise and show poor interrater reliability[2,13]. Radiological measurements are easier to standardize, but they are typically based on static images and do not capture the dynamic nature of patellar tracking or the influence of soft tissues on movement. Additionally, static measurements can only partially predict patellofemoral kinematics, and may therefore not be the optimal method to identify and quantify the patient specific cause of maltracking[16].

In recent years, several studies have investigated the potential of dynamic imaging in the diagnosis of knee disorders, particularly patellar maltracking. These studies have used various imaging modalities and have applied different movement tasks and loading conditions to answer a wide range of questions regarding patellar maltracking and its relation to knee kinematics and knee morphology[12,29,30,33,34]. Comprehensive review studies have concluded that dynamic imaging provides valuable insights into knee kinematics and pathologies and has the potential to be used for the diagnosis and quantification of knee disorders[18,27,36]. However, dynamic imaging is still largely confined to research settings and is not widely used in clinical practice[7].

There are several technology-specific challenges that limit the use of dynamic imaging techniques in clinical practice, in addition to practical issues inherent to the technology. For example, dynamic magnetic resonance imaging (MRI) involves a trade-off between temporal and spatial resolution and requires repeated movements and cooperation from the patient, which can be difficult for patients with painful knees[3,17]. On the other hand, dynamic ultrasound has excellent temporal resolution, but the field of view and image quality are limited[4].

There are also more fundamental challenges associated with dynamic imaging that hinder its use in clinical practice. The large amounts of data generated by dynamic imaging techniques requires time-consuming manual postprocessing and assessment, adding to the already high workload of radiologists[23]. Moreover, the majority of manual image analysis is performed on a single orthogonal view, ignoring crosstalk and

6

oversimplifying the complex three-dimensional character of patellar maltracking and knee kinematics[18]. In a previously published study, we applied a dynamic CT scanning protocol with fully automated postprocessing and analysis to 100 healthy subjects[10].

The aim of this pilot study is twofold: 1) to establish the feasibility of applying the proposed methods in daily clinical practice 2) to determine whether the methods are capable of distinguishing between healthy and pathological knee kinematics.

Methods

Ethical approval for this study was obtained from the institutional review board. Two dynamic CT datasets were acquired: 1) a normative dataset consisting of 100 healthy volunteers 2) a dataset of 21 patients diagnosed with objective patellofemoral instability (PFI).

To establish a normative database, 100 healthy subjects were included in line with the recommendation of the COnsensus-based Standards for the selection of health Measurement INstruments (COSMIN) workgroup[24]. Patients with recurrent PFI were included between 2018 and 2021, with the aim to include as much patients as possible.

For the normative dataset, one-hundred volunteers between 18 and 35 years were included. The maximum age was set at 35 to match the patient population and to exclude individuals with altered kinematics due to early onset osteoarthritis. Reports on dysfunction, pain or prior surgery were reason for exclusion. Further exclusion criteria were functional or congenital disorders and severe valgus or varus malalignment. The exclusion criteria were assessed through an intake interview conducted by the first author.

For the patient dataset, 21 patients diagnosed with recurrent patellar instability were included who were already required to undergo a conventional CT scan. Exclusion criteria were prior surgery, and inability to actively extend and flex the knee or age below 18 years.

For healthy subjects and patients, weight, length and BMI and were registered, for patients the dexterity of the affected knee was noted.

The CT scan protocol was equal for patients and healthy volunteers. A single high resolution static scan (voxelsize 0.71x0.71x0.80mm) was obtained for both legs while the subject was in supine position on the scanner table (Canon Aquilion One). The longitudinal field of view of the static scan was 500 mm and included the distal half of

the femur, the proximal half of the tibia and the full patella. The subject was moved to the end of the scanner table, and an angled pillow was placed in the popliteal fossa, with both legs hanging freely over the edge of the scanner table (see figure 1).

Figure 1. Overview of the scan protocol. a) A high resolution static scan is made of the patient in supine position on the scanner table. b&c) The subject is moved to the end of the scanner table and an angled pillow is placed in the popliteal fossa. The subject is asked to fully extend and flex both legs in approximately 11 seconds.

During the dynamic scan, subjects were asked to perform an extension-flexion movement from approximately 90° of flexion to full extension and back with both knees in roughly 11 seconds. The smoothness and speed of the movement was practiced prior to the actual scan. During the scan, 41 images were made. The field of view in the axial direction during dynamic scanning was 160 mm (voxelsize 0.976x 0.976x0.50). To ensure that the entire patella, the distal part of the femur and proximal part of the tibia were continuously within the field of view during the scan, a subject positioning protocol was used. The previously described technique was used to calculate all rotations and translations of the patella and tibia with respect to and in the femur coordinate system [10]. An overview of TF and PF rotations is given in figure 2a&b.

Two translations are of main importance in tibiofemoral and patellofemoral kinematics: anterior-posterior translation of the femoral condyles relative to the tibia and patellar mediolateral translation relative to the femur. Translation of the femoral condyles was separately calculated for the medial and lateral condyle, similar to Gray et al.[19]. The centroids of cylinders fitted through the lateral and medial epicondyles were projected onto the tibial plateau for the complete range of motion. When connected, the line through these points creates the projected trans-epicondylar axis. Condyle translation was calculated with respect to full tibiofemoral extension i.e. translation is zero at the smallest tibiofemoral flexion angle. An illustration of medial and lateral femoral condyle translation can be found in figure 2c.

6
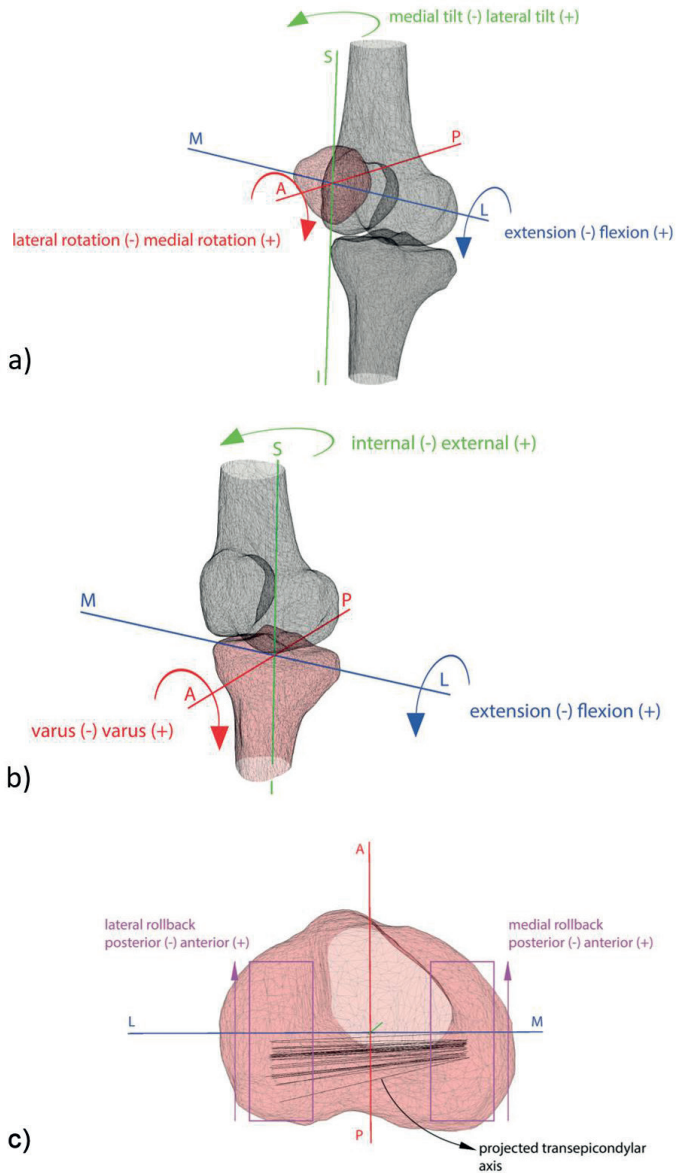
Figure 2. Overview of TF & PF rotations and translation of the medial and lateral femoral condyles. In this example a left knee is used. a) Patellofemoral rotations b) tibiofemoral rotations c) medial and lateral translation of the femoral condyle.

To determine whether there is an anterior or posterior position of the femoral condyles in full extension, the femorotibial rotation was calculated based on the static scans similar to Flury et al.[15]. A positive femorotibial rotation angle correlates with an external rotation of the tibia.

The patellar mediolateral translation relative to the femur was calculated by calculating the distance between the patellar and femoral coordinate system origin along the ML axis of the femur. As the aim was to compare mediolateral movement and not position, offsets in starting positions had to be negated. The mediolateral position at 30 degrees of tibiofemoral flexion was used as a reproducible starting point (i.e. set to zero), as the patella should be engaged in the femoral trochlea at that flexion angle in a "normal" knee.

Statistics
T-tests ($α= 0.05$) were used to determine if there were differences in age, height and BMI between patients and healthy subjects.

Normality of kinematic outcome metrics was determined for each tibiofemoral flexion angle with a Shapiro-Wilk test. Several kinematic measured showed a non-normal distribution for different flexion angles. For consistency, non-parametric tests Mann Whitney U tests ($α=0.05$) were performed to test differences between healthy individuals and patients for all flexion angles.

Results

One hundred healthy volunteers were successfully recruited and scanned with the dynamic scan protocol. Three volunteer datasets contained image artifacts that prohibited automatic segmentation and registration and were therefore excluded from analysis.

Twenty-one patients diagnosed with recurrent patellofemoral instability were included. Bilateral instability was diagnosed in 3 patients, bringing the total number of affected and included knees to 24. Both healthy subjects and patients signed an informed consent form prior to participating. All patients were able to complete the scan protocol without issues.

The complete datasets were successfully segmented and registered, and coordinate systems for the femur, patella and tibia were successfully calculated. Total analysis time was approximately 1.5 hours.

No significant differences were found in age (healthy = 24±3.5y, patients = 23±4.6y) or height (healthy = 1.74±0.09m, patients =1.74±0.07m). BMI of patients and healthy volunteers was different (p <0.001) (healthy = 19.2±2.8, patients = 24.1±4.0).

Knee movement was completely voluntary, without the use of rigs timers. As a result, not all subjects started at exactly 90° of flexion or were able to fully extend their knees to 0° within the scan time. This led to discontinuities in the data at flexion angles that were only met by

a limited number of individuals. To ensure that the figures are interpretable and not skewed by the limited number of patients that were able to reach the extreme flexion angles, the median and percentiles were only calculated and visualized for TF flexion angles that were reached by at least 50% of the subject. Fifty percent of the subjects reached 1-71° of flexion during the extension movement, and 1-77° during the flexion movement.

Tibiofemoral kinematics

The median internal/external tibia rotation of patients and healthy volunteers follows the same trend. At the beginning of the movement (at high flexion angles), this is a slight external rotation that rotates internally until about 15° of tibiofemoral flexion, after which a rapid internal rotation can be observed. The spread of the data is very similar for both groups and remains constant throughout the movement. From 70° of flexion to full extension during the extension movement and from full extension to 62° of flexion during the flexion movement, patients exhibit significantly more external tibia rotation than healthy subjects.

Both groups start the movement with a small varus rotation of the tibia with respect to the femur. In healthy volunteers there was a minor decrease in varus angle during the extension movement and a minor increase during flexion, where in patients this angle is more or less constant. Unlike internal external rotation, the dispersion of the data of both groups decreases as the flexion angle decreases. Overall, patients demonstrated less varus rotation of the tibia with respect to the femur between 78°-36° of TF flexion during the extension movement and 46°-56° of TF flexion during the flexion movement.

Both internal-/external- and varus/valgus rotation demonstrate a slightly different pattern and magnitude during the extension and flexion movement. The median, 25-75 percentile and region of significant difference of both rotations are visualized in figure 3a.

The medial condyle showed minimal anterior-posterior translation throughout the movement. Medial condyle translation demonstrates a similar trend for both groups, with a minor anterior translation below ±60°. Small differences were observed (~1°) at 15°-32° of TF flexion during the flexion movement.

Translation of the lateral condyle was significantly greater than medial and decreased with decreasing flexion angle. With the exception of low flexion angles during flexion movement, differences are observed between patients and volunteers, with patients showing greater translation. The median, 25-75 percentile and region of significant difference of femoral condyle translation is visualized in figure 3b.

Femorotibial rotation was larger (p=0.072) in patients (11.81±7.98°) than healthy subjects (8.20±6.45°).

Figure 3a. Median and 25-75 percentile of tibiofemoral kinematics for healthy volunteers (green) and patients (red). The bold line represents the median, the coloured area the 25-75 percentile. The dark coloured background indicates a statistically significant difference between patients and healthy volunteers. Patients show increased external rotation and reduced varus rotation of the tibia, compared to healthy subjects.

Femoral Rollback

Figure 3b. Median and 25-75 percentile of anteroposterior condyle translation for healthy volunteers (green) and patients (red). The bold line represents the median, the coloured area the 25-75 percentile. The shaded area indicates significant differences between patients and healthy subjects. Condyle translation was calculated with respect to full tibiofemoral extension i.e. translation is zero at the smallest tibiofemoral flexion angle. Patients show significantly greater posterior translation of the lateral condyle compared to healthy subjects.

Patellofemoral kinematics

The magnitude of the patellar flexion angle was roughly two thirds of the TF flexion angle throughout the complete motion. Trend and spread of patella flexion were similar between both groups. Small differences in patella flexion can be observed. At different tibiofemoral flexion angles healthy subjects demonstrate slightly greater patella flexion angles than patients.

Throughout the movement, patients exhibit larger lateral patella tilt than healthy subjects. The healthy subjects exhibit a small medial tilt at high flexion angles which decreases to a neutral position until ±20° of TF flexion. From there to full extension, lateral tilt increases to ±4°. The patients' patellas were tilted laterally throughout the complete movement, with a sharp increase in tilt seen from about 20° of tibiofemoral flexion. At full extension, a difference in patella tilt of approximately 12° was observed between the two groups.

Patellar rotation was similar between patients and healthy individuals and no significant differences were found. Both groups started at a median lateral rotation of ±4°, which gradually decreased to zero rotation at full extension.

The median, 25-75 percentile and region of significant difference of patellar flexion, tilt, and rotation are visualized in figure 4a.

Mediolateral translation of the patella with respect to the femur was similar between groups above ~45° of TF flexion. Throughout the complete movement spread of the data was similar for both groups. Patients exhibited considerably greater lateral translation below 30° of TF flexion during extension and flexion movement. At full extension, the median lateral translation was approximately 10 mm greater in patients than in healthy subjects.

The median, 25-75 percentile and region of significant difference of mediolateral translation of the patella is visualized in figure 4b.

6

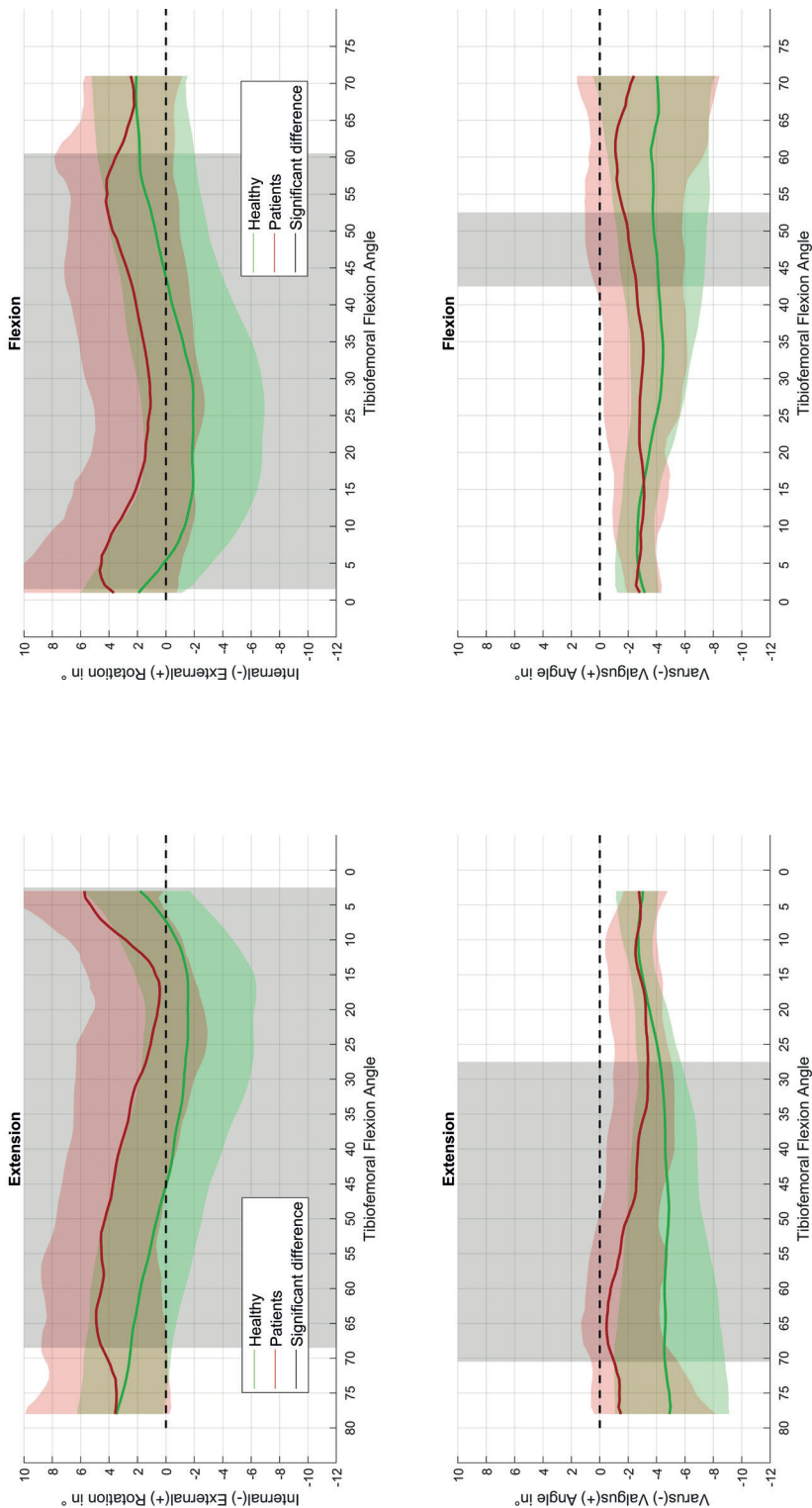## Patellofemoral Kinematics

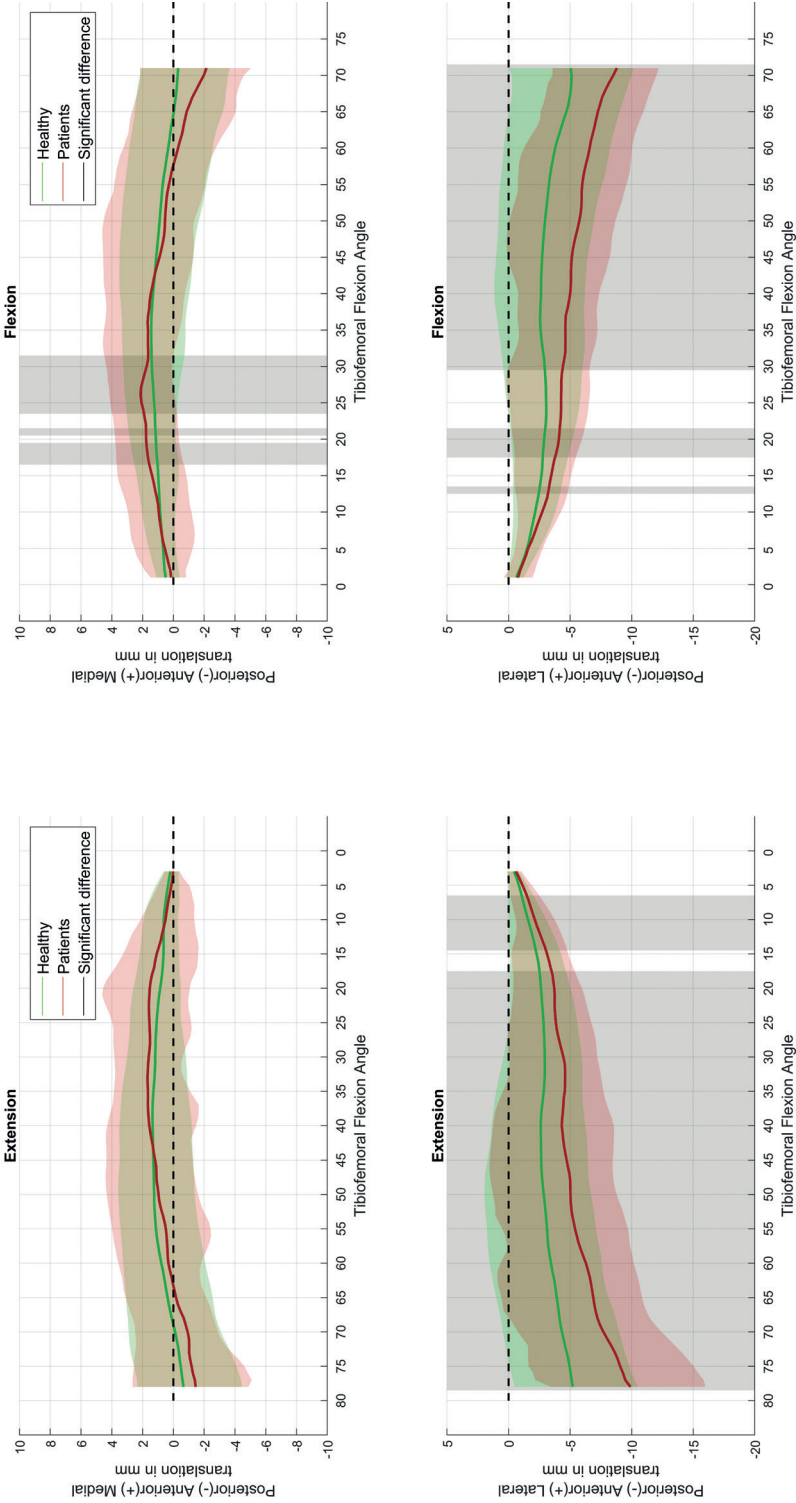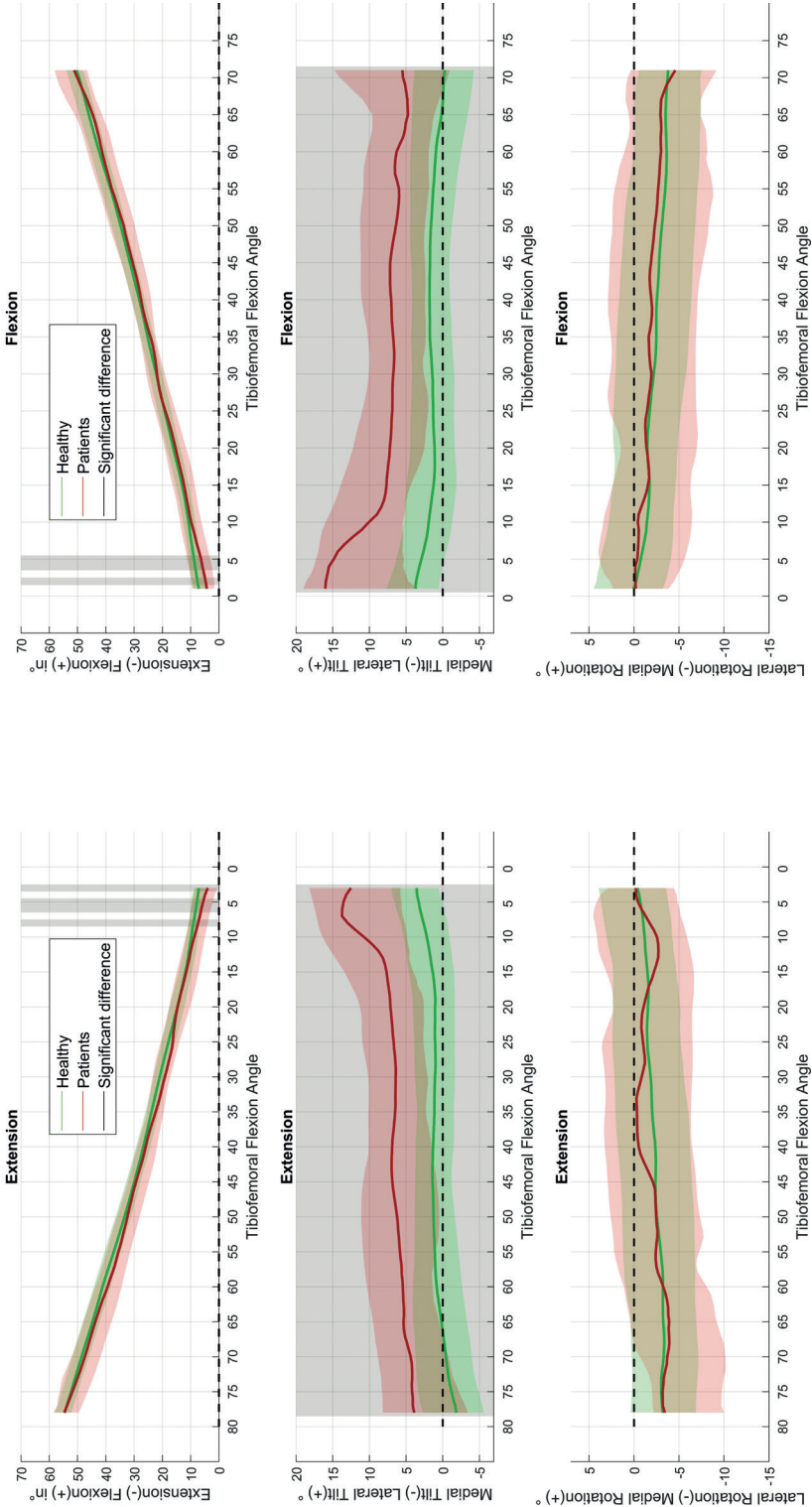**Figure 4a.** Median and 25-75 percentile of patellofemoral kinematics for healthy volunteers (green) and patients (red). The bold line represents the median, the coloured area the 25-75 percentile. The shaded area indicates significant differences between patients and healthy subjects. Lateral patellar tilt is significantly greater in patients compared to healthy subjects.
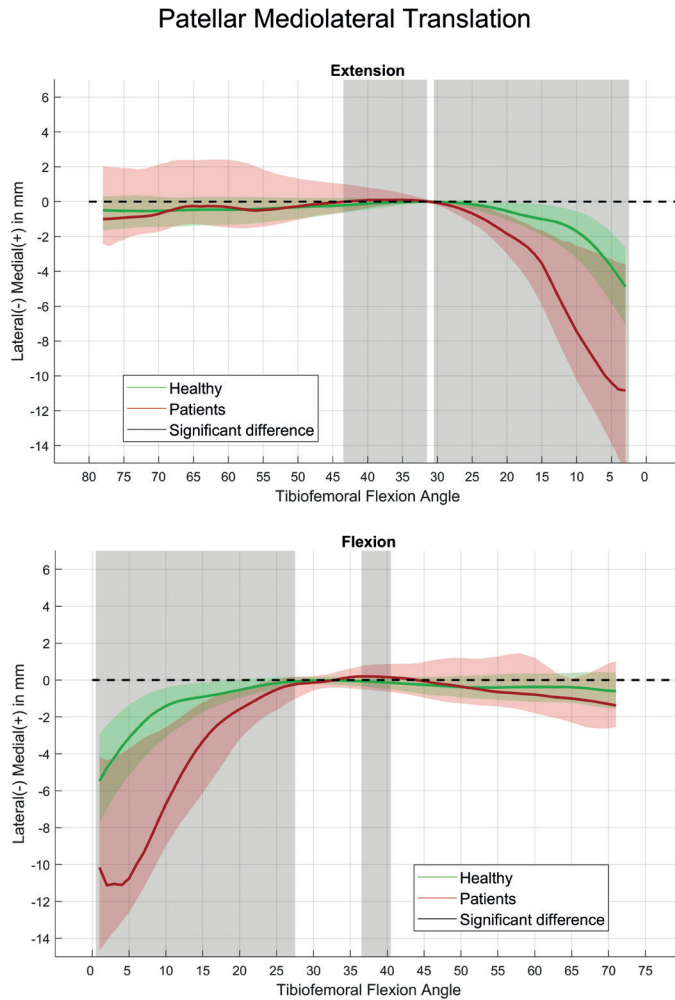
Figure 4b. Median and 25-75 percentile of patellar mediolateral translation for healthy volunteers (green) and patients (red). The thick line represents the median, the coloured area the 25-75 percentile. The shaded area indicates significant differences between patients and healthy subjects. Patients exhibit increased mediolateral tilt compared to healthy subjects.

Discussion

Multiple studies have underlined the potential of dynamic imaging for diagnosis and quantification of knee disorders[18,27,36]. Nevertheless, dynamic imaging remains a research exercise and is rarely applied in clinical practice due to a variety of reasons [7].

This study shows that dynamic CT imaging and the proposed analysis methods are suitable for use in daily clinical practice. The scan protocol is easy to perform and the

duration is short (~10 minutes). Analysis of the results is fully automatic, thereby not adding further to the already high workload of radiologists[23]. All study participants were able to complete the scanning protocol, indicating its feasibility even for patients with painful knees. Additionally, it is important that the method is able to distinguish between healthy and pathological kinematics, allowing for standardization of diagnosis and quantification of knee disorders.

This study addresses several challenges related to dynamic imaging that have been identified in previous studies and which impede accurate and robust diagnosis and quantification of patellofemoral disorders. For example, all outcomes are calculated in three-dimensional (3D) multiplane, taking crosstalk into account, improving the accuracy of the methods[31]. Additionally, image acquisition occurs during active muscle contraction, allowing for better diagnosis and study of maltracking disorders[18]. Another important advantage of the proposed method is that tibiofemoral and patellofemoral kinematics can be recorded simultaneously. While it is known that they influence each other, many studies only focus on one of the two. This offers opportunities to further investigate the relationship between them and understand the complex aetiology of patellofemoral disorders.

Previous studies have shown differences in knee kinematics among patients with different demographic characteristics and onset of patellofemoral instability, and have concluded that these should be analysed as separate groups[14,18,30]. Given the limited number of patients included in this study, it is underpowered to draw firm conclusions about differences in kinematics. Additionally, analysis methods have a significant impact on the values of knee kinematics found, making it difficult to directly compare these values with those from other studies [36]. Nevertheless, twenty-one patients were included in this study, exceeding the minimally recommended number of twelve for pilot studies[20]. Moreover, the trends and values found in this study and the differences between those of patients and healthy subjects are largely consistent with those reported in the literature.

The average body mass index (BMI) of the patient population was higher compared to that of the healthy volunteers, while the mean of both groups was within the healthy range (18.5 to 24.9). Nevertheless, BMI has been linked to changes in patellofemoral kinematics, which may impact the results of this study.

The internal/external rotation pattern of the tibia was similar for both patients and healthy subjects, characterized by external rotation of the tibia during the last 30° of tibiofemoral (TF) extension. This rotation pattern can be attributed to the screw home mechanism. Excessive tibial external rotation is a known secondary risk factor for PF

instability as it increases the Q-angle and lateral pull factor of the patellar tendon on the patella[5,8,11]. The current patient group also showed increased external translation, similar to the results of Souza et al [32]. Interestingly, Sheehan et al. reported increased internal rotation of the tibia in patients compared to healthy volunteers, a result that is difficult to explain from a biomechanical perspective[29].

Although the differences were small (±4°), the data suggest that patients had significantly less varus rotation (more valgus) than healthy subjects at high flexion angles. While pathological valgus alignment is associated with patellar instability and patellofemoral osteoarthritis, the values found in this study were not pathological and the median varus alignment of 3° near full extension was similar to the constitutional varus alignment found by Bellemans et al. [1,8,22].

Interestingly, patients not only exhibit increased femorotibial rotation, but also show a greater translation of the lateral femoral condyle. This raises questions about the cause-and-effect relationship. Morphological differences between groups, such as a greater radius difference between the lateral and medial condyles in patients, could potentially lead to a larger medial pivot, resulting in more external rotation. This could also cause increased valgus at high flexion angles. As patients often have different and underdeveloped distal femur and femoral trochlea compared to healthy knees, this is an interesting topic for further research.

Minor, yet, significant differences (±5°) were observed in patella flexion between groups, while the trend and spread of the data is similar. Although this may be a result of the difference in group size, alternatively it may be a result of patella alta, which causes the patella to reach the same patella flexion at higher tibiofemoral flexion angles in patients compared to healthy subjects. This may have a (small) effect on the described translations, as they are performed at 30° of tibiofemoral flexion due to the expected osseous engagement of the patella and femur.

Similar to previous studies, patients show increased patella tilt up to 12° in full extension[6,12,29]. Patella tilt rapidly increases during the last 20° of flexion to a greater extent in patients than in healthy individuals. The increased tilt appears to be present across the range of motion, but becomes constant at flexion angles greater than 20°. This may be explained by insufficient medial constraint due to MPFL rupture combined with a tight lateral retinaculum in patients and may even cause the greater external tibial rotation in patients, as the patellar tendon pulls more laterally at small flexion angles when the patella is engaged in the femoral trochlea. Since many patients develop symptoms during skeletal development, such a mechanism could influence skeletal

6

development, which would explain the differences in patella maltracking between young adults and adults demonstrated by Shen et al [30].

Patients demonstrated considerably greater mediolateral patella translation in the final 30° of the extension movement, resulting in approximately 9 mm more lateralization than in healthy subjects. In addition, the degree of increase in lateralization was significantly greater, causing the median to show a classic inverse J-sign as originally described by Post et al [25].

Several limitations of this study should be considered. Firstly, the scan protocol and analysis methods have a significant impact on the kinematic description. For example, the determination of the anatomical axes and the zeroing of translations directly affect the calculated values. Therefore, comparing the absolute numbers from this study to those in literature may not be realistic. However, it is important that analysis is performed consistently in order to accurately reflect differences between patients and healthy individuals. Using a fully automated analysis ensures this consistency and the one hundred healthy subjects included in the study provide a strong normative database for comparison. By definition, the calculation of translations requires the selection of a flexion angle where translations are zero, and the choice of this flexion angle logically affects the calculated values. The chosen tibiofemoral (TF) flexion angles of full extension and patellofemoral flexion at 30° are logical from a biomechanical perspective. In combination with the significant similarities between the values found in this study and those in the literature, the proposed methods seem to provide a good foundation for automatic kinematic analysis.

Secondly, as previously mentioned, various factors of the scan protocol and analysis method significantly affect the kinematic values found[18,21,36]. Examples of these include the calculation of anatomical coordinate systems and the zeroing of translations at a specific flexion angle. In previous research, we demonstrated that kinematics can be described with acceptable certainty using anatomical axis systems. For the zeroing of translations, the authors chose a flexion angle of 30° from a biomechanical perspective because at that angle the patella is fully engaged with the femoral trochlea. In the interpretation of the results, this should be taken into consideration.

Thirdly, different loading conditions and physiological activities result in different knee kinematics. The extension-flexion movement against gravity performed during the scan is simple, non-weightbearing, and not prone to error. Several studies have reported greater tibiofemoral and patellofemoral rotations and translations during non-weightbearing tasks compared to weightbearing tasks[9,32,35]. Therefore, the differences in knee kinematics found in this study may be greater than those found during

physiological loading. The large forces acting on the knee joint during weightbearing may reduce visibility of the effect of small but important structures such as the medial patellofemoral ligament on kinematics. As the cause of maltracking disorders is often multifactorial and diffuse, a non-weightbearing extension-flexion movement against gravity may offer more insight into the patient specific causes. Nonetheless, further investigation is needed and additional testing may be necessary to determine whether the current protocol is optimal for diagnosing and quantifying patellofemoral disorders.

Lastly, this study compared the different components of knee kinematics separately and per flexion angle. While this provides a useful comparison at the population level, relevant information at the individual level remains unexplored. For example, there may be correlations between the different components of knee kinematics, which, when properly analysed, could provide a deeper understanding of the patient-specific cause of maltracking. Although the aetiology of patellofemoral instability may be too complex to establish causality, discovering correlations can provide points of reference for future research.

In conclusion, the proposed method appears feasible for use in daily practice and the scan protocol is executable for both healthy subjects and patients with painful knees. Additionally, the method is able to distinguish between differences in knee kinematics between patients and healthy subjects, providing insights in this area. It offers the opportunity to easily scan a large number of patients and build a large kinematic database with patients of various demographic backgrounds and patellofemoral conditions, which may shed new light on the complex aetiology of patellofemoral instability.

6

References

1. Bellemans J, Colyn W, Vandenneucker H, Victor J (2012) The Chitranjan Ranawat Award: Is Neutral Mechanical Alignment Normal for All Patients?: The Concept of Constitutional Varus. Clin Orthop Relat Res 470:45–53

2. Best MJ, Tanaka MJ, Demehri S, Cosgarea AJ (2020) Accuracy and Reliability of the Visual Assessment of Patellar Tracking. Am J Sports Med 370–375

3. Borotikar B, Lempereur M, Lelievre M, Burdin V, Ben Salem D, Brochard S (2017) Dynamic MRI to quantify musculoskeletal motion: A systematic review of concurrent validity and reliability, and perspectives for evaluation of musculoskeletal disorders. PLoS One 12:1–26

4. Buzzatti L, Keelson B, Vanlauwe J, Buls N, De Mey J, Vandemeulebroucke J, Cattrysse E, Scheerlinck T (2021) Evaluating lower limb kinematics and pathology with dynamic CT. Bone Joint J 103-B:822–827

5. Camathias C, Pagenstert G, Stutz U, Barg A, Müller-Gerbl M, Nowakowski AM (2016) The effect of knee flexion and rotation on the tibial tuberosity–trochlear groove distance. Knee Surgery, Sport Traumatol Arthrosc Springer Berlin Heidelberg 24:2811–2817

6. Cilengir AH, Cetinoglu YK, Kazimoglu C, Gelal MF, Mete BD, Elmali F, Tosun O (2021) The relationship between patellar tilt and quadriceps patellar tendon angle with anatomical variations and pathologies of the knee joint. Eur J Radiol Elsevier B.V. 139:109719

7. Dandu N, Knapik DM, Trasolini NA, Zavras AG, Yanke AB (2022) Future Directions in Patellofemoral Imaging and 3D Modeling. Current Reviews in Musculoskeletal Medicine

8. Dejour D, Zaffagnini S, Arendt EA, Sillanpää P, Dirisamer F (2020) Patellofemoral Pain, Instability, and Arthritis. Dejour D, Zaffagnini S, Arendt EA, Sillanpää P, Dirisamer F (eds) JAMA - J. Am. Med. Assoc. Springer Berlin Heidelberg, Berlin, Heidelberg

9. Draper CE, Besier TF, Fredericson M, Santos JM, Gary S, Delp SL, Gold GE (2010) Differences in Patellofemoral Kinematics between Weight- Bearing and Non-Weight-Bearing Conditions in Patients with Patellofemoral Pain. J Orthop Res 29:312–317

10. Dunning H, van de Groes SAW, Buckens CF, Prokop M, Verdonschot N, Janssen D (2023) Fully automatic extraction of knee kinematics from dynamic CT imaging; normative tibiofemoral and patellofemoral kinematics of 100 healthy volunteers. Knee The Author(s) 41:9–17

11. Elliott CC, Diduch DR (2001) Biomechanics of patellofemoral instability. Oper Tech Sports Med 9:112–121

12. Esfandiarpour F, Lebrun CM, Dhillon S, Boulanger P (2018) In-vivo patellar tracking in individuals with patellofemoral pain and healthy individuals. J Orthop Res 36:2193–2201

13. Fabricant PD, Heath MR, Mintz DN, Emery K, Veerkamp M, Gruber S, Green DW, Strickland SM, Wall EJ, Shubin Stein BE, Parikh SN, Brady JM, Chambers CC, Ellis HB, Farr J, Heyworth BE, Koh JL, Kramer DE, Magnussen RA, Redler LH, Sherman SL, Tompkins MA, Wilson PL (2022) Many Radiographic and Magnetic Resonance Imaging Assessments for Surgical Decision Making in Pediatric Patellofemoral Instability Patients Demonstrate Poor Interrater Reliability. Arthrosc J Arthrosc Relat Surg The Arthroscopy Association of North America

14. Fick CN, Grant C, Sheehan FT (2020) Patellofemoral Pain in Adolescents: Understanding Patellofemoral Morphology and Its Relationship to Maltracking. Am J Sports Med 48:341–350

15. Flury A, Hodel S, Hasler J, Hooman E, Fucentese SF, Vlachopoulos L (2022) The winking sign is an indicator for increased femorotibial rotation in patients with recurrent patellar instability. Knee Surgery, Sport Traumatol Arthrosc Springer Berlin Heidelberg 30:3651–3658

16. Freedman BR, Sheehan FT (2013) Predicting three-dimensional patellofemoral kinematics from static imaging-based alignment measures. J Orthop Res 31:441–447

17. Garetier M, Borotikar B, Makki K, Brochard S, Rousseau F, Ben Salem D (2020) Dynamic MRI for articulating joint evaluation on 1.5 T and 3.0 T scanners: setup, protocols, and real-time sequences. Insights Imaging Insights into Imaging 11

18. Grant C, Fick CN, Welsh J, McConnell J, Sheehan FT (2021) A Word of Caution for Future Studies in Patellofemoral Pain: A Systematic Review With Meta-analysis. Am J Sports Med 49:538–551

19. Gray HA, Guan S, Thomeer LT, Schache AG, de Steiger R, Pandy MG (2019) Three-dimensional motion of the knee-joint complex during normal walking revealed by mobile biplane x-ray imaging. J Orthop Res 37:615–630

20. Julious SA (2005) Sample size of 12 per group rule of thumb for a pilot study. Pharm Stat 4:287–291

21. Kedgley AE, McWalter EJ, Wilson DR (2015) The effect of coordinate system variation on in vivo patellofemoral kinematic measures. Knee Elsevier B.V. 22:88–94

22. Kim C, Yeom S, Ahn S, Kang N, Park K, Jeon K (2022) Effects of Patellofemoral Pain Syndrome on Changes in Dynamic Postural Stability during Landing in Adult Women. Appl Bionics Biomech 2022:1–8

23. McDonald RJ, Schwartz KM, Eckel LJ, Diehn FE, Hunt CH, Bartholmai BJ, Erickson BJ, Kallmes DF (2015) The Effects of Changes in Utilization and Technological Advancements of Cross-Sectional Imaging on Radiologist Workload. Acad Radiol Elsevier Inc. 22:1191–1198

24. Mokkink LB, Prinsen CAC, Patrick DL, Alonso J, Bouter LM, de Vet HCW, Terwee CB (2019) COSMIN Study Design checklist for Patient-reported outcome measurement instruments. 1–31

25. Post WR, Teitge R, Amis A (2002) Patellofemoral malalignment: Looking beyond the viewbox. Clin Sports Med 21:521–546

26. Rathleff MS, Samani A, Olesen JL, Roos EM, Rasmussen S, Christensen BH, Madeleine P (2013) Neuromuscular activity and knee kinematics in adolescents with patellofemoral pain. Med Sci Sports Exerc 45:1730–1739

27. Rosa SB, Ewen PM, Doma K, Ferrer JFL, Grant A (2019) Dynamic Evaluation of Patellofemoral Instability: A Clinical Reality or Just a Research Field? A Literature review. Orthop Surg 11:932–942

28. Scott WN (2007) Insall and Scott, Surgery of the Knee. Vol 2, Capitulo 79, pp 1367–1407

29. Sheehan FT, Derasari A, Brindle TJ, Alter KE (2009) Understanding patellofemoral pain with maltracking in the presence of joint laxity: Complete 3D in vivo patellofemoral and tibio-femoral kinematics. J Orthop Res 27:561–570

30. Shen A, Boden BP, Grant C, Carlson VR, Alter KE, Sheehan FT (2021) Adolescents and adults with patellofemoral pain exhibit distinct patellar maltracking patterns. Clin Biomech Elsevier Ltd 90:105481

31. Shibanuma N, Sheehan FT, Stanhope SJ (2005) Limb positioning is critical for defining patel-lofemoral alignment and femoral shape. Clin Orthop Relat Res 434:198–206

32. Souza RB, Draper CCE, Fredericson M, Powers MDCM (2010) Femur Rotation and Patellofemo-ral Joint Kinematics: A Weight-Bearing Magnetic Resonance Imaging Analysis. 40:277–285

33. Tanaka MJ, Elias JJ, Williams AA, Carrino JA, Cosgarea AJ (2015) Correlation between Changes in Tibial Tuberosity-Trochlear Groove Distance and Patellar Position during Active Knee Ex-tension on Dynamic Kinematic Computed Tomographic Imaging. Arthrosc - J Arthrosc Relat Surg Arthroscopy Association of North America 31:1748–1755

34. Tanaka MJ, Elias JJ, Williams AA, Demehri S, Cosgarea AJ (2016) Characterization of patellar maltracking using dynamic kinematic CT imaging in patients with patellar instability. Knee Surgery, Sport Traumatol Arthrosc Springer Berlin Heidelberg 24:3634–3641

6

35. Victor J, Labey L, Wong P, Innocenti B, Bellemans J (2010) The influence of muscle load on tibiofemoral knee kinematics. J Orthop Res 28:419–428
36. Yu Z, Yao J, Wang X, Xin X, Zhang K, Cai H, Fan Y, Yang B (2019) Research Methods and Progress of Patellofemoral Joint Kinematics: A Review. J Healthc Eng Hindawi 2019

6

Chapter 7

Summary & General Discussion

Patellofemoral pain (PFP) is a musculoskeletal condition that is commonly associated with patellar maltracking, a condition in which the patella follows an unusual path to and through the femoral trochlea. Patellar tracking is governed by an intricate interaction between the soft tissue envelope, neuromuscular control and bony congruence of the patella and femur[1,2]. A disruption of this interaction can lead to patellar maltracking, or in severe cases, dislocation of the patella out of the femoral trochlear groove (TG). If such dislocations occur easily and frequent, this condition is called patellofemoral instability (PFI). Patella dislocation is painful, may cause damage to surrounding tissues and has been associated with development of osteoarthritis[3].

The primary treatment for PFI is conservative, but if conservative treatment is insufficient there are several surgical options to treat PFI, which aim to reconstruct normal movement and tissue loading. Since the cause of PFI is often complex and multifactorial, determining a patient-specific treatment plan can be challenging. The outcomes of surgical interventions for PFI varies and depends on the specific cause and severity of the condition[4,5]. To achieve optimal results, it is important to accurately diagnose and quantify the biomechanical cause of pain or instability in order to choose the optimal treatment.

Medical imaging plays a crucial role in the diagnosis and evaluation of the cause of PFI and patellar maltracking. Traditionally, imaging in clinical practice is done under static conditions, which does not take into account the dynamics of motion or the influence of ligaments, tendons, and muscles[6]. In recent years, various dynamic imaging techniques have been developed to improve the diagnosis of PFI, yet they are not widely used in clinical practice[7]. The aim of this thesis was to implement dynamic computed tomography (4DCT) imaging in the clinical evaluation of complex knee disorders in order to objectively quantify knee kinematics. The use of 4DCT imaging in the clinical evaluation of complex knee disorders can help to objectively quantify the impact of conditions such as PFI on knee movement, potentially leading to more patient-specific and effective treatment.

Thesis outline

To determine the cause and extent of PFI, several measurements have been developed that utilize static imaging. The Tibial Tuberosity – Trochlear Groove (TT-TG) distance is a widely used measurement to distinguish between healthy and pathological (mediolateral) insertion of the patellar tendon on the tibia. The TT-TG distance is commonly measured on a CT or Magnetic Resonance Imaging (MRI) scan and has absolute, yet debated, cut-off values that are dependent on the imaging modality[8]. In **chapter 3** it was examined whether, and to what extent, the TT-TG measurement is

7

affected by variations in patient orientation in the CT scanner during scanning. To this end, the TT-TG distance measurement was automated with a computer algorithm to ensure measurement consistency. The bilateral TT-TG distance of 100 healthy subjects was calculated on CT scans in the orientation the subject was scanned, and in simulated orientations where the subject was tilted up to 7 degrees with respect to the longitudinal axis of the CT scanner in the frontal plane. The results of this study showed that the TT-TG distance is sensitive to variations in subject orientation as the measured distance changes by approximately 1 mm per simulated degree of deviation. Moreover, during a routine CT scan, small to substantial alignment variations of 1.02±2.23° (range: -5.6° to 6.6°) can be observed which are poorly recognizable from the axial views on which the TT-TG is measured. Given the considerable effect of alignment variation on the TT-TG distance measurement, the degree of alignment variation during routine knee CT scans and the measurements' absolute cut-off values, the orthopaedic community should be aware of this sensitivity. Where possible, alignment correction should be applied during image postprocessing to minimise the ensuing differences and facilitate better intersubject comparison.

Knee movement and knee morphology are related, and altered knee morphology due to pathology or trauma can therefore affect movement and change tissue loading[9,10]. During surgical treatment of PFI and other conditions such as fractures of the tibia plateau, the aim of the surgeon is to perform anatomic reconstruction to restore function and to prevent complications. In **chapter 4** the symmetry of the left and right tibia plateau was established, to determine if left-right mirroring can be used for preoperative surgical planning of tibial plateau fractures. To this end, surface models of left and right tibia plateaus were mirrored and superimposed. Distances between the surface models were calculated and visualized in distance maps. The overall mean squared distances between correspondence points was 0.6276mm ± 0.0343mm, indicating that left and right tibia plateaus are highly symmetric. Furthermore, no locations on the tibia plateau were identified where the differences were structurally the highest. These results suggest that mirroring the contralateral side is a solid starting point for preoperative surgical planning of tibial plateau fractures. Since altered knee kinematics are often associated with abnormal anatomy, mirroring anatomy may provide a solution for patients with unilateral complaints. By further investigating the relationship between altered anatomy and kinematics, the cause of maltracking can be determined and a healthy joint can potentially be reconstructed based on the unaffected side.

Establishing normative knee kinematics is important to understand how knee disorders affect knee kinematics and how kinematics in patients differ from healthy individuals. **Chapter 5** describes the knee kinematics of 100 healthy subjects extracted from 4DCT. A 4DCT scan protocol was developed for imaging of an active knee movement.

Furthermore, a method was developed to automatically extract TF and PF kinematics from the imaging data. Knee kinematics found in this study were similar to those in literature, with key phenomena such as the screw home mechanism and femoral rollback being clearly visible. The scan protocol allows for high spatial and temporal resolution at a low radiation dose of 0.08 mSv. Due to its easy-to-execute protocol and automated analysis, this method allows implementation of 4DCT imaging in daily clinical practice. Despite the clear general kinematic patterns, one of the key findings was that considerable variation in knee kinematics can be observed in the healthy population that was analysed.

Multiple studies conclude that dynamic imaging provides valuable insights into (pathological) knee kinematics and underline the need for objective and accurate determination of subject-specific knee kinematics. Nevertheless, dynamic imaging remains a research exercise and is rarely applied in clinical practice. In **Chapter 6** twenty-one patients diagnosed with objective PFI underwent a 4DCT scan. The feasibility of 4DCT scanning and the automated analysis in clinical practice was determined, and it was examined whether the methods are capable of distinguishing healthy and pathological knee kinematics. Therefore, the TF and PF kinematics of these patients were compared to the normative kinematics of 97 healthy control subjects acquired in **Chapter 5**. All patients were able to successfully complete the protocol, all data was successfully segmented, registered, and coordinate systems for the femur, patella and tibia were calculated. The weight and length of both groups were equal, yet the patients had a higher body mass index (BMI). The results of this study indicate that both tibiofemoral and patellofemoral kinematics are affected in patients with recurrent PFI compared to healthy individuals. Patients exhibit increased external rotation of the tibia, a larger posterior translation of the lateral femoral condyle, more lateral translation of the patella, and a lower patella flexion at equal TF flexion. In addition, they show more lateral patella tilt over the entire range of motion. The fact that all patients were able to complete the scan protocol and that the automatic analysis is fast and able to distinguish between pathological and healthy knee kinematics makes it applicable in daily clinical practice.

General discussion

Diagnosing and quantifying knee disorders of a dynamic, multifaceted nature is a significant challenge. To optimize and standardize treatment of such disorders many attempts have been made to capture the effects of knee disorders on knee kinematics in both physical examination and radiological measurements. Because knee kinematics is such a complex and multifaceted phenomenon, there is a danger of oversimplification through interpretation of static, two-dimensional and orthogonal medical images. This

7

is supported by this thesis as it is demonstrated that the widely used TT-TG measurement has methodological inaccuracies that may affect clinical decision-making. Even seemingly simple rotational measurements contain complexities and are dependent on multiple (anatomical) factors. Innovations in the field of medical imaging and the development of new software- and artificial-intelligence algorithms, have the potential to better map such complex conditions without adding to the already high workload of clinicians. In this thesis the development of a 4DCT protocol and automated analysis for obtaining 3D knee kinematics is presented. The developed methods were applied to a large cohort of one hundred healthy subjects and a population of patients with patellofemoral conditions. The results of this thesis demonstrate the potential of 4DCT imaging combined with automated analysis in the diagnosis and quantification of orthopaedic disorders in clinical practice.

Normative kinematics

The established normative kinematics acquired in chapter 5 have the potential to serve as a benchmark for the future assessments of knee kinematics after TKA, ligament reconstruction, or patellofemoral interventions. The data offers important insights in the function and relation of TF and PF kinematics. An important finding is the considerable amount of variation in knee kinematics in both the healthy subject and patient group. While this variation complicates the interpretation and classification of the results, it confirms the complex aetiology of PF disorders as well as the need for novel and improved, objective diagnostic methods such as proposed in this thesis.

As described in chapter 5 and 6, part of the kinematic variation can be attributed to the scan protocol and analysis method[11–13]. For example, the freedom of movement and pace during the scan ensures that movement is as natural as possible. While this could be considered a strength of the methods, it does create heterogeneity in kinematic results, complicating analysis and comparison.

By using deterministic algorithms for determining knee kinematics, they can be determined in large cohorts in a consistent manner. The results of chapter 2 show that knee kinematics can be described with acceptable accuracy using anatomical coordinate systems. The differences in kinematic description between patients and healthy subject as a result of using such anatomical coordinate systems is therefore within acceptable limits. Consequently, the majority of variations are the result of actual differences between subjects in knee kinematics during a flexion extension movement. This demonstrates that apart from substantial variation in morphology and alignment, healthy individuals have highly variable knee kinematics[14]. As shown in Chapters 5 and 6, there is not only a considerable kinematic range within which healthy individuals move, but also considerable overlap with those of patients with patellofemoral

instability. Although there are clear differences in kinematic patterns, there are also patients with painful knees who show a kinematic pattern similar to that of healthy individuals, making it more complicated to distinguish them from each other. Thus definition of patella maltracking as a deviation from 'normal, healthy' patella tracking may be an oversimplified definition and needs to be refined. Understanding the nature and consequences of variation may offer new insights into the PF joint and in the definition of patella (mal)tracking. To fully utilize the diagnostic potential of 4DCT, more advanced analysis methods will need to be developed, which are able to distinguish possible differences in kinematic patterns at a functional level.

Patient kinematics

As demonstrated in chapter 6 4DCT imaging can be used in a clinical setting and the analysis methods are capable of identifying differences in three-dimensional knee kinematics between patients and healthy subjects. This allows the causes and effects of complex knee disorders to be quantitatively determined, without possibly subjective judgement of the treating physician.

To make the methods clinically feasible, they should possess a number of distinct properties. Firstly, the scan protocol enables imaging with both high spatial and temporal resolution while the examination time marginally differs from a routine CT examination. The movement during the scan is simple and easy to perform, and in contrast to dynamic MRI, there is no strictly timed, repeated movement required, making it also feasible for people with painful knee joints [17–19]. Finally, the automatic analysis enables fast and consistent kinematic assessment without causing additional burden to the radiologist.

4DCT imaging and automated analysis have the potential to make clinical decision making less dependent on static measurements with poor interrater reliability and which have an unclear relationship with dynamic knee movement[15,16]. The implementation of 4DCT in clinical practice makes it possible to scan large patient groups, facilitating the establishment of a kinematic database. By including confounding factors in the database, such as age of onset of disease and demographics, a database could play a key role in understanding the complex aetiology of PF disorders.

Quantitative analysis of pre- and postoperative kinematics are insightful for the surgeon and enables to further optimize surgery and confirm the preoperative surgical plan based on quantitative data of the joints' dynamic behaviour rather than relying on intraoperative intuition. This quantitative analysis can aid in understanding the effects of the procedure, leading to improved treatment and potentially better long-term outcomes.

7

Data analysis & Interpretation

In the realisation of this thesis it has become apparent, that dynamic imaging requires a fundamentally different method of image analysis and interpretation compared to conventional static imaging. Current diagnostic imaging relies heavily on human interpretation of orthogonal, 2D images, which can be challenging even for static images and ignores the complex 3D nature of knee disorders. As a result, various diagnostic measurements have been proposed to support clinicians in the diagnosis, evaluation and quantification of disorders to facilitate in clinical decision-making. In case of dynamic imaging, the conventional orthogonal views provide limited insights and are difficult if not impossible to interpret. Additionally, a multitude of data is captured compared to static scanning, which renders manual assessment too time consuming for clinical practice. Furthermore, repeated manual measurements increase the likelihood of introducing inter- and intrarater variability, rendering the measurements inaccurate. The methods presented in this thesis are fully automatic, and allow for consistent measurement of knee kinematics and comparison of knee kinematics between patient groups and healthy individuals, facilitating clinical decision making.

However, these methods require further optimization. The use of existing measurements designed for static images on dynamic images can result in underutilization of the diagnostic potential of dynamic imaging and lead to complex, difficult-to-interpret results that cannot be easily compared. Due to natural variability in morphology, pose and movement, measurements that appear straightforward and simple in conventional 2D become multidimensional and complex in a dynamic situation. Moreover, existing terminology can easily cause confusion, for example due to the rotation of coordinate systems of adjacent anatomical structures.

The implementation of dynamic imaging, whether from CT or another modality, therefore requires further development of automated, new measurements as well as standardized terminology specifically developed for dynamic images. Newly developed measurements should not rely on absolute, general cut-off values, but rather consider the variability that exists in different populations and the potential overlap between patients and healthy individuals. Through such novel measurements, new clinical guidelines can be established to better assist clinicians in making an accurate clinical evaluation and developing the optimal treatment plan.

Enhancing diagnostic & clinical value

In addition to the development of novel measurements for quantification of kinematics and anatomy, the diagnostic value of dynamic imaging can be further enhanced through advanced analysis methods. For example, the unique aspect of simultaneous acquisition of PF and TF kinematics of the current method could be fully utilized by use

of a multidimensional regression model. While various studies have shown that TF & PF kinematics influence each other, they are often still determined and analysed separately, potentially leaving important interrelationships undiscovered[20,21].

More in-depth analysis methods such as Functional Principal Component Analysis (FPCA), could clarify the variation present in the healthy population. FPCA is a statistical technique that allows reduction of dataset dimensions while preserving the majority of information. Subtle multidimensional differences in kinematics that are not readily visible may become apparent, the complexity of current datasets may be reduced and the cause and magnitude of variation may be further explained. By linking this information to anatomical variation, relations between morphology and function can be revealed. This provides guidance for the surgeon, who can better understand what to aim for during treatment and ensures that surgical interventions become more patient-suited.

Similarly, other sophisticated analysis methods could include clustering algorithms such as BDSCAN or BIRCH. As is the case in gait analysis, these may reveal possible different phenotypes in knee kinematics[22,23]. Comparing such phenotypes can explain the overlap in kinematics between patients and healthy individuals and potentially show which individuals are prone to instability. This could also potentially clarify why certain individuals develop PFI following a traumatic event such as tearing of an MPFL.

A major advantage of such advanced (AI) methods is that they are able to approach complex conditions from multiple dimensions simultaneously. By relating the altered anatomy as a result of surgery and the difference between pre- and postoperative kinematics and incorporating outcomes of musculoskeletal models, such methods can accurately map the effects of surgical treatment. As algorithms such as Generalized Adversarial Networks (GAN) are capable of creating new information, this may even be used to create a preoperative surgical plan. In such case, the post-operative kinematics could be (partially) predicted. However, this requires large amounts of pre- and postoperative 4DCT images that need to be combined with surgical outcomes.

Scan protocol & loading conditions
The methods presented in this thesis settle a number of technical challenges regarding dynamic imaging, as raised in recent review articles[6,11,13]. For instance, the active muscle contraction as applied during the 4DCT scan enhances the ability to diagnose patella tracking disorders[11]. Moreover, three dimensional kinematics calculation, take into account complex movement across multiple axes simultaneously and ensure consistency in measurements through deterministic calculations. These improvements

7

increase the accuracy and usability of the results and are an integral step towards broad clinical implementation of 4DCT imaging in clinical practice.

Nevertheless, a number of topics need to be investigated to determine whether the applied methods are optimal for diagnosing PF disorders. A considerable number of articles have compared the kinematic differences between closed chain and open chain movement, and in weightbearing and non-weightbearing situations and concluded there are considerable differences[24–29]. The movement and loading conditions during the current protocol are relatively simple, non-weight bearing, and not prone to potential traumatic events. Episodes of patella luxation are therefore not likely to occur during the scan. The results obtained in this thesis can therefore not be extrapolated to weightbearing situations. However, this does not necessarily indicate that particular loading conditions are superior to the other for diagnosing specific knee disorders. For example, multiple studies demonstrate that translations and rotations are greater in unloaded than loaded conditions[24,26,30]. This could imply that non-weightbearing conditions provide a more complete picture of the effect of all the structures affecting PF kinematics. Moreover, the differences between weightbearing kinematics and non-weightbearing kinematics seem to be smaller than intersubject variation[21]. However, determining and optimizing the clinical value of the protocol is an important topic for future research.

Recent studies have shown that, among other things, patients with different demographics and onset of PF disorders demonstrate distinct kinematic patterns[31,32]. In future research on kinematics between patients (and/or healthy volunteers), it is therefore important that these groups are clearly defined and differentiated in order to prevent unwanted variables from influencing the kinematic results. The method presented in this thesis provides the capability to scan the large number of patients required for this type of research.

Other areas of 4DCT application
While the focus of this thesis was dynamic imaging of the knee joint, minor adjustments of the developed protocol and analysis method allow for analysis of other joints. The main requirements for using this method for 4DCT imaging of other joints are that the joint (partially) fits within the dynamic field of view of the CT scanner and that movement relevant for diagnosis is possible within the gantry of the CT scanner.

Key examples of other joints include the wrist, ankle, and hindfoot. For example, 4DCT can be used to diagnose joint instability or trigger lunate syndrome at the wrist[33]. Given the limited size of the structures in the wrist, the combined high spatial and temporal resolution of 4DCT is vital for proper assessment. The limited joint size also

provides possibilities for the use of a loading rig to compare loaded and unloaded wrist kinematics. Similarly, 4DCT offers possibilities for assessment of ankle joint and hindfoot disorders which are frequently experienced during simple daily tasks and movements[17]. To avoid invoking pain during scanning, it is vital that images can be acquired quickly and without repetition, as is not the case for dynamic MRI. In the case of the ankle and foot, previous publications on other dynamic modalities have already established the foundation for determining anatomical axis systems, their reproducibility, and the definition of movements[34,35].

Despite the fact that X-ray imaging techniques (e.g. CT scans) of metal objects can result in substantial image artifacts, advancements in iterative and deep learning-based reconstruction algorithms have made it possible to significantly enhance image quality and minimize these artifacts. Using a slightly modified scanning and analysis method as utilized in this thesis, this allows for extraction of knee kinematics with a knee implant. As a result, 4DCT can be used to analyze knee kinematics in a clinically accessible manner which can be used to further optimize total knee replacement design and surgery. Firstly, by determining the effects of TKA by comparing pre- and postoperative kinematics and linking these results to surgical outcomes and patient satisfaction. Secondly, the kinematic alignment of existing knee implants can be planned patient-specific, or a (patient-specific) knee implants can be developed so that pre-diseased knee kinematics are more closely mimicked.

Conclusions

In conclusion, the results of this thesis show that the widely used TT-TG measurement is sensitive to patient orientation in the CT scanner, and that the high frequency and degree to which orientation deviations occur during routine CT exams may potentially affect clinical decision-making. Moreover, it is demonstrated that anatomical variation affects the determination of coordinate systems used to describe knee kinematics, but these systems can nevertheless be used to describe kinematics with reasonable certainty. Morphological analysis shows that the left and right tibia plateaus have highly similar shape, which may allow for the use of the contralateral side as a reference for reconstructing the knee joint in patients with unilateral complaints. The scan protocol and automated postprocessing presented in this thesis allow for extraction of knee kinematics in a clinical setting. Applying them to healthy subjects and PFI patients revealed considerable variation in both healthy and pathological knee kinematics, but highlighted clear differences between healthy subjects and patients. This new knowledge will contribute to improving the clinical evaluation and quantification of complex knee disorders and lead to further optimize treatment modalities for these patients.

7

References

1. Rathleff MS, Samani A, Olesen JL, Roos EM, Rasmussen S, Christensen BH, et al. Neuromuscular activity and knee kinematics in adolescents with patellofemoral pain. Med Sci Sports Exerc 2013;45:1730–9. https://doi.org/10.1249/MSS.0b013e318292be30.

2. Scott WN. Insall and Scott, Surgery of the Knee. Vol. 2, Capitulo 79, 2007.

3. Eijkenboom JFA, Waarsing JH, Oei EHG, Bierma-Zeinstra SMA, Van Middelkoop M. Is patellofemoral pain a precursor to osteoarthritis? Bone Jt Res 2018;7:541–7. https://doi.org/10.1302/2046-3758.79.BJR-2018-0112.R1.

4. Hiemstra LA, Peterson D, Youssef M, Soliman J, Banfield L, Ayeni OR. Trochleoplasty provides good clinical outcomes and an acceptable complication profile in both short and long-term follow-up. Knee Surgery, Sport Traumatol Arthrosc 2019;27:2967–83. https://doi.org/10.1007/s00167-018-5311-x.

5. Schneider DK, Grawe B, Magnussen RA, Ceasar A, Parikh SN, Wall EJ, et al. Outcomes after Isolated Medial Patellofemoral Ligament Reconstruction for the Treatment of Recurrent Lateral Patellar Dislocations. Am J Sports Med 2016;44:2993–3005. https://doi.org/10.1177/0363546515624673.

6. Rosa SB, Ewen PM, Doma K, Ferrer JFL, Grant A. Dynamic Evaluation of Patellofemoral Instability: A Clinical Reality or Just a Research Field? A Literature review. Orthop Surg 2019;11:932–42. https://doi.org/10.1111/os.12549.

7. Dandu N, Knapik DM, Trasolini NA, Zavras AG, Yanke AB. Future Directions in Patellofemoral Imaging and 3D Modeling 2022.

8. Dejour H, Walch G, Nove-Josserand L, Guier C. Factors of patellar instability: An <b>anatomic<b/> radiographic study. Knee Surgery, Sport Traumatol Arthrosc 1994;2:19–26. https://doi.org/10.1007/BF01552649.

9. Rood A, Hannink G, Lenting A, Groenen K, Koëter S, Verdonschot N, et al. Patellofemoral Pressure Changes After Static and Dynamic Medial Patellofemoral Ligament Reconstructions. Am J Sports Med 2015;43:2538–44. https://doi.org/10.1177/0363546515594447.

10. Fick CN, Grant C, Sheehan FT. Patellofemoral Pain in Adolescents: Understanding Patellofemoral Morphology and Its Relationship to Maltracking. Am J Sports Med 2020;48:341–50. https://doi.org/10.1177/0363546519889347.

11. Grant C, Fick CN, Welsh J, McConnell J, Sheehan FT. A Word of Caution for Future Studies in Patellofemoral Pain: A Systematic Review With Meta-analysis. Am J Sports Med 2021;49:538–51. https://doi.org/10.1177/0363546520926448.

12. Kedgley AE, McWalter EJ, Wilson DR. The effect of coordinate system variation on in vivo patellofemoral kinematic measures. Knee 2015;22:88–94. https://doi.org/10.1016/j.knee.2014.11.006.

13. Yu Z, Yao J, Wang X, Xin X, Zhang K, Cai H, et al. Research Methods and Progress of Patellofemoral Joint Kinematics: A Review. J Healthc Eng 2019;2019. https://doi.org/10.1155/2019/9159267.

14. Hochreiter B, Hess S, Moser L, Hirschmann MT, Amsler F, Behrend H. Healthy knees have a highly variable patellofemoral alignment: a systematic review. Knee Surgery, Sport Traumatol Arthrosc 2019. https://doi.org/10.1007/s00167-019-05587-z.

15. Fabricant PD, Heath MR, Mintz DN, Emery K, Veerkamp M, Gruber S, et al. Many Radiographic and Magnetic Resonance Imaging Assessments for Surgical Decision Making in Pediatric Patellofemoral Instability Patients Demonstrate Poor Interrater Reliability. Arthrosc J Arthrosc Relat Surg 2022. https://doi.org/10.1016/j.arthro.2022.03.033.

16. Freedman BR, Sheehan FT. Predicting three-dimensional patellofemoral kinematics from static imaging-based alignment measures. J Orthop Res 2013;31:441–7. https://doi.org/10.1002/jor.22246.

17. Borotikar B, Lempereur M, Lelievre M, Burdin V, Ben Salem D, Brochard S. Dynamic MRI to quantify musculoskeletal motion: A systematic review of concurrent validity and reliability, and perspectives for evaluation of musculoskeletal disorders. PLoS One 2017;12:1–26. https://doi.org/10.1371/journal.pone.0189587.

18. Garetier M, Borotikar B, Makki K, Brochard S, Rousseau F, Ben Salem D. Dynamic MRI for articulating joint evaluation on 1.5 T and 3.0 T scanners: setup, protocols, and real-time sequences. Insights Imaging 2020;11. https://doi.org/10.1186/s13244-020-00868-5.

19. Mazzoli V, Schoormans J, Froeling M, Sprengers AM, Coolen BF, Verdonschot N, et al. Accelerated 4D self-gated MRI of tibiofemoral kinematics. NMR Biomed 2017;30:1–11. https://doi.org/10.1002/nbm.3791.

20. McWalter EJ, Cibere J, MacIntyre NJ, Nicolaou S, Schulzer M, Wilson DR. Relationship between varus-valgus alignment and patellar kinematics in individuals with knee osteoarthritis. J Bone Jt Surg - Ser A 2007;89 A:2723–31. https://doi.org/10.2106/JBJS.F.01016.

21. Kefala V, Ali AA, Hamilton LD, Mannen EM, Shelburne KB. Effects of Weight-Bearing on Tibiofemoral, Patellofemoral, and Patellar Tendon Kinematics in Older Adults. Front Bioeng Biotechnol 2022;10:1–12. https://doi.org/10.3389/fbioe.2022.820196.

22. Zgolli F, Henni K, Haddad R, Mitiche A, Ouakrim Y, Hagemeister N, et al. Kinematic data clustering for healthy knee gait characterization. 2018 IEEE Life Sci Conf LSC 2018 2018:239–42. https://doi.org/10.1109/LSC.2018.8572119.

23. Mezghani N, Soltana R, Ouakrim Y, Cagnin A, Fuentes A, Hagemeister N, et al. Healthy knee kinematic phenotypes identification based on a clustering data analysis. Appl Sci 2021;11. https://doi.org/10.3390/app112412054.

24. Draper CE, Besier TF, Fredericson M, Santos JM, Gary S, Delp SL, et al. Differences in Patellofemoral Kinematics between Weight- Bearing and Non-Weight-Bearing Conditions in Patients with Patellofemoral Pain. J Orthop Res 2010;29:312–7. https://doi.org/10.1002/jor.21253.

25. Stensdotter AK, Hodges PW, Mellor R, Sundelin G, Häger-Ross C. Quadriceps Activation in Closed and in Open Kinetic Chain Exercise. Med Sci Sports Exerc 2003;35:2043–7. https://doi.org/10.1249/01.MSS.0000099107.03704.AE.

26. Fritz B, Fritz J, Fucentese SF, Pfirrmann CWA, Sutter R. Three-dimensional analysis for quantification of knee joint space width with weight-bearing CT: comparison with non-weight-bearing CT and weight-bearing radiography. Osteoarthr Cartil 2022;30:671–80. https://doi.org/10.1016/j.joca.2021.11.019.

27. Lacerda Nobre T. Comparison of Exercise Open Kinetic Chain and Closed Kinetic Chain in The Rehabilitation of Patellofemoral Dysfunction: an Updated Revision. Clin Med Diagnostics 2012;2:1–5. https://doi.org/10.5923/j.cmd.20120203.01.

28. Sadoghi P, Camp CL, Stuart MJ, Krych AJ, Levy BA, Bond JR, et al. The Tibial Tubercle–Trochlear Groove Distance: Letter to the Editor. Am J Sports Med 2013;41:NP51-2. https://doi.org/10.1177/0363546513510142.

29. Lullini G, Belvedere C, Busacca M, Moio A, Leardini A, Caravelli S, et al. Weight bearing versus conventional CT for the measurement of patellar alignment and stability in patients after surgical treatment for patellar recurrent dislocation. Radiol Medica 2021;126:869–77. https://doi.org/10.1007/s11547-021-01339-7.

30. Victor J, Labey L, Wong P, Innocenti B, Bellemans J. The influence of muscle load on tibiofemoral knee kinematics. J Orthop Res 2010;28:419–28. https://doi.org/10.1002/jor.21019.

7

31. Shen A, Boden BP, Grant C, Carlson VR, Alter KE, Sheehan FT. Adolescents and adults with patellofemoral pain exhibit distinct patellar maltracking patterns. Clin Biomech 2021;90:105481. https://doi.org/10.1016/j.clinbiomech.2021.105481.

32. Fick CN, Jiménez-Silva R, Sheehan FT, Grant C. Patellofemoral kinematics in patellofemoral pain syndrome: The influence of demographic factors. J Biomech 2022;130. https://doi.org/10.1016/j.jbiomech.2021.110819.

33. Kwong Y, Mel AO, Wheeler G, Troupis JM. Four-dimensional computed tomography (4DCT): A review of the current status and applications. J Med Imaging Radiat Oncol 2015;59:545–54. https://doi.org/10.1111/1754-9485.12326.

34. Makki K, Borotikar B, Garetier M, Brochard S, Ben Salem D, Rousseau F. In vivo ankle joint kinematics from dynamic magnetic resonance imaging using a registration-based framework. J Biomech 2019;86:193–203. https://doi.org/10.1016/j.jbiomech.2019.02.007.

35. Brown JA, Gale T, Anderst W. An automated method for defining anatomic coordinate systems in the hindfoot. J Biomech 2020;109. https://doi.org/10.1016/j.jbiomech.2020.109951.

7

Chapter 8

Nederlandse samenvatting

Patellofemorale pijn (PFP) is de medische benaming voor veelvoorkomende pijnklachten rond de knieschijf. PFP wordt geassocieerd met 'patella maltracking' waarbij het pad van de patella (knieschijf) naar en door een femorale trochlea (groeve in dijbeen) afwijkt van normaal. De tracking (sporing) van de patella is het gevolg van een complexe wisselwerking tussen zachte weefsels zoals spier en bindweefsel, neuromusculaire controle en de congruentie van de patella en het femur[1,2]. Een verstoring van deze interactie kan resulteren in patella maltracking of in ernstige gevallen tot een luxatie van de patella uit de trochlea. Indien dergelijke luxaties frequent en gemakkelijk voorkomen, spreekt men van patellofemorale instabiliteit (PFI). Zowel maltracking als luxaties zijn pijnlijk en kunnen schade aanbrengen aan omliggende weefsels. Daarnaast wordt het in verband gebracht met het ontstaan van artrose[3].

De primaire behandeling voor PFI is conservatief, maar indien deze behandeling onvoldoende resultaat boekt zijn er verschillende chirurgische behandelingen mogelijk. Deze behandelingen hebben als doel de gezonde beweging en weefsel belasting te reconstrueren. De oorzaak van PFI is vaak complex en multifactorieel, waardoor het bepalen van de optimale, patiënt specifieke behandelmethode even ingewikkeld is. Ook zijn de uitkomsten van de verschillende chirurgische interventies variabel en in grote mate afhankelijk van de onderliggende oorzaak en ernst van de aandoening[4,5]. Om het optimale resultaat te bereiken is het belangrijk om de biomechanische oorzaak van pijn of instabiliteit nauwkeurig te diagnosticeren en evalueren om vervolgens de optimale behandelmethode te bepalen.

Medische beeldvorming speelt een cruciale rol bij de diagnose en evaluatie van zowel PFI en patella maltracking als andere spierskelet aandoeningen. In de praktijk wordt deze beeldvorming veelal onder statische omstandigheden verkregen, waarbij de patiënt zo stil mogelijk ligt tijdens het maken van de scan. Aangezien PFI en patella maltracking bij uitstek aandoeningen zijn met een dynamische aard, wordt bij deze manier van beeldvorming het effect van beweging of de invloed van spieren, pezen en ligamenten op het sporen van de patella niet vastgelegd[6]. In de afgelopen jaren zijn om deze reden verschillende dynamische beeldvormingstechnieken ontwikkeld. Deze technieken zijn in staat de dynamische aspecten in kaart te brengen en kunnen mogelijk de diagnose en evaluatie van aandoeningen zoals PFI verbeteren. Helaas worden dergelijke dynamische beeldvormingstechnieken nauwelijks toegepast in de klinische praktijk en slechts sporadisch in wetenschappelijk onderzoek gebruikt[7]. Het doel van dit proefschrift was om dynamische computed tomography (4DCT) toe te passen bij de klinische evaluatie van patiënten met complexe knieaandoeningen om de kniekinematica (beweging van de knie) objectief te kunnen kwantificeren. Het gebruik van 4DCT biedt de mogelijkheid om het effect van aandoeningen zoals PFI op

de beweging van de knie te bepalen, waardoor effectievere en meer patiënt specifieke behandeling mogelijk wordt.

Thesis overzicht

Voor het beschrijven van kniekinematica wordt meestal gebruik gemaakt van anatomische coördinaten systemen (ACS). Het gebruik van dergelijken coördinaten systemen heeft de voorkeur boven alternatieven zoals de (finite) helical axis vanwege de relatief makkelijke visualisatie en interpretatie van de resultaten. Als gevolg van normale anatomische variatie in een (patiënt)populatie ontstaan echter inherente verschillen in de bepaling van het ACS. In de vergelijking van kinematica tussen personen kunnen daardoor verschillen ontstaan die niet zozeer het gevolg zijn van een bepaalde pathologie, maar van verschillen in de bepaling van het ACS. Hierdoor wordt het ingewikkeld om kniekinematica tussen patiënten of groepen te vergelijken en wordt het vaststellen van mogelijke relaties tussen veranderde beweging en knieaandoeningen moeilijker. In hoofdstuk 2 werd onderzocht in welke mate een ACS van de knie wordt beïnvloed door anatomische variatie van het bot. Hiervoor werd gebruikt gemaakt van statistical shape models om de vorm van de knie te parameteriseren. De resultaten van dit onderzoek laten zien dat het ACS van de patella het meest gevoelig is voor anatomische variatie ten opzichte van dat van het femur en tibia. Als gevolg vertoont de beschrijving van patellofemorale (PF) kinematica de meeste onzekerheid. De beschrijving van tibiofemorale (TF) en PF kinematica hadden een maximale onzekerheid van respectievelijk 5.0° en 13,5°. Hiermee werd aangetoond dat zelfs in knieën die qua vorm aanzienlijk afwijken van het gemiddelde, de kinematica met acceptabele nauwkeurigheid kan worden bepaald. Gezien het brede gebruik van ACS is het van belang dat de orthopedische gemeenschap zich bewust is van de (on)nauwkeurigheid van dergelijke systemen, in het bijzonder omdat verscheidene aandoeningen gepaard gaan met afwijkende anatomie.

Om de oorzaak en ernst van PFI te bepalen zijn verschillende metingen ontwikkeld op basis van beeldvormend medisch onderzoek. De Tibial Tuberosity – Trochlear Groove (TT-TG) afstand is een veel gebruikte meting om mogelijke pathologische laterale insertie van de patellapees op de tibia vast te stellen. De TT-TG afstand wordt gemeten op statische CT of MRI en heeft absolute maar betwiste afkapwaarden die afhankelijk zijn dan de modaliteit waarop de meting wordt gedaan [8]. In hoofdstuk 3 is onderzocht of, en in welke mate, de TT-TG meting wordt beïnvloed door veranderingen in de oriëntatie van de patiënt in de CT-scanner. Om consistentie van de meting te waarborgen werd de TT-TG meting geautomatiseerd met een computeralgoritme. De TT-TG afstand werd bilateraal gemeten op CT-scans van 100 gezonde proefpersonen. Dit werd gedaan in de oriëntatie waarin deze personen werden gescand, en in gesimuleerde oriëntaties

waarbij de proefpersonen tot 7° schuin lagen ten opzichte van de lengteas van de CT-scanner in het frontale vlak. De resultaten van dit onderzoek laten zien dat de TT-TG afstand gevoelig is voor oriëntatie van de patiënt en veranderde met circa 1 mm per gesimuleerde graad afwijking. Daarnaast werden tijdens het onderzoek variaties in uitlijning waargenomen (1,0±2,2° (bereik: -5,6° tot 6,6°)) die slecht zichtbaar zijn op de axiale aanzichten waarop de TT-TG afstand wordt gemeten. Gezien het effect van de patiënt oriëntatie op de meting, de mate waarin deze voorkomt, de absolute afkapwaarden van de meting en de rol van de meting bij klinische besluitvorming, dient de orthopedische gemeenschap zich bewust te zijn van deze gevoeligheden. Waar mogelijk moet tijdens het uitwerken van de beeldvorming een correctie worden toegepast om de effecten op de TT-TG afstand te minimaliseren en zo betere vergelijking binnen en tussen patiënten mogelijk te maken.

De morfologie van de knie en de manier waarop deze beweegt zijn aan elkaar gerelateerd. Door veranderingen in morfologie als gevolg van trauma of ziekte is het mogelijk dat de beweging en weefselbelasting verandert[9,10]. Om de functie en beweging van de knie te herstellen wordt bij de chirurgische behandeling van fracturen van zowel het tibiaplateau als PFI daarom vaak een anatomische reconstructie uitgevoerd. In hoofdstuk 4 werd de symmetrie van het linker en rechter tibia plateau onderzocht, om te bepalen of links-rechts spiegeling kan worden gebruikt als uitgangspunt voor preoperatieve chirurgische planning van tibia plateau fracturen. Hiervoor werden 3D computermodellen gemaakt van het linker en rechter tibiaplateau. De modellen van de rechter plateaus werden gespiegeld en geregistreerd op de linker plateaus waarna de afstand tussen de twee oppervlakken werd berekend en gevisualiseerd. De gemiddelde afstand tussen corresponderende punten op deze oppervlakken was 0,62 mm ± 0,03 mm. Daarnaast werd er geen specifieke locatie gevonden waar de verschillen structureel het grootst waren. Dit duidt op een grote mate van symmetrie tussen het linker en rechter tibiaplateau. Deze resultaten suggereren dat het spiegelen van de contralaterale zijde een goed uitgangspunt is voor preoperatieve chirurgische planning van fracturen in het tibiaplateau. Omdat veranderde kniekinematica vaak gepaard gaat met abnormale anatomie, biedt het spiegelen van de anatomie mogelijk een oplossing voor de behandeling van patiënten met unilaterale klachten van PFI. Door de relatie tussen veranderde anatomie en kinematica verder te onderzoeken, kan de oorzaak van maltracking worden vastgesteld en kan mogelijk de functie en beweging van een gewricht worden gereconstrueerd op basis van de contralaterale zijde.

Om het effect van aandoeningen op de beweging van de knie te kunnen bepalen, is het van belang om normatieve kniekinematica te bepalen. In hoofdstuk 5 werd de kniekinematica van 100 gezonde proefpersonen bepaald, door middel van 4DCT. Hiervoor werd een scan-protocol ontwikkeld om een actieve beweging van de knie in

8

beeld te brengen. Daarnaast werd een methode ontwikkeld om de TF & PF kinematica automatisch uit de beelden te extraheren. De waarden vertonen grote overeenkomsten met die uit bestaande publicaties en onthullen belangrijke biomechanische kenmerken zoals het screw home mechanisme en femorale rollback. Het ontwikkelde scan protocol maakt het mogelijk om dynamisch te scannen met hoge spatiele en temporale resolutie terwijl de effectieve stralingsbelasting voor de patiënt beperkt blijft tot 0,08mSv. Dankzij het eenvoudig uit te voeren protocol en de geautomatiseerde analyse maakt deze methode implementatie van 4DCT-beeldvorming in de dagelijkse klinische praktijk mogelijk. Hoewel duidelijke bewegingspatronen zichtbaar waren, is de aanzienlijke variatie in kinematica binnen deze gezonde populatie een belangrijke bevinding van dit onderzoek

Eerdere wetenschappelijke publicaties concludeerden dat dynamische beeldvorming waardevolle inzichten geeft in (pathologische) kniekinematica en onderstreepten het belang van nauwkeurige, objectieve en patiënt specifieke kniekinematica. Desondanks wordt dynamische beeldvorming nauwelijks toegepast in de klinische praktijk en blijft de inzet beperkt tot wetenschappelijk onderzoek. In hoofdstuk 6 werd bepaald in hoeverre 4DCT kan worden ingezet in de dagelijkse klinische praktijk voor de diagnose en evaluatie van PFI. Daarnaast werd onderzocht of de scan en analyse methoden gepresenteerd in hoofdstuk 5 in staat waren om gezonde en pathologische kniekinematica te onderscheiden. Eenentwintig patiënten met patellofemorale instabiliteit ondergingen een 4DCT scan. De TF & PF kinematica van deze patiënten werd vergeleken met de in hoofdstuk 5 verkregen normatieve data van 97 gezonde proefpersonen. De resultaten van deze studie laten zien dat zowel tibiofemorale als patellofemorale kinematica anders is bij patiënten met PFI vergeleken met gezonde proefpersonen. Hierbij laten patiënten toegenomen externe rotatie van de tibia zien, grotere translatie van de femorale laterale condyl, grotere laterale translatie van de patella en lagere patellofemorale flexie bij gelijke tibiofemorale flexie. Tot slot vertonen patiënten over de gehele beweging een grotere patella tilt. Dat alle patiënten ondanks pijnklachten in staat waren het protocol te voltooien, de succesvolle geautomatiseerde analyse en het vermogen onderscheid te maken tussen pathologische en gezonde knie kinematica, laat zien dat 4DCT toepasbaar is in de dagelijkse klinische praktijk in de diagnose en evaluatie van complexe knieaandoeningen.

De onderzoeken beschreven in dit proefschrift dragen bij aan de verdere verbetering van de klinische evaluatie en kwantificatie van complexe knieaandoeningen en kunnen leiden tot geoptimaliseerde behandeling voor patiënten.

Appendices

Dankwoord

Wie mij een paar jaar geleden had gezegd dat ik een PhD zou gaan doen had ik voor gek verklaard. Maar daar zit ik dan, een dankwoord te schrijven voor mijn proefschrift. Ik heb geen moment spijt gehad van de beslissing om dit promotieonderzoek te gaan doen. De afgelopen jaren heb ik met veel plezier gewerkt bij het Orthopaedic Research Laboratory (ORL). Ook heb ik veel leuke nieuwe mensen ontmoet en ontzettend veel geleerd. Ik ben erg dankbaar voor deze mooie periode en voor alle hulp die ik heb gekregen. Met het risico dat ik iemand vergeet wil ik specifiek een aantal mensen bedanken.

Beste Nico, dank voor jouw rol als promotor. Ik heb er veel respect voor hoe hard jij kunt werken en hoeveel balletjes je in de lucht kunt houden. De hoeveelheid inhoudelijke kennis die je daarnaast paraat hebt, is opzienbarend. Ondanks je volle agenda was je altijd bereikbaar voor feedback op artikelen en presentaties of het meedenken bij onderzoeksmethoden. Bedankt voor alles en denk goed om jezelf.

Daar is hij dan Sebastiaan, mijn publicatie d…… Ontzettend bedankt voor je enthousiasme en inzet in het onderzoek dat we gedaan hebben en voor alle keren dat je je gewicht in de strijd hebt gegooid als het project ergens vast liep. Je vervult veel verschillende functies in het ziekenhuis en op de afdeling. Ik vind het erg knap hoe snel je situaties weet in te schatten en hoe je je vinger op de zere plek weet te leggen. En ondanks dat ook nog zo vaak kunnen lachen… Dankjewel!

Dennis, dankjewel voor alle technische en procedurele hulp, maar ook voor het relativeren en je (goede) flauwe humor. Als ik door de bomen het bos niet meer zag had jij dat vaak al door. Ook heb je meer dan eens mijn agenda bewaakt door sarcastisch te zeggen: "Dat kan Hans wel doen, die heeft nog wel tijd over". Je bent het aanspreekpunt voor velen binnen het ORL en dat je vrijwel elk jaar als supervisor van het jaar wordt genomineerd, zegt volgens mij genoeg. Dankjewel!

Dr. Buckens, beste Stan, toen jij als radioloog betrokken werd bij het 4DCT project heeft het project echt vleugels gekregen. Je hebt meermaals mensen gemobiliseerd om het een of ander voor elkaar te krijgen. Ook proefkonijn spelen voor wilde ideeën zoals belaste 4DCT vond je geen probleem. Dankjewel voor je enthousiasme en inzet.

Willem-Jan, Koen en Mirte, de echte CT piloten. Dankjewel voor de vele proefscans en uren overwerk om de grote hoeveelheid gezonde vrijwilligers te scannen.

A

Ook alle proefpersonen die deel hebben genomen aan het 4DCT Knie onderzoek wil ik enorm bedanken. Zonder jullie enthousiasme en nieuwsgierigheid was het nooit gelukt deze mooie resultaten te verkrijgen.

Jasper & Martijn, dank dat jullie mijn paranimfen willen zijn. Ook bedankt voor de leuke jaren bij het ORL, de gezellig borrels en de ontelbare potjes tafelvoetbal. Martijn, toen ik in 2018 naast je kwam zitten was het gelijk raak. We hebben vaak (om foute dingen) de slappe lach gehad en je hakkelende presentatie na het legen van de minibar zal me altijd bijblijven. Jasper, dankjewel voor de broodnodige afleiding in de vorm van reisfoto's, tafelvoetbal en filmpjes van klusprojecten. Je maakt echt hele gave dingen, dus een je kunt altijd nog een carrière switch overwegen.

Corine, we zijn lang elkaars collega's geweest. Tijdens de studie, tijdens de stage, tijdens het afstuderen en later samen bij het ORL. Die streak is nu ten einde gekomen, dank voor alle leuke gesprekken en de 'lekkere' kopjes koffie. Heel veel succes & plezier in Barcelona.

Max, thanks voor de eindeloze debug sessies en het 'kijkewattiedoet' om er na anderhalf uur komma-staren achter te komen dat ik een domme typo had gemaakt. Je Matlab skills blijven onovertroffen, moet je misschien eens iets mee gaan doen…

Jason, Jasper T, Jasper vd G, Heleen, Anne vd B., Lennard, Kaylee, Anne R. Dankjewel voor jullie bijdrage aan dit project in de vorm van (master)stages, jullie enthousiasme en kritische vragen.

Beste Richard, dankjewel voor alle hulp. Of het nou ging om het regelen van minuscuul kleine boorkopjes (gemaakt in een 5-assige CNC machine ter grootte van $25m^3$ in een machinefabriek van een sigarettenfabrikant), hulp bij het onderwijs, of het ontwerpen en printen van een houder voor de oscillerende zaag (die uiteindelijk nooit is gebruikt). Niets was te gek en altijd met een lach. Dankjewel!

Beste Leon, dankjewel voor alle segmentaties die je hebt gedaan. Het was monnikenwerk maar essentieel om het 4DCT project een succes te maken.

Ook alle andere ORL collega's wil ik graag bedanken voor alle hulp en gezelligheid. De leuke BBQ's, uitjes zoals golfen, karten en kano varen (want suppen is tegen mijn principes) waren erg gezellig en ik ga ze zeker missen.

Ward & Bram, we kennen elkaar al lang en hebben met z'n drieën al veel meegemaakt. Mooie maar ook heftige dingen. Ik ben ontzettend blij dat we elkaar (ondanks dat we in

de uithoeken van het land wonen) altijd weer weten te vinden en precies verder gaan waar we gebleven waren.

Beste 'Burgerlijke Pikken', anders dan de appgroepnaam doet vermoeden zijn de avondjes en weekendjes alles behalve burgerlijk. Dank voor alle afleiding, gezelligheid, goede gesprekken en ook vooral de hele slechte gesprekken. Ik zie uit naar het volgende weekend!

Lieve Jan, Hanneke, Mark en Noor, dankjewel voor jullie warmte en jullie interesse in mijn promotie onderzoek en werk.

Lieve zussen, broer, zwagers, schoonzus, neefjes en nichtjes, bedankt voor jullie interesse in mijn onderzoek. Ik ben blij met jullie!

Lieve papa en mama, dankjewel voor jullie onvoorwaardelijke steun en hulp. Of het nu gaat om studie, werk of persoonlijke dingen, jullie staan altijd voor mij (en Iris & Juul) en dat is een ontzettend fijn gevoel.

Lieve Iris, toen ik deze promotie begon woonden we in een klein appartement in het centrum van Utrecht. Nu, ruim 4 jaar (en heel veel burgerpunten) later wonen we in een twee-onder-een-kap in een Vinex wijk en hebben we een dochter. Je bent er altijd voor me om te motiveren of te relativeren óf om een kopje thee te brengen tijdens de avonduren schrijven. Je bent de aller-aller beste en ik hou van jou!

En tot slot, lieve kleine Juul. Ik ben ontzettend trots op je en ik vind het fantastisch om jou te zien op je grote ontdekkingsreis. Ik dacht dat ik nieuwsgierig was, maar jij… Kus!

A

Curriculum Vitae

Hans Dunning was born on the 29th of January 1989 in Delfzijl. He obtained his VWO diploma from the Zernike College in Haren. He started the bachelor Mechanical Engineering at the University of Twente but stopped after 1 year.

After a year of working and traveling he started the bachelor Lifescience & Technology at the University of Groningen, with a major in Biomedical Engineering. After completion of the bachelor he started the master Biomedical Engineering at the University of Groningen. For his master thesis he completed an internship at the 3DLab of the Radboudumc, where he researched the optimal one-shape-fits-all geometry of a bone anchored tibia implant.

In 2017 he started as a research scientist at the Orthopaedics department to develop a minimally invasive tool for the treatment of bone metastasis. He authored a KWF Unique High Risk Project grant which was awarded in 2018.

In 2018 he started as a PhD at the Orthopaedic Research Laboratory focussing on the clinical implementation of dynamic CT imaging in complex knee realignment surgery. Currently he works as a R&D Scientist Imaging & Dosimetry and New Product Development Lead at Quirem Medical.

Data Management

This thesis is based on the results of medical-scientific research with human participants and was therefore subject to the Medical Research Involving Human Subjects Act (WMO). The studies were conducted in accordance with the ICH-GCP guidelines (Good Clinical Practice).

Prior to these studies, ethical approval was obtained from the 'Medical Ethical Committee Oost' under registration numbers: NL60392.091.17 (dose reduction study), NL72784.091.20 (healthy volunteers). Informed consent was obtained from all research participants.

To safeguard the availability, integrity and confidentiality of the data, organizational and technical measures were taken. Data were processed pseudonymised and key files were stored in accordance with institutional guidelines. Non image data was collected through electronic Case Report Forms (eCRF) using Castor EDC.

Data retention and publications

All image data is stored in dedicated image archives and will remain archived for the duration of 15 years. When signing informed consent all participants in the healthy volunteer study described in chapter 5 have, indicated that their image data may be used for future studies. However, institutional approval must be obtained for this purpose.

The scientific articles in this thesis have been published open access, in line with the institutional preference.

A

PhD Portfolio

Department: Orthopaedic Research Laboratory
PhD period: 01**/07/2018 – 01/07/2022**
PhD Supervisor(s): **Prof. N. Verdonschot**
PhD Co-supervisor(s): **Dr. S.A.W. van de Groes, Dr. D. Janssen**

Training activities	Hours
Courses	
• RIHS - Introduction course for PhD candidates (2018)	15.00
• Scientific Integrity for PhD candidates (2018)	28.00
• RIHS PhD introduction course (2018)	21.00
• Musculoskeletal Modeling by Multibody Dynamics (2018)	112.00
• Statistiek voor promovendi met SPSS (opfriscursus) (2018)	56.00
• EBrok course (2018)	42.00
• Scientific Writing for PhD candidates (2019)	84.00
• Projectmanagement for PhD candidates (2019)	56.00
• Radboudumc - Scientific integrity (2019)	20.00
Conferences	
• PhD Retreat (2018) (oral presentation)	28.00
• World Congress of Biomechanics (2018) (poster presentation)	49.00
• PhD Retreat (2019) (poster presentation)	14.00
• NOV Jaarcongres (2019) (oral presentation)	14.00
• ESSKA 2022 Paris (2022) (poster presentation)	42.00
Teaching activities	
Lecturing	
• Belasting & Belastbaarheid (2018)	11.20
• Meet the PhD (2018)	56.00
• Orthopaedic Biomechanics in Motion 2019 (2019)	21.00
• Minor Introduction: Moving Questions (2019)	2.80
• Belasting & Belastbaarheid 2019 (2019)	11.20
• Belasting & Belastbaarheid 2020 (2020)	11.20
• Orthopaedic Biomechanics in Motion 2020 (2020)	21.00
Supervision of internships / other	
• Master internship, Jason Verspeek, Medicine, 6 months (2018)	56.00
• Master internship, Jasper Twilt, Technical Medicine, 3 months (2018)	21.00
• Master internship, Jasper van der Graaf, Technical Medicine, 12 months (2019)	112.00
• Master internship, Heleen van den Nieuwenhof, Technical Medicine, 3 months (2019)	21.00
• Master internship, Anne van den Brekel, Technical Medicine, 3 months (2019)	21.00
• Master internship, Lennard van Karnenbeek, Technical Medicine, 3 months (2020)	21.00
• Master internship, Kaylee van Duren,, Technical Medicine, 3 months (2021)	21.00
• Master internship, Anne van den Brekel, Technical Medicine, 12 months (2021)	112.00
• Master internship, Anne Rook, Technical Medicine, 18 months (2022)	140.00
Total	**1240.40**